Distribution Agreement

In presenting this thesis or dissertation as a partial fulfillment of the requirements for an advanced degree from Emory University, I hereby grant to Emory University and its agents the non-exclusive license to archive, make accessible, and display my thesis or dissertation in whole or in part in all forms of media, now or hereafter known, including display on the world wide web. I understand that I may select some access restrictions as part of the online submission of this thesis or dissertation. I retain all ownership rights to the copyright of the thesis or dissertation. I also retain the right to use in future works (such as articles or books) all or part of this thesis or dissertation.

Signature:

_____ _____

Alicia Ann Cutler Date

Analyses of aging and heterogeneity in nuclei of multinucleated skeletal muscle cells

By

Alicia Ann Cutler

Doctor of Philosophy

Graduate Division of Biological and Biomedical Science

Biochemistry, Cell, and Developmental Biology

_____	_____
Anita H. Corbett, Ph.D. Advisor	Grace K. Pavlath, Ph.D. Advisor
_____	_____
Winfield S. Sale, Ph.D. Committee Member	Maureen A. Powers, Ph.D. Committee Member
_____	_____
James Q. Zheng, Ph.D. Committee Member	Nicholas T. Seyfried, Ph.D. Committee Member

Accepted:

_____

Lisa A. Tedesco, Ph.D.
Dean of the James T. Laney School of Graduate Studies

_____

Date

Analyses of aging and heterogeneity in nuclei of multinucleated skeletal muscle cells

By

Alicia Cutler

B. S. Brigham Young University, 2012

Advisors: Anita Corbett, Ph.D. and Grace Pavlath, Ph.D.

An Abstract of

A dissertation submitted to the Faculty of the

James T. Laney School of Graduate Studies of Emory University

In partial fulfillment of the requirements for the degree of

Doctor of Philosophy

In Biochemistry Cell and Developmental Biology

2017

Abstract

Analyses of aging and heterogeneity in nuclei of multinucleated skeletal muscle cells

By Alicia Cutler

The primary cell type of skeletal muscle is the myofiber. Myofibers are multinucleated containing thousands of nuclei all sharing a single, common cytoplasm. Despite all nuclei sharing the same cytoplasm, individual nuclei differ in key characteristics. Although the nucleus is the major site of gene regulation, the muscle nucleus has been underexamined because of technical limitations including contamination with non-myofiber derived nuclei and inability to selectively analyze individual nuclei. In this dissertation, we overcome these difficulties and demonstrate that nuclei in a single myofiber differ in nuclear import as a potential mechanism for achieving variation in nuclear content and function among nuclei in a single cell. We also present an approach to selectively isolate myonuclei, the first detailed myonuclear proteome, and changes that occur in the myonuclear proteome with aging. This work reinforces the significance of variation among myonuclei and emphasizes the importance of examining nuclear activity on the level of individual nuclei. Additionally, we show that we have developed the technical approach needed to pursue myonuclear-specific studies. Together our findings lay the foundation for careful examination of the myonuclear proteome, transcriptome, and epigenome in response to muscle growth, regeneration, exercise, and disease.

Analyses of aging and heterogeneity in nuclei of multinucleated skeletal muscle cells

By

Alicia A Cutler

B.S., Brigham Young University, 2012

Advisors: Anita Corbett, Ph.D. and Grace Pavlath, Ph.D.

A dissertation submitted to the Faculty of the

James T. Laney School of Graduate Studies of Emory University

In partial fulfillment of the requirements for the degree of

Doctor of Philosophy

In Biochemistry Cell and Developmental Biology

2017

Acknowledgements

I gratefully acknowledge my two wonderful mentors: Grace Pavlath and Anita Corbett. Grace is an incredible role model with her unwavering professionalism, remarkable efficiency, and unfailing optimism. After meeting with her I always felt like I knew what the next step was and was excited to do it. Her faith in and optimistic support of my career has made all the difference in the course I have taken. Anita is a remarkable example of dedicated service to important causes in science; she readily makes room among her many time commitments and responsibilities for those things she cares deeply about. I am thankful for her investment in my development as a scientist. I was fortunate to have a dedicated thesis committee who provided valuable insights into the logic of my project and technical expertise that solved so many of my problems. Collaboration with them enabled me to develop specialized expertise that would otherwise have been infeasible. The friendship and comradery of my lab mates made coming to work a joy. I am profoundly grateful for their support and problem-solving insights during stressful times and for being the inspiration for some particularly brilliant musical parodies. I appreciate the example of my classmates; together we pushed each other to excellence. The support of my friends helped keep me sane and was a valuable reserve of knowledge on statistics, computer programming, and edible plants. Finally, I am grateful to my family for their support and encouragement. In particular, my parents, who instilled me with a love of science and a passion for learning, my inspirational Grandmother, my brother Chris, who was always available to bounce ideas off and lend a hand, and my sister Sarah for reading and correcting my papers. I thank the many people who contributed to my success.

Table of Contents

Chapter 1: Background and Significance 1
Introduction 2
1.1 Skeletal muscle 3
1.1.1 Myogenesis 4
1.1.2 Aging Muscle 6
1.2 Nucleocytoplasmic transport 8
1.2.1 Nuclear envelope 9
1.2.2 Nuclear pore complex 11
1.2.3 Nuclear transport receptors 17
1.3 Multinucleated cells 20
1.3.1 Multinucleated single-celled organisms 21
1.3.2 Multinucleated cells in multicellular organisms 23
1.4 Summary 30
1.5 Figures 33
Chapter 2: Non-equivalence of nuclear import among nuclei in multinucleated skeletal muscle cells 38
2.1 Summary 39
2.2 Introduction 40
2.3 Results 44
2.3.1 Nuclear import varies among nuclei within single cultured multinucleated myotubes 44
2.3.2 Independence of nuclear import pathways in cultured myotubes 48
2.3.3 Variation in cNLS import among myofiber nuclei in situ 51
2.3.4 Nuclear import varies with muscle differentiation 54
2.4 Discussion 55
2.5 Methods 66
2.6 Tables 75
2.7 Figures 76
Chapter 3: Biochemical isolation of myonuclei employed to define changes to the myonuclear proteome that occur with aging 92
3.1 Summary 93
3.2 Introduction 94
3.3 Results 96
3.3.1 Isolation of pure intact nuclei 96

3.3.2 Isolated nuclei are predominantly myonuclei 97
3.3.3 Increased depth of proteomic detection in myonuclear proteome 99
3.3.4 The myonuclear proteome changes with age 100
3.3.5 Myonuclei share common aging pathways with brain nuclei 102
3.4 Discussion 104
3.5 Experimental Procedures 108
3.6 Tables 107
3.7 Figures 112
Chapter 4: Discussion and future directions 121
Appendix 1: Biochemical isolation of myonuclei from mouse skeletal muscle tissue 134
Appendix 1.1 Abstract 135
Appendix 1.2 Background 135
Appendix 1.3 Materials and Reagents 136
Appendix 1.4 Equipment 138
Appendix 1.5 Procedure 139
Appendix 1.6 Optional alternative approach 146
Appendix 1.7 Data analysis 147
Appendix 1.8 Notes 148
Appendix 1.9 Recipes 148
References 153

List of tables

Table 2.1 NLS sequences and associated nuclear transport receptors

Table 3.1 Myonuclear proteins that change significantly with age

Table 3.2 Brain nuclear proteins that change significantly with age

List of figures

Figure 1.1 Cellular composition of skeletal muscle

Figure 1.2 Myogenesis

Figure 1.3 Nuclear transport

Figure 2.1 Some but not all nuclei within myotubes import a fluorescent nuclear import reporter

Figure 2.2 Nuclear import depends on the NLS

Figure 2.3 A single nucleus with a myotube can import through multiple import pathways, a single import pathway, or no detectable import pathway

Figure 2.4 cNLS nuclear import varies among nuclei within single myofibers

Figure 2.5 Rates of cNLS nuclear import can vary between regions of a single myofiber

Figure 2.6 Nuclear import varies during myogenesis *in vitro*

Figure 2.7 Nuclear number compared to percent import positive nuclei

Figure 2.8 cNLS nuclear import and Nup levels

Figure 2.9 Purity of purified recombinant proteins

Figure 3.1 Workflow for isolating nuclei from skeletal muscle

Figure 3.2 Isolated nuclei are predominately myonuclei

Figure 3.3 Nuclear proteins are enriched in purified nuclei

Figure 3.4 Aging of the myonuclear proteome

Figure 3.5 Comparison of age-related alterations in muscle and brain nuclear proteomes

Figure A.1 Muscle dissection

Figure A.2 Pre-ultracentrifugation preparation

Figure A.3 Loading ultracentrifugation tubes

Figure A.4 Unloading ultracentrifugation tubes

Figure A.5 Purified myonuclei

List of abbreviations

BSA	Bovine serum albumin
cNLS	Classical nuclear localization sequence
CMP	Complete mini protease
CyTOF	Mass cytometry
DAPI	4’,6-diamidino-2-phenylindole
DAVID	Database for Annotation, Visualization and Integrated Discovery
ECL	Elastin, collagen, laminin
EGFP	Enhanced green fluorescent protein
ER	Endoplasmic reticulum
EU	Ethynyl uridine
FBS	Fetal bovine serum
FG	Phenylalanine glycine repeat
FAP	Fibroadipogenic progenitor cell
FITC	Fluorescein isothiocyanate
FDR	False discovery rate
FRAP	Fluorescence recovery after photobleaching
GA	Gastrocnemius
GO	Gene ontology
GST	Glutathione S-transferase
HAT	Histone acetyl transferases
HDAC	Histone deacetylase

INM	Inner nuclear membrane
INTACT	Isolation of nuclei tagged in specific cell types
IPTG	Isopropyl β-D-1-thiogalactopyranoside
KEGG	Kyoto Encyclopedia of Genes and Genomes
LFQ	Label free quantitation
MGC	Multinucleated giant cells
MTJ	Myotendinous junction
NES	Nuclear export sequence
NET	Nuclear envelope transmembrane
NLS	Nuclear localization sequence
NMJ	Neuromuscular junction
NPC	Nuclear pore complexes
NTR	Nuclear transport receptors
O-GlcNAc	O-linked N-Acetylglucosamine
ONM	Outer nuclear membrane
RF	Rectus femoris
SD	Standard deviation
SE	Standard error
SR	Sarcoplasmic reticulum
SSC	Side scatter
$T_{1/2}$	Time to half recovery
WGA	Wheat germ agglutinin

Chapter 1: Background and Significance

Chapter 1: Background and Significance

Introduction

Proper function of skeletal muscle tissue is critical for survival and quality of life. As in any tissue, proper function relies on correct gene expression. Unlike other tissues, the primary cell type in skeletal muscle is multinucleated. This plurality of nuclei adds a layer of complication to regulating gene expression Thousands of nuclei sharing a common cytoplasm introduces new variables like nuclear position, age of a nucleus, and interaction with other nuclei that could affect nuclear activity. Whether nuclear activity is coordinated among nuclei or is regulated by each nucleus independently is unknown as is the effect of factors like nuclear position and age. By extension, how different states like growth, regeneration, exercise, or aging affect muscle nuclei is largely unknown. Nucleocytoplasmic transport regulates which proteins enter and leave the nucleus and thereby broadly modulates nuclear activity. This dissertation will examine nuclear import in multinucleated skeletal muscle cells and changes to the myonuclear proteome that occur in aging. This chapter highlights the basic properties of skeletal muscle, nucleocytoplasmic transport, and multinucleated cells. First, skeletal muscle and its properties in development and aging are examined. Second, the primary components of nucleocytoplasmic transport are presented with particular emphasis on nuclear import. Third, the basic properties of multinucleated cells, how they are formed, and any differences among nuclei within a single cell are reviewed.

1.1 Skeletal muscle

Skeletal muscle is the most massive tissue in the body, making up 40–50% of a human body's mass (Ten Broek, Grefte et al. 2010). Critical bodily functions including breathing, swallowing, and moving require skeletal muscle function. In addition to its role in contraction, skeletal muscle also plays a major role in the immune response and in metabolic homeostasis and thermal homeostasis in mammals. Skeletal muscle is the primary amino acid reserve, supplying the body with nutrients when protein or glucose intake is limited (Cahill 1970, Biolo, Zhang et al. 1995). When the body is exposed to cold, skeletal muscle shivering is induced as a means of thermogenesis (Jubrias, Vollestad et al. 2008, Nakamura and Morrison 2011). Shivering is also induced in response to infection as a means of thermogenesis to combat the pathogen (Cooper, Preston et al. 1976). Survival depends on proper development and maintenance of skeletal muscle.

Skeletal muscle tissue is made up of many different cell types (Figure 1.1). Crucial supporting cells in a muscle include afferent neurons, muscle spindles that sense the muscle length, endothelial cells that make up blood vessels, and fibroblasts that help deposit extracellular matrix. Some cells present in small numbers in uninjured muscle expand their populations dramatically to support tissue repair following injury; these cell populations include muscle resident stem cells called satellite cells (Mauro 1961), fibroadipogenic progenitor cells (FAPs) (Joe, Yi et al. 2010), and macrophages (Tidball and Villalta 2010). While all of these cell types play an important role in supporting and maintaining skeletal muscle, the primary cell type in muscle is large multinucleated myofibers. Myofibers can extend from a muscle's origin to its insertion site. The ends of a myofiber are specialized to form a myotendinous junction that anchors the cell. A neuromuscular junction in the

middle of the myofiber, where a motor neuron synapses onto the myofiber, conveys action potentials signaling the myofiber to contract. The body of a myofiber is densely packed with contractile units called sarcomeres. The principle components of a sarcomere are actin and myosin. Myosin motors move along actin filaments, shortening the sarcomere and contracting the myofiber. Four major isoforms of myosin heavy chain exist, and each has a different rate of contraction. Fast cycling myosin motors are found in myofibers relying predominantly on glycolytic phosphorylation while slower cycling myosin is found in myofibers relying on oxidative phosphorylation (Schiaffino and Reggiani 1994). The composition of slow and fast myofiber types in a muscle affects the muscle's performance in both maximal force and time to fatigue. In conclusion, nuclei in skeletal muscle stem from many different cell type, several types of myofibers, and different myofiber regions.

1.1.1 Myogenesis

During embryogenesis, cells from the myotome or from the precordal mesoderm migrate and differentiate into muscle precursor cells called myoblasts (schematized in Figure 1.2A). Precursor cells differentiate to committed post-mitotic myocytes, which fuse to form immature myofibers (Reviewed in (Buckingham 1992)). Myofibers form in two waves during embryonic development. Primary myofibers form first and tend to be slow twitch myofibers (Draeger, Weeds et al. 1987, Buckingham, Bajard et al. 2003). The second wave of myofibers form around primary myofibers and produce various kinds of fast twitch myofibers (Ross, Duxson et al. 1987, Harris, Duxson et al. 1989). This initial embryonic phase of myogenesis gives way to the fetal phase mostly defined by growth. Postnatally muscles continue to grow and reserve precursor cells are designated to become

satellite cells (Reviewed in (Tajbakhsh 2005)). However, muscle satellite cells remain relatively active throughout juvenile development as muscle continues to grow, up until three months of age in mice (Pawlikowski, Pulliam et al. 2015). Growth and maintenance of skeletal muscle in juveniles and adults depends on satellite cells. Satellite cells activate from quiescence and divide. In an asymmetric cell division, one daughter cell returns to quiescence, maintaining the satellite cell pool; the other daughter cell differentiates and fuses into a myofiber (Kuang, Kuroda et al. , Shinin, Gayraud-Morel et al. 2006). To summarize, developmental myogenesis relies on several rounds of progenitor differentiation and incorporation to produce highly ordered skeletal muscle tissue.

Skeletal muscle is a highly regenerative tissue. Following injury, a series of coordinated events result in regeneration of the injured site (schematized in Figure 1.2B). First, M1 pro-inflammatory macrophages invade the site of injury and break down the damaged tissue (Tidball and Villalta 2010). Fibroadipogenic progenitor cells proliferate rapidly during this time and are potentially involved in stimulating the activation of satellite cells and promoting matrix deposition (Lemos, Babaeijandaghi et al. 2015). The macrophages then shift from pro-inflammatory M1 macrophages to anti-inflammatory M2 macrophages (Tidball and Villalta 2010), and FAPs undergo apoptosis (Lemos, Babaeijandaghi et al. 2015). Satellite cells proliferate and produce a large number of muscle progenitor cells. These progenitors differentiate and either fuse into existing damaged myofibers or fuse with each other, forming new, smaller myofibers (Reviewed in (Ratnayake and Currie 2017)). Sometimes myofibers regenerate with branches, which reduce myofiber functionality and resistance to mechanical stress (Pichavant and Pavlath 2014). Myonuclei in regenerated myofibers are localized in the center of the myofiber

rather than the periphery and remain in the center of the myofiber for months after the injury has healed. Thus, following injury multiple cell types all participate in a tightly coordinated regenerative program that results in full regeneration of skeletal muscle tissue.

Myogenesis can be modeled *in vitro* using cultured muscle precursor cells (schematized in Figure 1.2C). These cells are proliferative when cultured in growth media containing serum. However, when transferred to serum-free media, the progenitor cells differentiate and fuse, forming large multinucleated myotubes (Bondesen, Mills et al. 2004). This culture system likely best models the type of myogenesis that takes place during regeneration.

1.1.2 Aging Muscle

Starting around age 30 in humans, muscle mass and strength begin an overall decline, and the rate of decline increases rapidly after age 60 (Metter, Conwit et al. 1997, Bassey 1998, Frontera, Hughes et al. 2000). The loss of muscle mass and strength results from hypoplasia (loss of muscle cells) and atrophy (reduction in the size of the remaining muscle cells). In addition, motor units undergo a switch from fast motor units to slow motor units (Campbell, McComas et al. 1973), increasing delays in reaction time and increasing the risk of loss of balance and falls. Decreased muscle function increases morbidity and decreases quality of life for the elderly. Reduced muscle strength is associated with reduced mobility (Marsh, Rejeski et al. 2011, Dufour, Hannan et al. 2013) and greater risk of falls (Cesari, Kritchevsky et al. 2005, Landi, Liperoti et al. 2012) and disability (Newman, Kupelian et al. 2006, Xue, Walston et al. 2011).

The functional and physiological changes in aging muscle are accompanied by changes in the transcriptome and epigenome. mRNA levels are altered in aging: transcripts related to metabolism are depleted in older muscle, while transcripts related to inflammation and damage response are enriched (Zahn, Sonu et al. 2006, Kim, Park et al. 2014, Su, Ekman et al. 2015). These changes reflect functional changes like myofiber type switching. miRNA expression and DNA methylation also change with age. Levels of miRNAs regulating transcripts involved in transcription and differentiation are altered (Kim, Park et al. 2014). Aging is also correlated with global DNA hypermethylation (Zykovich, Hubbard et al. 2014). While there are established connections between altered gene expression and the loss of muscle mass and function, the molecular mechanisms driving a shift in gene expression remain elusive.

The changes in transcript levels with age are also accompanied by proteomic changes in aging muscle. Approximately 10% of proteins in rat skeletal muscle change significantly with age (Capitanio, Vasso et al. 2009). Most age-associated changes in human and rodent skeletal muscle are detected in contractile and metabolic proteins (Baraibar, Gueugneau et al. 2013, Holland, Dowling et al. 2014). Sarcomeric and metabolic proteins are orders of magnitude more abundant than other proteins in the tissue, so these proteins dominate any proteomic analysis to the exclusion of low abundance proteins. In mouse and human samples ~50% of proteins identified and ~80% of peptide reads are from contractile proteins (Carberry, Zweyer et al. 2014, Deshmukh, Murgia et al. 2015, Cutler, Dammer et al. 2017). Examination of aging muscle in nematodes, which have relatively lower levels of sarcomeric proteins than mammalian muscle, revealed a greater variety of changes, including changes in levels of proteins functioning in transcription termination,

mRNA degradation, proteosomal function, and ribosomal proteins (Copes, Edwards et al. 2015). The results from aging nematodes indicate that substantial changes occur in skeletal muscle with aging but are undetectable by current sample preparation techniques. Increased detection of underrepresented proteins, including nuclear proteins, would likely identify more muscle-specific aging changes.

Little is known about the effects of aging on myonuclei. The average half-life of a human myonucleus is 15 years (Spalding, Bhardwaj et al. 2005), so some nuclei have been incorporated in a myofiber for more than 30 years. Nuclear proteins are among the longest lived in a cell; histones and some nuclear pore components turn over on the order of decades (Toyama, Savas et al. 2013). This low turnover rate of nuclei and nuclear proteins suggests that wear and tear of decades of use could affect nuclear composition and integrity. Indeed, nuclear pore proteins accumulate oxidative damage with age, which results in decreased exclusion of cytoplasmic proteins from the nuclear compartment (D'Angelo, Raices et al. 2009). Likely, other nuclear proteins also undergo changes in levels or modification as skeletal muscle ages. However, prior to the work presented in Chapter 3 (Cutler, Dammer et al. 2017), most nuclear proteins were undetectable by proteomic analysis of whole skeletal muscle tissue.

1.2 Nucleocytoplasmic transport

In eukaryotic cells, transcription is separated from translation by the nuclear envelope. Genes are transcribed inside the nucleus, and the transcript is exported and then translated in the cytoplasm. Any proteins with nuclear function must then be imported into the nucleus. Nucleocytoplasmic transport (schematized in Figure 1.3) is controlled to

maintain regulation of gene expression and to protect the genome. Transport in and out of the nucleus passes through nuclear pore complexes (NPC), the gateway through the nuclear envelope (Schmidt and Görlich 2016). Most proteins and RNA require nuclear transport receptors to facilitate transport. Nuclear import proceeds as nuclear transport receptors (NTR) bind to nuclear localization signals in the cargo protein. The complex of NTR and cargo then translocate through the NPC into the nucleus. Once inside the nucleus, the NTR is bound by RanGTP. This induces a conformational change, which releases the cargo into the nucleoplasm. Many NTRs can mediate both import and export. An NTR-RanGTP complex can bind to a nuclear export sequence (NES) motif in a target protein. Together, the complex moves through the NPC to the cytoplasm. When RanGTP encounters RanGAP1, in the cytoplasm it induces hydrolysis of GTP, which causes a conformational change that dissociates the complex. The cargo and NTR are released (Schmidt and Görlich 2016). To replenish nuclear pools of RanGTP, RanGDP is bound by NTF2 and imported into the nucleus (Corbett and Silver 1996) where the RanGDP is converted to RanGTP by interaction with RCC1. The directionality of nuclear transport depends on maintaining higher concentrations of RanGTP in the nucleus and RanGDP in the cytoplasm. This concentration gradient is achieved by localizing RCC1 to the nucleus and RanGAP1 to the cytoplasm (reviewed in (Tran, King et al. 2014)).

1.2.1 Nuclear envelope

The nuclear envelope is a double membrane sequestering the nucleus from the rest of the cell; the primary mode of crossing the nuclear envelope is through nuclear pores. The outer nuclear membrane (ONM) is continuous with the endoplasmic reticulum and

contains some ribosomes. The ONM is also decorated with several proteins specific to the ONM, which function to connect the nucleus to the surrounding cytoskeleton and correctly position the nucleus in the cell. The inner nuclear membrane (INM) interacts with nuclear lamins, chromatin, and other nucleoplasmic proteins through nuclear envelope transmembrane proteins (NETs), most of which specifically localize to the INM. LINC complexes, composed of SUN domain proteins on the nucleoplasmic side and KASH domain proteins on the cytoplasmic side, connect the cytoskeletons of the nucleus and cytoplasm (Tapley and Starr 2013), provide for transduction of mechanical signaling (Uzer, Thompson et al. 2015), and maintain the correct spatial separation between the INM and ONM (Voeltz and Prinz 2007). SUN domain proteins interact with nuclear lamins as well as chromatin. KASH domain proteins interact with actin, microtubules, and intermediate filaments. Together these linker and cytoskeletal proteins help to maintain overall nuclear structure and protect the nucleus from shear force. The nuclear envelope is not simply a passive barrier supported by active cytoskeletal proteins. Rather, nuclear envelope restructuring is important for proper differentiation of embryonic stem cells (Voeltz and Prinz 2007, Smith, Zhang et al. 2011) and pathology results if the nuclear envelope or underlying lamins are compromised (Worman, Östlund et al. 2010). In summary, the nuclear envelope separates the nuclear compartment from the cytoplasm, helps to coordinate communication between nucleus and cytoplasm, and forms is actively involved in regulating nuclear processes.

1.2.2 Nuclear pore complex

The NPC is a massive protein complex that forms the gateway through the nuclear envelope, connecting the nucleus with the cytoplasm. Composed of multiple copies of ~30 nucleoporins (Nups) in eightfold symmetry, the NPC is a staggering ~120 MDa complex extending approximately 125 nm from the cytoplasmic fibrils to the nuclear basket (Tran and Wente 2006). The central channel can expand so that it is large enough to accommodate transport of ribosome subunits (Kohler and Hurt 2007). The NPC regulates movement into and out of the nucleus. Ions and molecules smaller than 40 kDa freely diffuse through the nuclear pore while molecules larger than 40 kDa require the assistance of nuclear transport receptors to travel through the NPC. A single NPC can accommodate more than 1,000 transport events per second (Ribbeck and Gorlich 2001) and a nucleus has thousands of NPCs to fill the constant need for cargo delivery.

While the exact structure of the NPC and precise mechanism of selective transport have not been determined, some of the roles of NPC components in these processes have been established. Nup84 plays a role in regulating positioning and spacing of NPCs in the nuclear envelope (Tran, King et al. 2014), and the transmembrane proteins POM121, NDC1, and Nup210 anchor the NPC in the nuclear envelope (Terry, Shows et al. 2007). Structural Nups of the Nup107-160 complex (Nups160, 107, 133, 96, 85, 43, 37, Sec13, Seh1, and ELYS) provide the NPC's general architecture (Walther, Alves et al. 2003, Terry, Shows et al. 2007). These core structural Nups are very stably associated in the NPC, and the same protein can persist in the complex for years in post-mitotic cells (Savas, Toyama et al. 2012, Toyama, Savas et al. 2013). Other Nups associate with the NPC more dynamically, with dwell times ranging from hours to seconds (Rabut, Doye et al. 2004).

Among these more dynamic Nups are the proteins that make up the cytoplasmic face of the nuclear pore, the hydrophobic Nups of the central channel, and the proteins that make up the nuclear basket.

A cargo's passage through the NPC begins and ends with interaction with cytoplasmic filaments and the nuclear basket. Cytoplasmic filaments are made up of Nup358 and Nup214. Long filamentous domains of these proteins extend into the cytoplasm and provide binding sites for transport proteins. Nuclear import begins with binding of NTR-cargo complexes to cytoplasmic filaments. Nuclear export terminates with RanGAP-mediated dissociation of NTR-cargo complexes. RanGAP1 binds to Nup358, localizing it to the nuclear envelope (Tran and Wente 2006), although in *Arabadopsis thaliana*, correct localization is not required to maintain nuclear transport if RanGAP1 maintains GAP activity (Boruc, Griffis et al. 2015). In contrast, loss of cytoplasmic filament proteins Nup358 or Nup214 inhibits nuclear transport (Tran and Wente 2006, Sabri, Roth et al. 2007, Hutten, Flotho et al. 2008). On the nuclear side of the nuclear pore, the nuclear basket is the starting point for nuclear export and the ending point of nuclear import. The nuclear basket, which extends from the NPC into the nucleoplasm, is comprised of TPR, Nup50, and Nup153. The nuclear basket is an important docking site for NTRs entering and leaving the NPC. Loss of Nup153 inhibits nuclear transport (Tran and Wente 2006). Cytoplasmic filaments and the nuclear basket provide interaction sites for the first and last steps of nuclear transport.

The NPC central channel is filled with long, unstructured hydrophobic Nup repeats. These repeats include variations of a phenylalanine glycine (FG) motif (Tu and Musser 2011, Powers and Forbes 2012). Nups 153, 98, 62, 58, 54, and 45 all have hydrophobic

FG-repeat-containing motifs and contribute to the mesh-like barrier of the central channel. Only Nup98 is indispensable to maintaining the NPC permeability barrier (Hülsmann, Labokha et al. 2012), but subclasses of FG motifs found in some of the FG Nups are required for RNA (Terry and Wente 2007) and protein transport. The FG Nups are responsible for the NPC selective barrier, protecting the genome and gene expression by excluding most proteins from the nucleus while allowing nuclear proteins to enter the privileged compartment.

The NPC is not static. The levels of NPC components incorporated in the complex vary in response to signaling, stress, and differentiation. Additionally, the post-translational modifications of NPC proteins are dynamic. By modulating the NPC composition and modifications, nucleocytoplasmic transport can be fine-tuned without interrupting the almost constant exchange of molecules between the nucleus and cytoplasm of a cell. The impact of tissue specificity, differentiation, post-translational modification, and aging on the NPC and nuclear transport will be discussed in detail below.

1.2.2.1 Tissue specificity and the nuclear pore complex

NPCs differ across tissues in both which components are present in the NPC and in the levels to which they are incorporated. Similarly, loss or depletion of individual Nups can have tissue-specific phenotypes. Nup210 is selectively expressed in mature skeletal muscle and neuronal tissue (D'Angelo, Gomez-Cavazos et al. 2012, Gomez-Cavazos and Hetzer 2015). The levels of Nup50 in the nuclear pore vary across different tissues with highest incorporation in testes (Guan, Kehlenbach et al. 2000). Nup88 is highly expressed in inner medullary collecting duct cells in the kidney but not expressed in the cells of the cortex. Additionally, Nup88 levels increase in collecting duct cells in response to kidney

osmotic stress (Andres-Hernando, Lanaspa et al. 2008). In *Drosophila*, loss of Nup88 causes trachea-specific phenotypes (Uv, Roth et al. 2000). Mice hemizygous for Nup96 have impaired immune systems but lack other phenotypes (Faria, Levay et al. 2006). Nup133 knockout mice fail to appropriately differentiate neurons, but other tissues develop normally (Lupu, Alves et al. 2008). Increased levels of Nup358 in keratinocytes is associated with psoriasis (Yasuda, Sugiura et al. 2014). Why some NPC components are tissue-specific and why the loss of individual Nups induces tissue-specific defects is largely unknown. The specificity could result from tissue-specific protein or RNA cargos that require interaction with specific Nups for transport or from Nup functions unrelated to the nuclear pore.

1.2.2.2 Post-translational modifications and the nuclear pore complex

The post-translational modifications of nuclear pore proteins are dynamic and affect nuclear import. Most Nups are subject to phosphorylation; FG Nups are additionally subject to O-GlcNAc glycosylation. These modifications can affect association of the Nups with the nuclear pore, Nup interaction with NTRs, or interactions between Nup FG repeat motifs (Tran and Wente 2006, Kosako and Imamoto 2010). ERK-mediated phosphorylation of Nups 50, 153, 214, (Kosako and Imamoto 2010) and 62 (Nardozzi, Lott et al. 2010) decreases their interaction with a specific NTR, importin β (Kosako and Imamoto 2010). Introducing non-phosphorylatable Nups into the nuclear pore causes impaired RNA export and altered gene expression (Regot, de Nadal et al. 2013). O-GlcNAc glycosylation of FG Nups increases the permeability of the nuclear pore to NTRs (Hulsmann, Labokha et al. 2012). Varying the post-translational modifications on specific Nups can increase or decrease nuclear transport.

Post-translational modifications of Nups are dynamic and change in response to stress, differentiation, or other signaling events. For example, oxidative stress blocks nuclear transport by phosphorylation of Nup153, Nup88 (Kodiha, Tran et al. 2009), Nup62, and Nup214 (Sekimoto and Yoneda 2012) and O-GlcNAc modification of Nups 153 (Kodiha, Tran et al. 2009), 62, and 214 (Sekimoto and Yoneda 2012). Oxidative stress also decreases the stability of Nup358 (Crampton, Kodiha et al. 2009). Changes in modification state can change Nup association with the nuclear pore. Altered modifications in response to oxidative stress lead to accumulation of Nup 98 (Crampton, Kodiha et al. 2009) and Nup153 (Kodiha, Tran et al. 2009) in the nucleus. Preventing O-GlcNAc modification decreases the stability of Nup62 and reduces the incorporation of Nup62 and Nup88 at the nuclear pore (Mizuguchi-Hata, Ogawa et al. 2013). In summary, Nup modification state is modulated to regulate nuclear transport in response to physiological changes.

1.2.2.3 Differentiation and the nuclear pore complex

The NPC undergoes changes in composition and modification during differentiation. Nup133 is preferentially expressed in dividing progenitor cells and is down regulated as mouse embryonic stem cells and neuronal progenitor cells differentiate (Lupu, Alves et al. 2008). Nup210 is not expressed in progenitor cells but is expressed upon differentiation of muscle and neuronal cells. Ectopic expression of Nup210 in proliferating myoblasts is sufficient to drive accelerated differentiation into myotubes (D'Angelo, Gomez-Cavazos et al. 2012). Nup358 and Nup50 are additionally required for proper muscle cell differentiation. Lack of Nup50 negatively impacts fusion of muscle progenitor cells (Buchwalter, Liang et al. 2014). Nup358 is expressed throughout development, but the amount of Nup358 present at each nuclear pore increases as myoblasts differentiate.

Depletion of Nup358 prevents differentiation of myoblasts into myocytes (Asally, Yasuda et al. 2011). Similarly, Sec13 is expressed in most tissues, but a mutation in the gene specifically results in a defect in retinal development (Niu, Hong et al. 2014). Not only does the composition of the nuclear pore change with differentiation, but the post-translational modifications also change. For example, as human embryonic stem cells differentiate, there is an overall decrease in Nup phosphorylation (Rigbolt, Prokhorova et al. 2011). These examples have shown that cellular differentiation is accompanied by changes in the NPC. In most cases the effects of these changes are unknown; NPC changes could affect differentiation by changing the localization of proteins regulating gene expression or the export of specific transcripts. Conversely, the effects could be mediated by Nups acting in roles other than those described in nuclear transport.

1.2.2.4 Aging and the nuclear pore complex

In humans and mice, the core NPC proteins can persist in the NPCs of post-mitotic cells for years before being turned over (Savas, Toyama et al. 2012, Toyama, Savas et al. 2013). This extremely long half-life can lead to accumulation of damage to these proteins. In aged mice and *C. elegans*, oxidative damage to Nups compromised the nuclear pore's permeability barrier and cytoplasmic proteins usually excluded from the nucleus aggregated in the nucleoplasm (D'Angelo, Raices et al. 2009). A compromised NPC permeability barrier results in protein mislocalization that can negatively impact nuclear function and resulted in aberrant gene expression.

1.2.2.5 Roles for Nups beyond the nuclear pore complex

The first described role for many Nups was their involvement in the NPC. It can be tempting to assume that cellular phenotypes associated with changes in protein levels or

post-translational modification of Nups are the result of altered nuclear transport. However, many Nups have additional functions besides their role in the NPC. For example, Nups 50, 153, and 98 are involved in regulating transcription, and their dwell times at the nuclear pore vary with the cell's transcriptional activity (Buchwalter, Liang et al. 2014). Nup210 modulates the balance between apoptosis and survival in differentiating muscle cells independent of its association with the NPC (Gomez-Cavazos and Hetzer 2015). Proteins of the nuclear basket are involved in mRNA quality control, chromatin compartmentalization, and transcription regulation (Reviewed in (Strambio-De-Castillia, Niepel et al. 2010, Saroufim, Bensidoun et al. 2015)). Several Nups bind to chromatin, playing a role in genome spatial organization in the nucleus (Schmid, Arib et al. , Franz, Walczak et al. 2007). Some Nups even have roles outside the nucleus, for example, Sec13 is a crucial component of the COPII coat complex, which is necessary for trafficking vesicles between the ER and the Golgi apparatus (Niu, Hong et al. 2014). The diverse roles of NPC components highlight the potential crosstalk between nuclear transport and other cellular processes.

1.2.3 Nuclear transport receptors

NTRs are transport proteins and adapter proteins that recognize cargo proteins and mediate binding to transport proteins. Adapter proteins mostly belong to the karyopherin alpha family (Kapα), while transport proteins belong to the karyopherin beta family (Kapβ). In mammals, 19 different Kapβs have been identified. Each Kapβ has distinct import, export, or bidirectional transport activity. Kapβs each recognize specific cargo proteins or RNAs; thus, each Kapβ and its associated cargos comprises a distinct import

pathway. Kapβs interact with FG Nups, which allows them to move through the NPC with their cargo proteins. Several Kapβs require specific Nups to be present at the NPC in order to translocate through the NPC. Interaction studies revealed that Kapβ2 interacts with Nup98 (Fontoura, Blobel et al. 2000); Kapβ1 interacts with Nup153 (Chen and Xu 2010); and Imp8 interacts with Nup93 and Nup358 (Chen and Xu 2010). Reduced Nup53 levels at the NPC during interphase blocks Kap121-mediated import (Makhnevych, Lusk et al. 2003). Nup214 is required for U1 snRNP import but not cNLS import (Lott and Cingolani 2011). Nup88 knockout in *Drosophila* does not affect mRNA export or cNLS-mediated import but blocks the import of a subset of nuclear proteins (Uv, Roth et al. 2000). In *Drosophila* S2 cells, Nups 75, 93, 205, and 50 and Sec 13 are required for SMAD transport; however, depletion of these Nups does not affect cNLS import. Conversely, depletion of Nup54 decreased cNLS import but did not affect SMAD transport (Chen and Xu 2010). Individual Kapβs' specific Nup requirements have prompted the hypothesis that distinct transport routes through the NPC exist (Tran and Wente 2006). Eleven of the 19 mammalian Kapβs can facilitate nuclear import (Chook and Suel 2011). Of the import-mediating Kapβs, KapB1 and KapB2 recognize well-defined motifs and transport many verified cargos. Less is known about the other members of the Kapβ family.

Kapβ1 primarily recognizes protein and RNA cargos through adaptor proteins. As a heterodimer, Kapβ1 and Snurportin1 bind the m3G cap of snRNPs (Huber, Cronshagen et al. 1998). The complex of Kapβ1 and a Kapα recognize the classical NLS (cNLS). The first NLS identified, the cNLS motif, is a short stretch of basic amino acids (Kalderon, Richardson et al. 1984). Multiple variations of the motif exist, including mono partite, a series of seven basic amino acids (Kalderon, Richardson et al. 1984), and bipartite, eight

basic amino acids separated by a linker (Robbins, Dilworth et al. 1991); the length of the linker determines the affinity of the motif for Kapα (Lange, McLane et al. 2010). Each variation has differing affinity for the many different Kapαs (reviewed in (Marfori, Mynott et al. 2011)). In addition to the cargos that are bound by Kapβ1 as a heterodimer with an adaptor protein, many proteins are bound directly by Kapβ1 without an adaptor protein. These cargos do not contain a cNLS and bind to several other binding sites on Kapβ1 distinct from the sites where Snurportin and Kapαs bind. Some cargos which bind directly to Kapβ1 include parathyroid related protein (PTHrP), histones, Smads, and ribosomal proteins (Chook and Suel 2011).

Kapβ2 recognizes and binds the PY-NLS. Unlike the cNLS, the PY-NLS is longer, with 15–30 amino acids, and more complex (Lee, Cansizoglu et al. 2006). Because of the complexity of the PY-NLS, a diverse set of sequences all contain the motif. PY-NLS-containing proteins include the mRNA binding progeins FUS, HuR, and many of the hnRNPs. Like Kapβ1, which transports cargos lacking the cNLS, Kapβ2 also transports cargos lacking the PY-NLS. These cargos bind to sites distinct from those where the PY-NLS is bound (Jakel and Gorlich 1998).

The NLS recognized by Kapβ3 is as yet incompletely defined. Many of the identified cargo proteins bind to multiple Kapβs and thus have redundant import pathways (Chook and Suel 2011). Several cargos, including Nup53 (Soniat, Cagatay et al. 2016), appear to be specifically imported by Kapβ3. Based on import studies in yeast Kapβ3 imports cargos more slowly than other NTRs and is likely involved in transporting cargos with more regulated localization (Timney, Tetenbaum-Novatt et al. 2006).

In conclusion, cargos entering and leaving the nucleus require NTRs to facilitate nuclear transport. NTRs bind to a NLS or NES in the cargo protein. Distinct NLSs or NESs are recognized and bound by each NTR. The best characterized NLS is the cNLS which is bound by the complex of a Kapα and Kapβ1. Non-cNLSs can be bound by Kapβ1 without Kapα or by another Kapβ. Many cargo proteins have redundant nuclear import pathways, so care is required when choosing NLSs to examine specific nuclear import pathways.

1.3 Multinucleated cells

Multinucleated cells feature multiple nuclei all sharing a common cytoplasm. This arrangement presents unique challenges and capabilities not encountered by mononucleated cells. Nuclear position in a cell, nuclear content, and nuclear activity must be regulated for each nucleus. Having multiple nuclei allows the possibility for each of these factors to be regulated differently in each nucleus and in many multinucleated cells at least one nuclear characteristic is differentially regulated. Examining the mechanisms by which nuclei are independently regulated in a specific type of multinucleated cell can inform understanding of potential mechanisms at work independently regulating individual nuclei in other multinucleated cells.

Multinucleated cells can form by mitosis uncoupled from cytokinesis (Orias, Cervantes et al. 2011) or by fusion of post-mitotic cells (Gupta, Athanikar et al. 2014) (Huppertz and Gauster 2011). Nuclei sharing a common cytoplasm can differ from one another morphologically (Couteaux and Pecot-Dechavassine 1973, Bruusgaard, Liestøl et al. 2003, Rosser and Bandman 2003, Iwamoto, Mori et al. 2009), compositionally (Etxebeste, Ni et al. 2008, Iwamoto, Mori et al. 2009), and functionally (Fontaine and

Changeux 1989, Jasmin, Lee et al. 1993, Ellery, Cindrova-Davies et al. 2009, Youn, Takada et al. 2010). These differences among nuclei can be ascribed to differences in NPC composition (Iwamoto, Mori et al. 2009), nuclear position and relation to other nuclei (Anderson, Eser et al. 2013), concentration of cytoplasmic factors (Illmensee and Mahowald 1974, Anderson and Nusslein-Volhard 1984, Schupbach and Wieschaus 1986), and age of the nucleus (Heazell, Moll et al. 2007, Mayhew 2014). While these factors affect nuclear behavior in a common cytoplasm, other variables affecting nuclear position, nuclear division, chromatin arrangement, and gene expression in multinucleated cells contribute and remain undiscovered. Below, we will discuss some examples of multinucleated cells found in both single celled and multicellular organisms.

1.3.1 Multinucleated single-celled organisms

Single-celled eukaryotes are a broad, diverse group. Several classes of single-celled organisms are multinucleated. Examining the complexity of regulating multiple nuclei without the added complexity of a cell's interaction with its neighbors has been a valuable tool in understanding the basic biology of nuclear function and mechanisms of selectively modulating individual nuclei within a single cell.

1.3.1.1 Cillates

Cilliates form a class of Protists that are free living, ciliated, single celled organisms. Ciliates are binucleated, containing two nuclei that are distinct both morphologically and functionally. The smaller micronucleus is the germline nucleus, while the larger macronucleus is the somatic nucleus. The macronucleus is polyploid, containing many mini-chromosomes that independently replicate. Gene expression during vegetative

growth is regulated from the macronucleus. The micronucleus is relatively inactive during vegetative growth but is responsible for sexual reproduction and, after reproduction, gives rise to a new macronucleus (reviewed in (Orias, Cervantes et al. 2011)).

The best characterized Ciliate is *Tetrahymena thermophila*, which has been extensively used as a model organism to investigate nuclear functions. In *T. thermophila,* different cargo proteins are transported to the micro and macro nuclei. This is achieved by nucleus-specific Nup incorporation. The NPCs of the micro and macro nuclei share the same overall architecture and the core structural Nups. However, distinct isoforms of other Nups are specifically incorporated into NPCs of each nucleus; this allows distinct Kapα homologs to be targeted to the micro and macro nucleus (Malone, Falkowska et al. 2008, Iwamoto, Mori et al. 2009). By mislocalizing nucleus-specific Nups to the wrong nucleus, the localization of cargo proteins can be reversed (Iwamoto, Mori et al. 2009). Thus, *Tetrahymena*, and possibly all ciliates, achieve differences among nuclei in a single cytoplasm by regulating the composition of NPCs in each nucleus.

1.3.1.2 Slime molds

Multiple species of syncital fungi have been identified; the nuclear activity of five have been studied: *Neuropora crassa, Ashbya gossypii, Ceratocystis fagacearum, Fusarium oxysporum,* and *Aspergillus nidulans.* These fungi grow from germinated spores. As they grow, the nucleus divides and both daughter nuclei remain in the common cytoplasm. Large fungi can accumulate hundreds of nuclei. The nuclei of *C. fagacearum* all undergo mitosis together. In *F. oxisporum* and *A. nidulans*, coordinated waves of nuclear division sweep through the cell. In contrast, *N. crassa* and *A. gossypii* nuclei progress through the cell cycle independently of one another (Gladfelter, Hungerbuehler et

al. 2006). Nuclei as close as 1–2 μm can be in different mitotic stages (Gladfelter, Hungerbuehler et al. 2006). These differences in nuclear activity are not due to different cellular domains, because nuclei are mobile and move through different regions of the cells (Anderson, Eser et al. 2013). Neither can they be attributed to differences in subcellular cyclin localization, because the concentration of cyclins does not vary among nuclei, despite being in different stages of mitosis (Gladfelter, Hungerbuehler et al. 2006). Two properties that contribute to asynchronous division are nuclear spacing and lineal relation to other nuclei. Nuclear spacing increases before mitosis; artificially decreasing nuclear spacing increases synchronicity of nuclear division (Anderson, Eser et al. 2013). Tracking the lag times between nuclear divisions revealed that the two daughter nuclei of a single nuclear division had more similar lag times between divisions than the lag times of other nuclei. This similarity in time to nuclear division in daughter nuclei perdured regardless of their position in the cell (Anderson, Eser et al. 2013). Nuclear transport receptors distribute evenly among nuclei (Markina-Inarrairaegui, Etxebeste et al. 2011), but some transcription factors are selectively targeted to a subset of nuclei located at the apex of the cell (Etxebeste, Ni et al. 2008). Thus, multiple mechanisms likely regulate differences among nuclei in syncytial fungi.

1.3.2 Multinucleated cells in multicellular organisms

Most cells in multicellular organisms are mononucleated, and multinucleated cells are the exception. However, specific cell types are multinucleated. Multinucleation in multicellular organisms can result from mitosis uncoupled from cytokinesis, as is found in single-celled organisms. Additionally, multinucleated cells can arise from fusion of

mononucleated progenitor cells. What advantage multinucleation provides is unknown. One explanation is that polyploidyization helps increases metabolic output capacity and is capable of maintaining larger cells (Ravid, Lu et al. 2002). Subcompartmentalization into individual nuclei could facilitate regular distribution of gene expression throughout large cells or provide a mechanism to differentially regulate gene expression among nuclei.

1.3.2.1 *Drosophila* embryo

The *Drosophila* syncytial blastoderm is formed by uncoupled mitosis of the early *Drosophila* zygote. The nucleus of a fertilized egg divides many times without undergoing cytokinesis until there are 256 nuclei. These nuclei migrate to the periphery of the egg, forming the syncytial blastoderm. The nuclei of the blastoderm continue to divide until there are approximately 6,000 nuclei present in a common cytoplasm. At this point, nuclei are encompassed by plasma membrane and the cellular blastoderm is formed surrounding the yolk sac (Mavrakis, Rikhy et al. 2009). While the nuclei all divide in synchrony, they remain independent of each other in several important ways. First, the nuclei for the germline cells are specified and remain distinct from somatic nuclei during the syncytial blastoderm phase (Illmensee and Mahowald 1974). Second, gene expression differs among nuclei (Lehmann and Nüsslein-Volhard 1986). Third, each nucleus is equipped with an endoplasmic reticulum and a Golgi apparatus with minimal exchange between the trafficking systems of neighboring nuclei (Frescas, Mavrakis et al. 2006). Fourth, prior to cellularization of the syncytia, the plasma membrane near each nucleus is polarized, in some cases differently from the neighboring section of membrane, in preparation to become apical, basolateral, or junctional (Mavrakis, Rikhy et al. 2009). These differences among nuclei are largely due to the subcellular concentration of maternally loaded mRNA

(Illmensee and Mahowald 1974, Anderson and Nusslein-Volhard 1984, Schupbach and Wieschaus 1986). In summary, nuclei in the *Drosophila* syncytial blastoderm divide synchronously but independently regulate gene expression and protein trafficking. The differences among these nuclei result from differences in the cytoplasm surrounding the nuclei.

1.3.2.2 Macrophage derived giant multinucleated cells

Macrophages are immune cells that recognize and engulf invading pathogens. Under certain circumstances macrophages can fuse to form specialized cells to battle serious infection or maintain bone and calcium homeostasis.

Multinucleated giant cells (MGC) are very large multinucleated immune cells that form in response to unusual immunological stress. Granulomatous conditions like tuberculosis (Williams and Williams 1983, Sakai, Okafuji et al. 2012) or HIV (Dargent, Lespagnard et al. 2000), embedded foreign material (Anderson, Rodriguez et al. 2008), and fat necrosis can all induce formation of histologically distinct varieties of macrophage-derived MGC (Gupta, Athanikar et al. 2014). These cells can contain between two and two hundred nuclei (Mariano and Spector 1974). While the stimulus for fusion and histology of the MGC differs, in each case the basic function of the cells is to isolate large particles of what is recognized as foreign matter in a tissue that cannot be broken down (McNally and Anderson 2011). Whether multinucleation is an adaptive response or simply a marker of pathology is unknown. It is also unclear if the nuclei function independently or synchronously.

Osteoclasts are multinucleated cells formed by fusion of macrophages responsible for bone resorption. Most osteoclasts contain around 20 nuclei, and nuclear number

correlates with resorption pit size (Youn, Takada et al. 2010). Unlike most of the other multinucleated cells in multinucleated organisms, which can persist in some cases for decades, osteoclasts are relatively short-lived with the average half-life of 14.4 hours (Kawaguchi, Manabe et al. 1999). Nuclei in a single osteoclast can differ in chromatin arrangement, protein content, and production of osteoclast-specific transcripts (Youn, Takada et al. 2010). The driving mechanism for these differences among nuclei is unknown, and no differences in steroid receptor localization, global transcription, or global nuclear import have been detected (Boissy, Saltel et al. 2002, Youn, Takada et al. 2010).

1.3.2.3 Syncytiotrophoblast

The placenta is made up of the embryonic chorion and maternal decidua basalis. There are three main layers of the chorion: the extraembryonic mesoderm contains the blood vessels that supply the developing embryo, and the cytotrophoblast and syncytiotrophoblast drive invasion of the endometrium and myometrium, securing access to maternal oxygen and nutrients. The syncytiotrophoblast forms by fusion of terminally differentiated cytotrophoblast cells (Huppertz and Gauster 2011). Nuclei within the syncytiotrophoblast differ in transcriptional activity and chromatin organization. Assaying several markers of transcriptional activity revealed variation among nuclei, including some nuclei that were negative for all markers examined (Ellery, Cindrova-Davies et al. 2009). Similarly, nuclei differed in chromatin organization: some nuclei have open chromatin while others have high levels of heterochromatin (Fogarty, Ferguson-Smith et al. , Ellery, Cindrova-Davies et al. 2009). High levels of clustered nuclei with dense chromatin is associated with prenatal pathologies, including eclampsia (Mayhew 2014). These clusters of nuclei are exacerbated by hypoxia (Heazell, Moll et al. 2007). Nuclei with dense

chromatin tended to be those with no detectable transcriptional activity. These nuclei could be older defunct nuclei or condensed chromatin, and lack of transcription could be markers of dead or dying nuclei.

1.3.2.4 Cardiomyocytes

Cardiomyocytes are the contractile cells of the heart. They rhythmically contract and communicate rapidly with neighboring cells through gap junctions. Cardiomyocytes can be polyploid and multinucleated. In humans, 30–60% of cardiomyocytes are binucleated, and virtually all are tetraploid or more (Walsh, Ponten et al. 2010). The current model of cardiac development states that the human cardiomyocytes proliferate in fetal development, but that within the first few neonatal weeks cytokinesis is inhibited in cardiomyocytes. As the heart continues to grow through the first 10 years of life, cardiomyocytes increase in ploidy, with or without nuclear division. While very low levels of cardiomyocyte generation persist into adulthood, almost all new myocyte nuclei are produced by endoreplication (Bergmann, Bhardwaj et al. 2009). Stress associated with aging or hypertension results in increased ploidy or multinucleation of cardiomyocytes (Soonpaa and Field 1998, Schipke, Banmann et al. 2014), which can be partially reversed by reducing the load on the heart (Wohlschlaeger, Levkau et al. 2010). Differences among nuclei in cardiomyocytes have yet to be studied.

1.3.2.5 Hepatocytes

In mammalian neonates, all hepatocytes are diploid. As the organism develops, an increasing proportion of hepatocytes are polyploid. In the healthy adult human liver, 30–50% of hepatocytes are polyploid (Kudryavtsev, Kudryavtseva et al. 1993, Seglen 1997); in adult rats 90% of hepatocytes are (Nadal and Zajdela 1967, Saeter, Schwarze et al. 1988).

Polyploid hepatocytes can be mononucleated or multinucleated. In healthy liver, binucleated hepatocytes form by incomplete cytokinesis. Interestingly, these binucleate hepatocytes can progress through the cell cycle and divide normally, giving rise to two mononucleated 4n daughter cells (Guidotti, Bregerie et al. 2003). Chronic active hepatitis or ingestion of toxic substances induces widespread increase of hepatocytes with 3 or more nuclei (Richey, Rogers et al. 1977, Scampini, Nava et al. 1993). Nuclei in multinucleated hepatocytes are morphologically similar to each other and to nuclei in surrounding mononucleated hepatocytes (Scampini, Nava et al. 1993). However, nuclei within the same hepatocyte can be in different phases of the cell cycle replicating and dividing independently of each other (Shalakhmetova, Umbayev et al. 2009). The mechanisms regulating this independent replication of nuclei within a single cell are unknown.

1.3.2.6 Skeletal muscle

As described above, myofibers are formed by fusion of mononucleated precursor cells. Nuclei in specialized regions differ from nuclei in the contractile body of a myofiber both functionally and morphologically. Nuclei located at the neuromuscular junction and at the myotendonous junction are more tightly clustered than nuclei elsewhere in the myofiber (Couteaux and Pecot-Dechavassine 1973, Bruusgaard, Liestøl et al. 2003, Rosser and Bandman 2003). Myotendonous junction nuclei produce more transcripts for sarcomeric proteins than other myonuclei (Dix and Eisenberg 1990). Nuclei at the neuromuscular junction produce transcripts, including N-CAM, 43k-rapsyn, S-laminin (Moscoso, Chu et al. 1995), acetylcholine esterase (Jasmin, Lee et al. 1993), acetylcholine receptor subunits α (Fontaine and Changeux 1989), and ε (Brenner, Witzemann et al.

1990), which are produced by no other myonuclei. This specialization of nuclei in specialized regions of a myofiber reflects the distinct needs of these regions.

In addition to differences between nuclei located in specialized regions and nuclei in the body of a myofiber, non-specialized nuclei differ in gene expression and accumulation of nuclear proteins. Some but not all nuclei in a single multinucleated muscle cell accumulate NFATc1 (Abbott, Friday et al. 1998), NFAT5 (O'Connor, Mills et al. 2007), myogenin (Ishido, Kami et al. 2004, Ferri, Barbieri et al. 2009), MyoD (Ishido, Kami et al. 2004, Yamamoto, Csikasz et al. 2008), Myo18B (Salamon, Millino et al. 2003), or myostatin (McPherron, Lawler et al. 1997, Artaza, Bhasin et al. 2002). Similarly, some but not all nuclei within a muscle cell produce α skeletal actin, troponin 1 slow (Newlands, Levitt et al. 1998), or myostatin (Artaza, Bhasin et al. 2002). What role these differences among nuclei play in myofiber biology remains unclear. Differences among nuclei have been characterized for more than 30 years; the mechanisms regulating these differences remain unknown.

1.3.2.7 Abnormal cells

Even cells that under normal circumstances are mononucleated can become multinucleated under sufficient stress. For example, prolonged hypertension or repeated insult induces multinucleation in vascular smooth muscle cells (Hixon, Obejero-Paz et al. 2000). Multiple cell types in an undescended testis are multinucleated (Bianchi, Boekelheide et al. 2017). Epithelial cells are multinucleated in several types of dermatosis and herpes infection (Cohen, Paravar et al. 2014). A hallmark of cancer cells is abnormal morphology. Fusion (Calderaro, Couchy et al. 2017) and mitosis without cytokinesis (Ariizumi, Ogose et al. 2009) can both give rise to multinucleated cancer cells, both in

disease progression and as a side effect of treatment. Various types of cancer exhibit abnormal multinucleated cells: hepatic (Calderaro, Couchy et al. 2017), bone (Divisato, di Carlo et al. 2017), bladder (Nawar, Olsen et al. 2016), breast (Cozzolino, Ciancia et al. 2014, Trichia, Ignatova et al. 2016), and colon (Wu, Ji et al. 2013). Treatment of cancer cells with ionizing radiation induces formation of multinucleated cancer cells from a small percentage of the population (Puck and Marcus 1955, Puck and Marcus 1956). Multinucleated cancer cells can give rise to mononucleated daughter cells contributing to cancer relapse (Vitale, Senovilla et al. 2010, Erenpreisa, Salmina et al. 2011, Weihua, Lin et al. 2011, Kaur, Rajendra et al. 2015). Although many cell types can become multinucleated in response to extreme stress or infection, these states likely represent a pathological response indicative of failure of normal cellular processes rather than a physiological response to productively respond to the environmental insult.

1.4 Summary

Skeletal muscle is a highly specialized tissue necessary for critical functions including locomotion, swallowing, and respiration. The primary cell type in muscle tissue is myofibers, which are unique among a body's cells in that they are long lived, multinucleated cells, that form by fusion in the absence of injury or infection. Maintaining muscle function relies on proper gene expression throughout a myofiber. This fundamental process is complicated by the thousands of nuclei sharing a common cytoplasm in a single skeletal muscle fiber. Nuclei within the same cell can differ in gene expression and protein accumulation. If they differ in other ways and how differences among individual nuclei are established was unknown. One potential regulatory mechanism is modulation of nuclear

transport. In Chapter 2, I will present our findings that activity of nuclear import pathways and rates of cNLS nuclear import vary among nuclei a single skeletal muscle cell. This variation correlates with differentiation state, position in a cell, and injury. The heterogeneity of nuclear import among nuclei and the responsiveness to multiple stimuli suggest that nuclear import could play a role in establishing or maintaining differences among myonuclei.

Failure to maintain skeletal muscle function results in loss of fitness and increased frailty. In aging, muscle strength is reduced; this functional decline is accompanied by transcriptomic and proteomic changes. The causative force driving these changes has not been determined. One contributing factor could be age-specific changes in the nuclear proteome leading to altered gene expression. However, because sarcomeric and metabolic proteins are highly abundant in skeletal muscle tissue, signal from the much lower abundance nuclear proteins is eclipsed rendering them undetectable from whole muscle tissue. Unfortunately, nuclei are difficult to isolate from muscle tissue and there was no existing method to satisfactorily purify myonuclei. In Chapter 3, I will present a method that I optimized to selectively isolate myonuclei from skeletal muscle tissue. I apply this purification method to detect age-specific differences between the myonuclear proteomes of young and old muscle.

In Chapter 4, I will examine the implications of the findings presented in Chapters 2 and 3 as well as future directions toward understanding the regulation of individual nuclei in multinucleated muscle cells. Differences in nuclear import among nuclei provides the foundation for examining the mechanisms governing differences among individual nuclei. The method to isolate myonuclei lays the technical ground work for investigating

individual nuclei. Defining the biochemical and signaling mechanisms differentiating individual nuclei and the consequences of these differences will require development of new reagents to selectively label nuclei and modifications of interest and techniques with the resolution to examine multiple parameters on the level of single nuclei. These advances should be pursued because the findings will elucidate a basic process of skeletal muscle biology, inform understanding of other multinucleated cells, and could unveil potential therapeutic targets to treat sarcopenia and osteoporosis.

1.5 Figures

Figure 1.1: Cellular composition of skeletal muscle. Skeletal muscle is composed of many different cells types. Nuclear number estimates are based on abundance of mononucleated cell types measured by flow cytometry (Joe, Yi et al. 2010) and the abundance of satellite cell nuclei in muscle sections (Shi and Garry 2006).

Figure 1.2: Myogenesis. A During embryonic myogenesis, a primary wave of myoblasts differentiates into primary myofibers. Later, a second wave of myoblasts differentiates and fuses to form secondary myofibers. During fetal and juvenile development, myofibers hypertrophy and mature. **B** When myofibers are injured regeneration restores the damaged muscle tissue. First, the damaged myofiber is cleared by macrophages. Satellite cells activate and proliferate. These newly generated myoblasts differentiate and fuse either into the remaining myofiber or with each other. The resulting regenerated myofiber may have centrally located nuclei and branches. **C** Myogenesis can be modeled *in vitro.* Cultured myoblasts differentiate upon serum deprivation. Differentiated myocytes fuse to form large multinucleated myotubes.

Figure 1.3: Nuclear transport. A Nuclear import depends on nuclear transport receptors (NTR) binding to a nuclear localization sequence (NLS) in a cargo protein. Together, the complex transports through the nuclear pore complex. Multiple NLSs exist each of which is recognized and bound by a distinct NTR. Once inside the nucleus the NTR-cargo protein complex is dissociated by binding of RanGTP. **B** The NTR-RanGTP complex can bind

nuclear export signals in cargo proteins or mRNA caps. The complex of NTR-RanGTP and cargo moves through the nuclear pore to the cytoplasm. Interaction with RanGAP located on the cytoplasmic face of the nuclear pore induces hydrolysis of GTP and a subsequent conformational change releasing the cargo and NTR from RanGDP. **C** RanGDP is imported back into the nucleus by NTF2. Once in the nucleus, GDP is exchanged for GTP regenerating RanGTP.

Figure 1.1

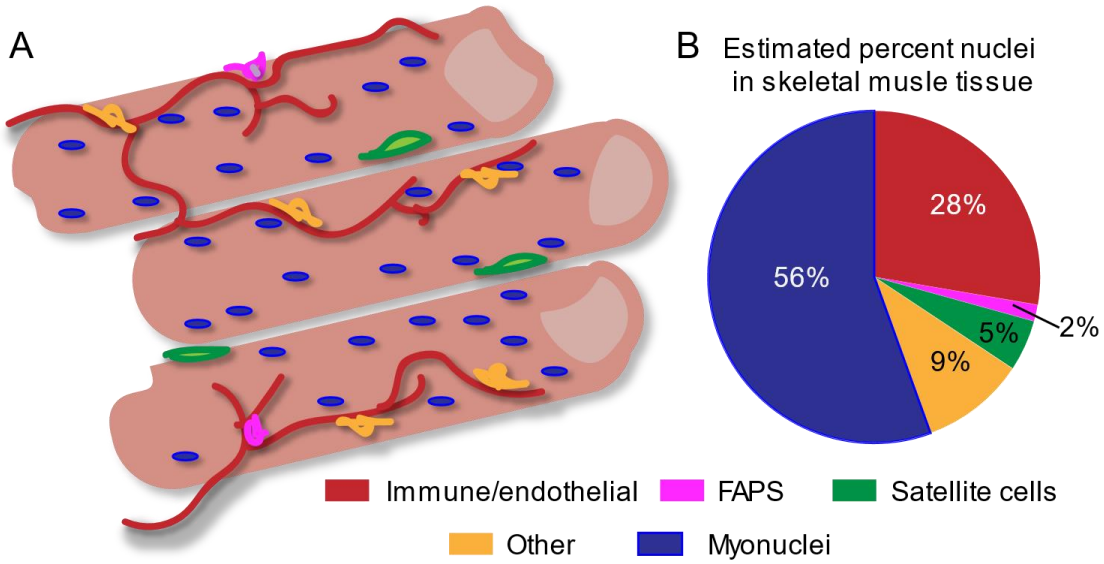
A
B
Estimated percent nuclei
in skeletal musle tissue
28%
2%
5%
9%
56%
Immune/endothelial
FAPS
Satellite cells
Other
Myonuclei

Figure 1.2

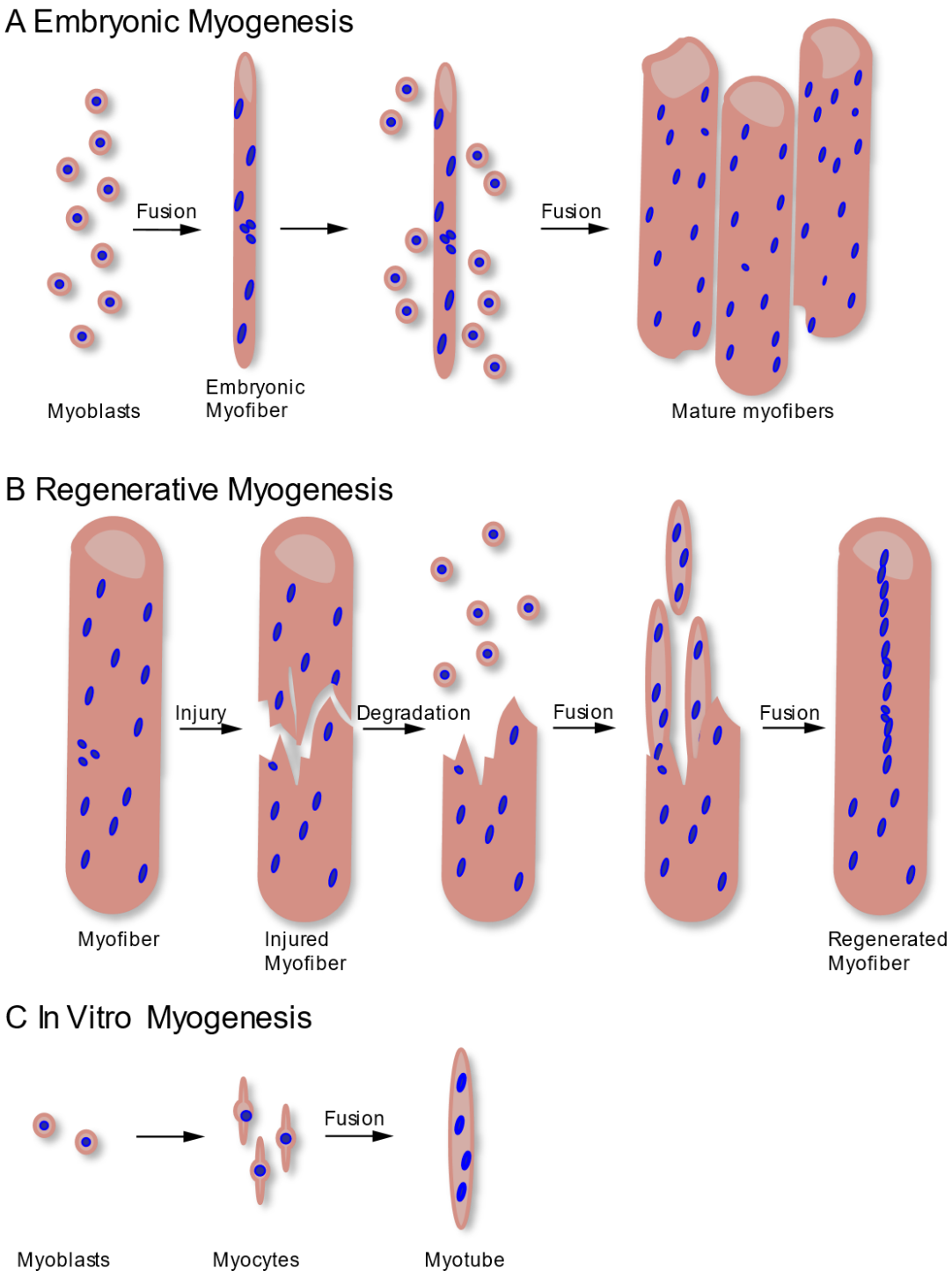
A Embryonic Myogenesis
Fusion
Fusion
Myoblasts
Embryonic Myofiber
Mature myofibers
B Regenerative Myogenesis
Injury
Degradation
Fusion
Fusion
Myofiber
Injured Myofiber
Regenerated Myofiber
C In Vitro Myogenesis
Fusion
Myoblasts
Myocytes
Myotube

Figure 1.3

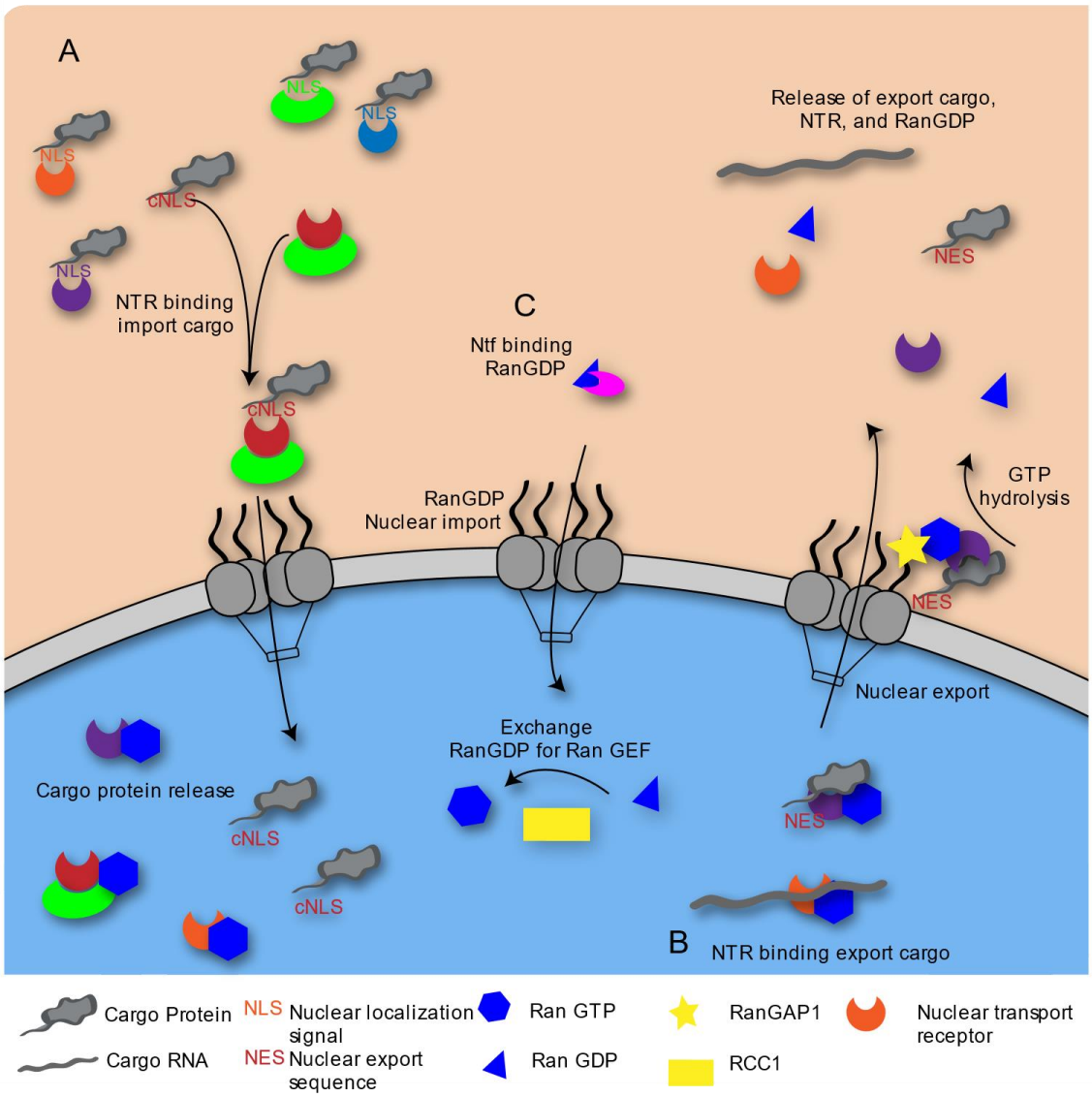
A
NLS
NLS
NLS
NLS
cNLS
NTR binding
import cargo
cNLS
C
Ntf binding
RanGDP
RanGDP
Nuclear import
Release of export cargo,
NTR, and RanGDP
NES
GTP
hydrolysis
NES
Nuclear export
Exchange
RanGDP for Ran GEF
Cargo protein release
cNLS
cNLS
NES
B
NTR binding export cargo
Cargo Protein
Cargo RNA
NLS Nuclear localization signal
NES Nuclear export sequence
Ran GTP
Ran GDP
RanGAP1
RCC1
Nuclear transport receptor

Chapter 2: Non-equivalence of nuclear import among nuclei in multinucleated skeletal muscle cells

A portion of this chapter has been submitted to Journal of Cell Science and is under revision:

Cutler, A.A., J.B Jackson, A.H. Corbett, G.K. Pavlath, *Non-equivalence of nuclear import among nuclei in multinucleated skeletal muscle cells.*

Jennifer Jackson contributed the initial data acquisition for Figure 2.1E.

Chapter 2: Non-equivalence of nuclear import among nuclei in multinucleated skeletal muscle cells

2.1 Summary

Skeletal muscle is primarily composed of large myofibers containing thousands of post-mitotic nuclei distributed throughout a common cytoplasm. Protein production and localization in specialized myofiber regions is critical for muscle function. Myonuclei differ in transcriptional activity and protein accumulation but how these differences among nuclei sharing a cytoplasm are achieved is unknown. Regulated nuclear import of proteins is one potential mechanism to spatially and temporally regulate transcription in individual myonuclei. The best characterized nuclear localization signal (NLS) in proteins is the classical NLS (cNLS) but many other NLS motifs exist. We examined cNLS and non-cNLS reporter protein import using in vitro generated multinucleated muscle cells, revealing that cNLS and non-cNLS nuclear import differs among nuclei in the same cell. Investigation of cNLS nuclear import rates in isolated myofibers ex vivo confirmed differences in nuclear import rates among myonuclei. Analyzing nuclear import throughout myogenesis revealed that cNLS and non-cNLS import vary during differentiation. Together, our results suggest that spatial and temporal regulation of nuclear import pathways may be important in muscle cell differentiation and protein regionalization in myofibers.

2.2 Introduction

Skeletal muscle is critical for survival and quality of life as it is required for respiration, ingestion, and locomotion. The primary cell type of skeletal muscle is the myofiber, which is a very large, long-lived contractile cell containing thousands of post-mitotic nuclei. Myofibers are initially formed by fusion of differentiated precursor cells during embryogenesis. Additional muscle precursor cells continue to fuse as the muscle grows and matures. In the event of muscle injury, resident stem cells proliferate, differentiate and fuse with myofibers leading to regeneration in the area of injury. The process of differentiation and fusion has been well modeled *in vitro* and results in the formation of multinucleated muscle cells called myotubes. How gene expression is coordinated among multiple nuclei in myofibers to produce proteins necessary to maintain proper muscle function remains an open question.

A single myofiber can extend the entire length of a muscle and has three distinct regions: the myotendinous junction (MTJ) on either each end of the myofiber which anchors the myofiber to the tendon; the body of the myofiber which is primarily responsible for contraction; and the neuromuscular junction (NMJ) where a motor neuron synapses onto the myofiber. Each of these regions requires certain proteins to function properly. Although they exist in a common cytoplasm, nuclei in the specialized regions of the NMJ and the MTJ differ from other nuclei in the myofiber. Nuclei close to the MTJ are more tightly packed than elsewhere in the myofiber (Bruusgaard et al., 2003, Rosser and Bandman, 2003). When a muscle is stressed by stretching, nuclei at the MTJ increase production of myosin heavy chain (Dix and Eisenberg, 1990), one of the major components of the contractile sarcomere. The 3-8 nuclei at the NMJ are also tightly clustered and are

larger and rounder than other nuclei in the myofiber (Couteaux and Pecot-Dechavassine, 1973). In addition to morphological differences, some proteins are selectively associated with NMJ nuclei, such as Syne-1, a component of the LINC complex which connects the nuclear lamina to the cytoskeleton (Apel et al., 2000). Additionally, some transcripts including N-CAM, 43k-rapsyn, S-laminin (Moscoso et al., 1995), acetylcholine esterase (Jasmin et al., 1993), acetylcholine receptor subunits α (Fontaine and Changeux, 1989), and ε (Brenner et al., 1990), are produced exclusively or preferentially by NMJ nuclei while transcripts for actin and myosin, some of the most highly expressed proteins in myofibers, are seldom produced by NMJ nuclei (Moscoso et al., 1995). While these differences between nuclei in specialized regions and other nuclei have been well described, how these nuclei are distinguished from other nuclei within the syncytia is unknown.

While the differences between specialized and non-specialized nuclei have been well established, nuclei in non-specialized regions also differ from one another in protein accumulation and gene expression. Differences among nuclei in single muscle cells have been detected both *in vivo* and *in vitro.* Some but not all nuclei in a single multinucleated muscle cell accumulate NFATc1 (Abbott et al., 1998), NFAT5 (O'Connor et al., 2007), myogenin (Ferri et al., 2009, Ishido et al., 2004), MyoD (Ishido et al., 2004, Yamamoto et al., 2008), Myo18B (Salamon et al., 2003) or myostatin (McPherron et al., 1997, Artaza et al., 2002). Additionally, within a single myofiber some nuclei accumulate EndoG, an apoptosis associated endonuclease, and undergo DNA fragmentation in response to muscle atrophy while others do not (Dupont-Versteegden et al., 2006). Similarly, some but not all nuclei within a muscle cell produce α skeletal actin, troponin 1 slow (Newlands et al., 1998), or myostatin (Artaza et al., 2002). This compartmentalization of gene expression

likely allows for regional production of proteins necessary for proper muscle cell function. Despite the functional significance of this nonequivalence among myonuclei in multinucleated muscle cells both *in vivo* and *in vitro*, the molecular mechanisms governing differential protein localization and regulation of gene expression are unknown.

One mechanism that could dictate accumulation of proteins in some nuclei but not others in multinucleated muscle cells is regulated nuclear import. The nucleus is compartmentalized from the cytoplasm by the nuclear envelope which contains nuclear pore complexes (NPC) that mediate movement of molecules between the nuclear and cytoplasmic compartments. Small molecules and ions can freely diffuse through NPCs while proteins larger than 40 kDa must be bound by nuclear transport receptors to traverse the NPC. Nuclear transport receptors bind to a nuclear localization signal (NLS) within a cargo protein and mediate the movement of the cargo through the NPC. Once in the nucleus, a small GTPase, RanGTP, binds to the nuclear transport receptor triggering a conformational change that release the cargo inside the nucleus. The nuclear transport receptor bound by RanGTP is recycled to the cytoplasm where RanGTP is converted to RanGDP releasing the nuclear transport receptor. The nuclear transport receptor is then free to import a new cargo protein. The directionality of nuclear transport is maintained by localizing the Ran guanine nuclear exchange factor, RCC1, to the nucleus and the Ran GTPase activating proteins to the cytoplasm (Tran et al., 2014, Chook and Süel, 2011). Nuclear transport maintains privileged access of proteins to the nuclear compartment protecting the genome and facilitating gene regulation.

A number of distinct NLS sequences within cargo proteins have been characterized. The most common NLS is the classical nuclear localization signal (cNLS). Proteins

containing a cNLS are imported to the nucleus by the nuclear transport receptor heterodimer comprised of importin α and importin β. Importin α recognizes and binds to the cNLS in the cargo protein and acts as an adapter for importin β binding. Importin β mediates translocation of the complex through the NPC. While the cNLS is the most common NLS, many proteins contain non-classical NLSs (non-cNLS) whose import is mediated by direct binding to a nuclear transport receptor from the importin β superfamily. These nuclear transport receptors do not require an importin α adapter but rather directly bind the non-cNLS in the cargo protein and facilitate movement through the NPC. With the exception of the PY-NLS, which is recognized and imported by the nuclear transport receptor transportin, few of the non-cNLSs have been convincingly characterized to have a conserved motif or bind directly to specific, non-redundant nuclear transport receptors. Understanding of these less characterized non-cNLS import pathways is currently based on studies of individual protein cargoes. The diversity of NLSs could provide for specialization of the nuclear transport system for classes of cargo proteins.

Multinucleated muscle cells present an intriguing biological system; many nuclei all sharing the same common cytoplasm nonetheless behave differently. We investigated nuclear import as a potential mechanism of achieving differences in nuclear activity. Here we present our findings of differences in nuclear import among myonuclei within the same skeletal muscle cell. Using an *in vitro* import assay, we show that nuclei in myotubes *in vitro* differ from one another in the activity of classical and non-classical nuclear import pathways. The activity of these nuclear import pathways also varied at different stages of myogenesis. We further identified differences in the rates of nuclear transport among nuclei in myofibers *ex vivo* by using fluorescence recovery after photobleaching (FRAP). These

findings highlight the remarkable variability of nuclei within the same muscle cell, exposed to the same cytoplasmic factors and identify a potential mechanism for achieving diversity in protein accumulation and nuclear activity among myonuclei within a single muscle cell.

2.3 Results

2.3.1 Nuclear import varies among nuclei within single cultured multinucleated myotubes

To analyze nuclear import in multinucleated myotubes, we adapted an established *in vitro* nuclear import assay (Moore and Schwoebel, 2001). Primary mouse myotubes were generated *in vitro* by inducing differentiation and fusion of precursor myoblasts. In this adaptation of the assay, illustrated in Figure 2.1A, the myotube plasma membrane was permeabilized with digitonin, which selectively extracts cholesterol, leaving the nuclear envelope intact. The cytoplasm was washed out and the permeabilized cells were incubated with an import cocktail containing reticulocyte lysate which provides soluble nuclear transport factors, an energy regenerating system, and a fluorescent nuclear import reporter containing multiple copies of a classical nuclear localization sequence (cNLS). The reporter is approximately 78 kDa, which is above the size exclusion limit of the NPC (Lénárt et al., 2003), making this cargo dependent on facilitated nuclear import to enter the nucleus. After the incubation, excess reporter was removed by washing and the cells were fixed and examined by fluorescence microscopy. Because the cell cytoplasm has been removed, this assay specifically assesses intrinsic differences among nuclei in import of the fluorescent nuclear import reporter.

When all components of the import cocktail were present, nuclear import was readily detectable (Fig 2.1B). However, if reticulocyte lysate (lysate) or the energy

regenerating system (E) was omitted, nuclear import did not occur. These results are consistent with the requirement for nuclear transport factors and energy in the form of RanGTP for nuclear import to occur (Adam et al., 1990, Newmeyer et al., 1986). Furthermore, if the cells were treated with wheat germ agglutinin (WGA), which binds to glycosylated nucleoporin (Nup) residues (Hanover et al., 1987) and thereby blocks the NPC (Finlay et al., 1987), nuclear import was abolished. When cells were incubated with the complete import cocktail at 0°C, nuclear import was also blocked consistent with the temperature dependence of nuclear import (Adam, 2016, Adam et al., 1990). Together, these results indicate that the import of the fluorescent nuclear import reporter detected by this assay is mediated by active transport proceeding through the NPC.

To analyze whether nuclear import varies among myonuclei within a single myotube, nuclear fluorescence was manually scored following the *in vitro* nuclear import assay using fluorescence microscopy. Nuclei within myotubes containing 4-17 nuclei were scored either as positive for the nuclear import reporter (cNLS-positive) or negative for the nuclear import reporter (cNLS-negative). Within single multinucleated myotubes, we observed that not all the nuclei were cNLS-positive (Fig 2.1C): 71% of myotubes contained at least one cNLS-negative nucleus. Of the 1422 nuclei analyzed in 227 myotubes with both cNLS-positive and cNLS-negative nuclei, 69% of nuclei were cNLS-positive. The number of nuclei per myofiber did not affect percent of cNLS-positive nuclei (Fig 2.7) To examine whether cNLS-negative nuclei resulted simply from completely blocked NPCs, we incubated digitonin permeabilized myotubes with fluorescent dextrans. The 70 kDa dextran is above the size exclusion limit for NPCs and so is excluded from intact nuclei; the 10 kDa dextran is below this size cut off and can freely diffuse through NPCs (Adam,

2016). We found that 94% of nuclei appropriately excluded the 70 kDa dextran and 100% of nuclei were permeable to the small 10 kDa dextran (Fig 2.1D). These results indicate that nuclei were not damaged by digitonin permeabilization and that cNLS-negative nuclei within myotubes do not result from blocked NPCs. Armed with the knowledge that this assay reliably evaluates nuclear import and that differences among nuclei in myotubes are due to intrinsic nuclear characteristics, we investigated whether there was a connection between the position of a nucleus within a myotube and nuclear import of the fluorescent reporter. We defined the two nuclei at each end of a myotube as end nuclei and the other nuclei in the myotube as middle nuclei (Fig. 2.1E). Our results indicate that cNLS-negative nucleus can be located in any position within a myotube. However, the two nuclei on either end of a myotube are cNLS-negative significantly more frequently than predicted by random distribution (Fig 2.1E).

The fluorescent import reporter used in the initial experiments contained up to 20 cNLS peptides conjugated to a single BSA protein (Fig. 2.1). This high concentration of cNLS peptides allowed us to examine the nuclear import system at saturation. However, endogenous proteins typically contain a single encoded NLS. To better model nuclear import, we used a more biologically relevant reporter containing GST, a single cNLS, and EGFP (GST-cNLS-EGFP). At 60.6 kDa, this reporter is larger than the diffusion limit of the NPC and so relies on facilitated, nuclear transport receptor-mediated import to enter the nucleus. A fluorescent reporter with a mutant cNLS which is not bound by importin α and consequently does not accumulate in the nucleus or on the nuclear envelope (Butel et al., 1969, Rapp et al., 1969) was used as a control. The import assay was performed in myotubes using the reporter with a single cNLS sequence as schematized in Figure 2.2A.

Like the reporter with the multiple cNLS peptides conjugated to BSA, some but not all nuclei were cNLS-positive (Fig 2.2B). Nuclei within myotubes containing more than 6 nuclei were visualized by fluorescence microscopy and EGFP integrated intensity measured by an automated image analysis pipeline. To establish background fluorescence, we used the peak fluorescence intensity of nuclei incubated with the mutant cNLS reporter. Nuclei within myotubes incubated with the cNLS reporter with fluorescence higher than this background were defined as cNLS-positive and those with fluorescence less than or equal to the background level were defined as cNLS-negative (Fig 2.2C). As expected, performing the *in vitro* import assay with the new reporter containing a single cNLS yielded fewer cNLS-positive nuclei (25%; n=5 independent experiments with 150 nuclei per experiment) compared to the reporter containing up to 20 cNLS peptides (Fig.1; 69% cNLS-positive). Concerned that the fluorescent reporter could be concentrated in some areas of the nucleus, we examined multiple planes of focus through nuclei. When these myotubes were examined by confocal fluorescence microscopy, we confirmed that on no plane of focus were cNLS-negative nuclei more fluorescent than those incubated with the mutant cNLS reporter (Fig 2.2D). Thus, the encoded cNLS and mutant cNLS results provide confidence that active nuclear import can be tracked in these multinucleated cells. That differences in nuclear import among nuclei are detected using two distinct reporter cargos additionally lends confidence that the differences represent actual variation in nuclear import activity among these nuclei.

Having determined that some nuclei were cNLS-negative, we hypothesized that these nuclei could be dormant or simply inactive thus we examined transcription as a marker of general nuclear activity. To analyze transcription in myotubes, cultures were

incubated with alkyne-modified 5-ethynyl uridine (EU), a uracil analog which is incorporated into newly synthesized RNA, and nuclei were subsequently visualized using chemoselective ligation of Alexa Fluor 594 azide with the EU (Fig 2.2E). Surprisingly, 95% of 680 nuclei in four independent experiments were EU-positive indicating that almost all nuclei in myotubes are transcriptionally active (Fig 2.2F) even though 75% of nuclei are cNLS-negative for the GST-cNLS-EGFP reporter. Together these results indicate that differences in cNLS nuclear import among nuclei within single myotubes are not the result of using a saturated NLS reporter or an artifact of the plane of focus. Furthermore, these results demonstrate that cNLS-negative nuclei are still transcriptionally active.

2.3.2 Independence of nuclear import pathways in cultured myotubes

Having determined that some nuclei within individual myotubes are cNLS-negative but almost all nuclei are transcriptionally active, the question naturally arose as to whether these nuclei can import proteins through other non-cNLS dependent nuclear import pathways. To address this question, fluorescent reporters for specific non-classical nuclear import pathways were required. Many proteins have poorly defined NLSs and are imported by uncharacterized or redundant nuclear transport factors. We selected NLS sequences from proteins with a well-defined NLS which were characterized to be directly bound and imported by a single specific nuclear transport receptor. We identified three such proteins for analysis: hnRNPA1, Nup53, and PTHrP (Table 2.1) and cloned each of these three non-classical NLSs (non-cNLS) into the GST-NLS-EGFP reporter used above and into a GST-NLS-mCherry reporter of comparable size (61.2 kDa and 57.3 kDa respectively). We

expressed and purified the recombinant proteins such that for the cNLS, mutant cNLS and each non-cNLS we had a EGFP and a mCherry fluorescent reporter protein. Each of these reporters differed from the others only in which NLS was included allowing us to compare different import pathways.

Using these reporters, we performed the nuclear import assay making systematic pairwise comparisons between the cNLS reporter and one of the non-cNLS reporters (Fig 2.3A). In these pairwise comparisons, the assay was always performed in duplicate with the reciprocal fluorophores. For example, given three coverslips with myotubes from the same culture, one was incubated with equal concentrations of GST-cNLS-EGFP and GST-hnRNPA1 NLS-mCherry while the other coverslip was incubated with equal concentrations of GST-hnRNPA1 NLS-EGFP and GST-cNLS-mCherry. The third coverslip was incubated with equal concentrations of the control reporters: GST-mutant cNLS-EGFP and GST-mutant cNLS-mCherry. For each pairwise comparison, some nuclei were import-positive for one, both, or neither pathway (Fig 2.3B). Nuclei were identified by fluorescence microscopy and the fluorescence intensities of the EGFP and mCherry channels were measured by an automated image analysis pipeline. The percentage of nuclei that were cNLS-positive only, cNLS and non-cNLS positive, non-cNLS-positive only, or positive for neither NLS was calculated for each reporter (Figure 2.3C).

As illustrated in Figure 2.3C, for the hnRNP NLS and cNLS reporters 54% of nuclei were negative for both reporters, 32.2% of nuclei were cNLS-positive and hnRNP NLS-negative, 7.2% of nuclei were positive for both reporters, and 6.6% of nuclei were positive for only the hnRNP NLS. In the comparison of the PthrP NLS and cNLS reporters, 70.5% of nuclei were negative for both reporters, 21.7% were cNLS-positive and PthrP-negative,

5.9% were positive for both reporters, and 0.7% were positive for only the PthrP NLS. In the comparison of Nup53 NLS and cNLS, 78% of nuclei were negative for both reporters, 14.7% were cNLS- positive and Nup53-negative, 4.8% were positive for both reporters, and 2.1% were positive for only the Nup53 NLS. These data demonstrate that individual nuclei can be positive for one, multiple, or no import pathway.

To examine the degree of independence between the cNLS and non-cNLS reporters in individual nuclei, we compared the percentage of nuclei which were only non-cNLS-positive to those which were both non-cNLS- and cNLS-positive. We found that the degree of overlap with the cNLS reporter varied for each non-cNLS reporter and that the percentage of nuclei that were positive for both the cNLS and non-cNLS reporter protein differed significantly from the percentage predicted by random distribution of active nuclear import pathways among nuclei (Fig 2.3D). The hnRNPA1 NLS and cNLS reporters overlapped the least as only 45% of hnRNPA1 NLS positive nuclei were positive for both reporters. For the Nup53-NLS and cNLS reporter pairing, 69% of Nup53 NLS-positive nuclei were also cNLS-positive. In contrast, 95% of the PTHrP NLS positive nuclei were positive for both the PTHrP NLS and cNLS reporters. The high degree of overlap with the PTHrP NLS and cNLS reporters compared to the other non-cNLS reporters is not surprising because both these NLSs rely on importin β; the cNLS additionally requires importin α (Kalderon et al., 1984) while the PTHrP-NLS is importin α independent (Cingolani et al., 2002, Lam et al., 2001). Together, these data support the conclusion that the cNLS import pathway is the predominant mode of nuclear import for myonuclei and that each import pathway can be differentially regulated in individual nuclei.

2.3.3 Variation in cNLS import among myofiber nuclei ex vivo

While cultured myotubes are large compared to other cell types *in vitro,* relative to myofibers *in vivo,* they are quite small and lack the extensive subcellular specialization found in myofibers. To examine whether nuclear import is also variable among nuclei in myofibers as well as in cultured myotubes, we performed fluorescence recovery after photobleaching (FRAP) on isolated myofibers allowing us to examine nuclear import *ex vivo*. Myofibers were isolated from the gastrocnemius muscles of mice constitutively expressing cNLS-tdTomato (Prigge et al., 2013). These myofibers exhibit strong nuclear fluorescence with very little fluorescence in the cytoplasm (Fig 2.4A). To determine if we could monitor nuclear transport by FRAP, we measured fluorescence over time of unbleached nuclei, partially bleached nuclei, bleached cytoplasm, and fully bleached nuclei (schematic Fig 2.4B). Unbleached nuclei maintained their fluorescence over the course of the 94-minute assay with only minor decreases in fluorescence over time (Fig 2.4C-D). This result demonstrates the photostability of cNLS-tdTomato in the absence of photobleaching. When a portion of a nucleus was bleached, the region rapidly recovered to the level of the unbleached area of the nucleus, with a time to half recovery ($T_{1/2}$) of 0.5 ±0.02 SD seconds (Fig 2.4E-F). A section of bleached cytoplasm also quickly recovered fluorescence, with a time to half maximal recovery ($T_{1/2}$) of 5.4 ±0.14 SD seconds (Fig 2.4G). The substantially longer $T_{1/2}$ of the bleached cytoplasm relative to the nucleoplasm could reflect reduced mobility in the cytoplasm resulting from tightly packed, highly ordered myofibrils. These two controls demonstrate both that technically the experiment can detect bleaching and recovery and that the rates of diffusion of cNLS tdTomato within

either the nucleus or the cytoplasm of a myofiber are rapid and highly consistent. When a whole nucleus was bleached however, it recovered fluorescence much more slowly then when only a portion of the nucleus was bleached with a rate best modeled by a quadratic function (Fig 2.4H-I). This dramatically slower rate in conjunction with the 95 kDa size of the tdTomato molecule, which is well above the diffusion limit of NPCs, supports the validity of the FRAP assay to detect nuclear import rates.

To assess whether nuclei within the same myofiber differed in cNLS nuclear import rates we performed FRAP on several nuclei in a single myofiber. When multiple nuclei within a region of a single myofiber were bleached, we observed a clear variation in the rate of fluorescence recovery among nuclei with times to half recovery ($T_{1/2}$) ranging from 15-146 minutes (Fig. 2.4I). To determine if this variability in $T_{1/2}$ was observed in other myofibers, we examined 26 myofibers isolated from 4 different mice. We found that within any given myofiber the $T_{1/2}$ of nuclei varied, with both the median $T_{1/2}$ and degree of $T_{1/2}$ variability differing among myofibers (Fig 2.4J). Hypothesizing that distinct classes of nuclei could exist within myofibers: those importing rapidly and those importing more slowly, we compared the rates of nuclear import of all 128 nuclei examined and found that the rates of import reflect a single broad population with median $T_{1/2}$ equal to 45 minutes and not distinct subpopulations (Fig 2.4K).

Given the variability in ranges of nuclear import rates among different myofibers and the correlation between nuclear import and nuclear position within a myotube in the *in vitro* import assay (Fig 2.3C), we compared nuclear import rates between nuclei in two different non-NMJ regions of the same myofiber. We also compared the rates of populations of nuclei located at the NMJ and nuclei in non-NMJ regions of the same fibers

(Figure 2.5A). The NMJ is a well characterized, easily identifiable, specialized region of the myofiber containing a cluster of acetylcholine receptors (AChR) (Couteaux and Pecot-Dechavassine, 1973). We identified the neuromuscular junction on individual myofibers by fluorescent bungarotoxin staining of AChR (Figure 2.5B). By comparing nuclei in two non-NMJ regions in a single myofiber (4-9 nuclei in each region), we determined that the median and range of $T_{1/2}$ could differ significantly between the two non-NMJ regions of the same fiber (Figure 2.5C). Comparing the population of nuclei directly beneath the NMJ and paired nuclei in non-NMJ regions of the myofiber revealed no difference between the NMJ nuclei and non-NMJ nuclei (Figure 2.5D). These results indicate that while NMJ nuclei differ from other nuclei in the myofiber transcriptionally, they do not differ in cNLS nuclear import rates, however nuclei in two non-NMJ regions can differ significantly in rate of nuclear import.

Variation in nuclear import rates could affect cellular response to physiological stimuli, consequently we resolved to examine if nuclear import was affected by physiological stress. Skeletal muscle injury is one type of stress with a well-defined anatomical nuclear phenotype. After injury, skeletal muscle regenerates and many of the nuclei incorporated during regeneration are localized in the center of the myofiber rather than the periphery (Figure 2.5E). To determine whether central nuclei differed from non-central nuclei with respect to nuclear import rates, we compared $T_{1/2}$ of nuclei in myofibers isolated from injured gastrocnemius muscle 21 days post injury, the contralateral gastrocnemius, and the gastrocnemius isolated from uninjured mice (schematic in Figure 2.5F). When fluorescence recovery is modeled by quadratic equation, the recovery of some nuclei plateaus before half recovery is reached (Figure 2.5G). Consequently, these nuclei

are never projected to reach $T_{1/2}$. Calculations indicate that 8% of nuclei from the uninjured muscle and 4% of nuclei from the contralateral muscle would never reach $T_{1/2}$. In contrast, the fluorescent recovery of 20% of nuclei in injured myofibers plateaued before reaching $T_{1/2}$ (Figure 2.5H). The nuclei in injured myofibers for which a $T_{1/2}$ could be calculated recovered significantly more slowly (median $T_{1/2}$=123 minutes) than the nuclei in myofibers isolated from uninjured control mice (median $T_{1/2}$=62 minutes). Surprisingly, the nuclei in myofibers isolated from the contralateral leg also recovered significantly more slowly (median $T_{1/2}$=109 minutes) than nuclei from uninjured mice (Figure 2.5I). Together these findings demonstrate that nuclear import is responsive to muscle injury both in regenerating myofibers and in myofibers distant from the site of injury, suggesting systemic coordination of reduced nuclear import rates following injury.

2.3.4 Nuclear import varies with muscle differentiation

Interested in the decreased rate of nuclear import in newly regenerated myofibers, we examined whether global changes in nuclear import occur during differentiation. To model differentiation in a synchronized system, we took advantage of an *in vitro* model of myogenesis. During *in vitro* myogenesis in response to a depletion of growth factors, mononucleated myoblasts cease proliferating and differentiate to become myocytes. Subsequently, myocytes fuse with each to form multinucleated myotubes. We differentiated pure cultures of primary mouse myoblasts *in vitro* and performed the *in vitro* import assay using the fluorescent cNLS reporter (Fig. 2.2) at myoblast (0 hours), myocyte (18 hours), and myotube (48 hours) stages of differentiation (Fig 2.6A). We found that the proportion of nuclei that were cNLS-positive varied across the stages of differentiation.

The highest proportion of nuclei were cNLS- positive at the myoblast (25%) and myotube (21%) stages while only 9% of myocyte nuclei were cNLS-positive (Fig 2.6B).

Curious that such a low percentage of myocyte nuclei was cNLS-positive, we investigated whether the frequency of import of non-cNLS pathways also changed with myogenesis. We used pairwise comparisons of cNLS and non-cNLS reporters as in Figure 3. In the PTHrP NLS and cNLS and the Nup53 and cNLS reporter pairings, the percentage of nuclei positive for only the non-cNLS reporter did not change significantly across differentiation In contrast, the percentage of nuclei positive for only hnRNPA1 NLS was significantly higher at the myocyte stage (20.7%) than either the myoblast (7.5%) or myotube (9.6%) stages. This preferential import of the hnRNPA1 reporter occurred to the exclusion of the cNLS reporter. Together these results support that differentiation state affects nuclear import.

2.4 Discussion

Our study illustrates that nuclear import varies among nuclei in the same multinucleated muscle cell. Nuclei within *in vitro* generated myotubes differed from one another in accumulation of fluorescent reporter proteins indicating differential usage of the cNLS import pathway and non-cNLS import pathways. Additionally, rates of cNLS import varied among nuclei in isolated myofibers. Variation in nuclear import correlated with nuclear position within the cell and progression through myogenesis. These differences in nuclear import among muscle nuclei could play a role in differentiation and in establishing regional specialization in mature myofibers.

While some but not all nuclei were cNLS-positive, virtually all nuclei were transcriptionally active as determined by EU incorporation. The finding that all nuclei were transcriptionally active differs from reports of variability in transcriptional activity among nuclei within myofibers *in vivo* (Kirby et al., 2016). The difference between these results and our findings could reflect a higher transcriptional demand in cultured myotubes than in mature tissue. Conversely, it could be the result of technical differences in dosage, administration, and duration of EU labeling.

Examination of non-cNLS import pathways revealed that, like the cNLS pathway, some but not all nuclei were positive for the non-cNLS pathways. Individual nuclei could be positive for one, both, or neither examined import reporter. Variation in nuclear import could represent a mechanism for achieving diversity among myonuclei in a single cell. Nuclear transport is affected by NPC composition, post translational modification of Nups, the RanGTP gradient between the nucleus and the cytoplasm, levels and modification state of nuclear transport receptors, and levels and modification state of the cargo protein (Sekimoto and Yoneda, 2012, Hung and Link, 2011). The *in vitro* import assay specifically examines nuclear intrinsic variables: the RanGTP gradient among nuclei, variable NPC composition, or post-translational Nup modification. Thus, while additional variables likely contribute to regulating nucleocytoplasmic transport *in vivo*, the differences in nuclear import that we identified among myonuclei are rooted in intrinsic nuclear properties.

NPCs regulate movement into and out of the nucleus. The complexes are made up of multiple copies of ~30 nucleoporins (Nups) and can serve as scaffolding for localizing other proteins to the nuclear envelope. Changes to the NPC or associated proteins can affect

nuclear transport. Among the proteins that bind to the specific Nups are two enzymes critical to maintaining the RanGTP gradient: RCC1, the Ran guanine nucleotide exchange factor localized in the nucleus; and RanGAP1, the Ran GTPase activating protein localized to the cytoplasm (Tran and Wente, 2006). Disruption of the RanGTP gradient results in protein mislocalization, particularly of very large proteins (Snow et al., 2013, Lyman et al., 2002). The nuclear import reporters used in the experiments presented here are relatively small, so most probably the differences in nuclear import are due to NPC differences among nuclei, not RanGTP gradient disruption.

One type of NPC difference among myonuclei that could drive differential import pathways is composition of the NPC. Stoichiometric levels of Nups in the NPC can affect nuclear import (Crampton et al., 2009, Gustin and Sarnow, 2002, Gustin and Sarnow, 2001). While the core NPC proteins are incorporated into the nuclear envelope as it reforms after mitosis and experience minimal exchange over the lifetime of the cell (Savas et al., 2012), many of the peripheral Nups dynamically associate with the NPC (Toyama et al., 2013). Some Nups specifically interact with chromatin proteins, enzymes, or nuclear transport receptors. For example, specific Nups are required for SMAD nuclear transport. If these Nups are depleted by RNAi, SMAD import, mediated by Imp8 and Imp7 (Xu et al., 2007), is decreased but cNLS import is unaffected (Chen and Xu, 2010). Similarly, other Nups are required for cNLS import (Sabri et al., 2007). Because some Nups transiently associate with the NPC, import pathway activity in myonuclei could be dynamically regulated by modulating NPC composition. We set out to determine if there were differences in NPC composition between cNLS-positive and cNLS-negative nuclei by measuring immunofluorescence intensity of FG Nups, Nup358, RanGAP1, and Kapβ

(Fig 2.9A). All proteins we examined showed similar variability in fluorescence intensity (Fig 2.9B). To determine is small changes in fluorescence intensity correlated with nuclear import we performed immunocytochemistry for Nup358 in the context of the nuclear import assay (Fig 2.9C). We did not detect any correlation between fluorescence intensity and cNLS import (Fig 2.9D). However, it should be noted that our system lacked the sensitivity to definitively confirm or exclude differences in NPC composition between cNLS-positive and cNLS-negative nuclei.

Post-translational modification of Nups rather than changes in the composition of the NPC could also explain differences in nuclear transport among myonuclei. Both phosphorylation and O-GlcNAc glycosylation of Nups are dynamic transient modifications that change in response to cellular physiology (Kodiha et al., 2009, Regot et al., 2013, Crampton et al., 2009). At least 10 of the 30 Nups are subject to O-GlcNAc modification (Miller et al., 1999, Hulsmann et al., 2012). Increased O-GlcNAc modification of Nups can decrease association of nuclear export factors with the NPC and consequently decrease nuclear export (Crampton et al., 2009). In addition, at least 20 Nups can be phosphorylated (Rigbolt et al., 2011). Dynamic ERK-mediated phosphorylation of Nups 50, 153, and 214 leads to decreased binding of importin β and decreased nuclear import (Kosako et al., 2009). In contrast, another study found that treatment of HeLa cells with phosphatase inhibitors decreased importin-mediated import (Kehlenbach and Gerace, 2000). In yeast, hyperphosphorylation of the NPC decreased nuclear export while incorporation of non-phosphorylatable Nups into the NPC altered gene expression (Regot et al., 2013). Thus, transient post translational modifications of the Nups could result in nucleus to nucleus differences in nuclear import within a single muscle cell.

Identifying the biochemical mechanisms responsible for the differences in nuclear import among nuclei is technically challenging. Standard biochemical assays would require large amounts of purified cNLS-positive nuclei separated from cNLS-negative nuclei. Furthermore, many Nups have additional nuclear functions unrelated to their role at the NPC (Gomez-Cavazos and Hetzer, 2015, Buchwalter et al., 2014, Morchoisne-Bolhy et al., 2015). Thus, Nup protein levels in a nucleus may not reflect the amount of a Nup at the nuclear pore. NPC heterogeneity within a single nucleus would also complicate analysis. A myonucleus has approximately 360,000 NPCs (Asally et al., 2011). Therefore, even if an individual nucleus could be biochemically analyzed, the result would represent the average of a large population which could vary within a single nucleus (Kinoshita et al., 2012). Post-translational modifications would be difficult to identify because many of the modifications which impact nuclear transport occur in hydrophobic regions. These regions are highly repetitive and share homology between Nups which reduces confidence in detecting the modifications and in assigning detected modifications to a single protein. Additionally, each NPC contains 16-32 copies of each Nup (Hetzer and Wente, 2009) and individual copies of the same Nup may not all be modified in the same way. This level of NPC complexity decreases the probability of detecting the modification using an approach that examines a population of nuclei. As additional techniques are developed, identifying the biochemical mechanisms regulating differences in nuclear import among nuclei sharing a common cytoplasm will become increasingly feasible.

We not only studied nuclear import in cultured myotubes but also examined cNLS nuclear import rates by FRAP in isolated myofibers. Nuclei within individual myofibers differed in the rate of nuclear import. While individual nuclei could differ greatly in import

rate, the import rates of all nuclei examined formed a single broad population. Skeletal muscle cells are post-mitotic multinucleated cells with strong specialized regionalization. Comparing the population of nuclei associated with one specialized region, the NMJ, to the overall population of nuclei revealed no difference in cNLS import rates. Thus, although nuclei associated with the neuromuscular junction are distinct from nuclei located elsewhere in the myofiber both in protein content (Apel et al., 2000) and transcript production (Moscoso et al., 1995, Brenner et al., 1990, Jasmin et al., 1993, Fontaine and Changeux, 1989), these differences are not due to variation in cNLS nuclear import rates. The specialization of NMJ nuclei could be achieved through selective activation of non-cNLS import pathways only in NMJ nuclei or through subcellular enrichment of NMJ targeted cargo only in cytoplasm surrounding NMJ nuclei. .

When we examined the median rate of nuclear import between two morphologically non-specialized regions of a single myofiber, we found that median rate and range could vary significantly between different regions of the same myofiber. A study which described variability in expression of both housekeeping and muscle-specific genes among nuclei noted that while nuclei producing housekeeping gene transcripts were randomly distributed throughout a myofiber, nuclei producing muscle-specific transcripts clustered together separated by clusters of nuclei not producing transcripts (Newlands et al., 1998). This selective distribution of nuclei producing muscle-specific transcripts prompted the authors to suggest the existence of domains in a myofiber that could be defined functionally rather than morphologically. Our finding that the median and range of nuclear import rates can vary significantly between two morphologically non-specialized regions of a myofiber could support this model.

Skeletal muscle is a highly regenerative tissue. Following injury, a series of coordinated events result in regeneration of the injured site. After damaged tissue is cleared, muscle resident stem cells or satellite cells proliferate and produce a large number of muscle progenitor cells. These progenitors differentiate and either fuse into existing damaged myofibers or fuse with each other, forming new, smaller myofibers (Ratnayake and Currie, 2017). Myonuclei in regenerated myofibers are localized in the center of the myofiber rather than the periphery and remain in the center of the myofiber for months after the injury has healed (Wada et al., 2008). Why nuclei in regenerated myofibers centralize and what, if any, effect centralization has on nuclear activity remain open questions. We examined cNLS nuclear import after regeneration and found that the $T_{1/2}$ of nuclei in regenerated myofibers was significantly slower than that of control nuclei. A nucleus surrounded by dense myofibrils could have reduces access to diffusible proteins resulting in apparent decreased transport rates. However, the $T_{1/2}$ of nuclei in myofibers isolated from the contralateral limb was also significantly slower than uninjured control. Nuclei in these uninjured, contralateral myofibers remain at the periphery of the myofiber but none the less also experienced decreased cNLS import rates. Thses observations support that the change in nuclear import rates in response to injury is not the result of decreased diffusion. That the increased $T_{1/2}$ also occurs in nuclei in the contralateral limb suggest some systemic factor regulating nuclear import in response to injury. Circulating hepatocyte growth factor activator (HGFA), which is activated on injury to a tissue, induces a state of readiness in satellite cells distant from the location of the injury (Rodgers et al., 2014, Rodgers et al., 2017). Thus, a circulating factor could similarly mediate changes in nuclear transport in response to tissue injury.

Interested in the slower rates of cNLS import observed in regenerated myofibers, we wondered whether slower nuclear transport was related to differentiation. We examined cNLS and non-cNLS import pathways across the different stages of myogenesis in primary mouse muscle cells. This analysis revealed that nuclear import is dynamic across differentiation. Additionally, the proportion of import attributable to each pathway changed as differentiation progresses. A previous study that examined steady-state nucleocytoplasmic localization of fluorescent cNLS reporters in myoblasts and myotubes formed by differentiation of the C2C12 murine muscle cell line reported differing distributions of the reporter between myoblasts and myotubes but concluded that there was no difference in nuclear import between the two stages rather that the nuclear export rates differed between the two stages (Asally et al., 2011). However, the technical details of the approaches used to examine nuclear transport differed greatly between the previous study and the current work: microinjection versus digitonin permeabilization; inclusion versus exclusion of a nuclear export sequence in the reporter protein; and duration of the time course. Thus, the differences in these findings are likely technical. Our conclusion that nuclear import varies with differentiation were based on experiments conducted in permeabilized cells, indicating that nuclear inherent differences are responsible for the nuclear import variability we detected. Similarly, a comparison of steady-state localization of a fluorescent nuclear import and nuclear export reporter protein in myotubes and myoblasts treated with polyethylene glycol to induce fusion found that multinucleated myoblasts were more like mononucleated myoblasts than multinucleated myotubes (Asally et al., 2011). This finding indicates that differentiation of a nucleus has a greater impact on nuclear transport than simply existing in a multinucleated environment. Our observed

changes in nuclear import with differentiation could result in part from the stress of serum starvation to induce differentiation as various kinds of cellular stress induce changes in nuclear transport (Kodiha et al., 2009, Regot et al., 2013, Yasuda et al., 2006, Kodiha et al., 2008). Whether resulting from a stress response or regulated differentiation-related changes, the alterations in nuclear import are most likely mediated by changes to the NPC.

While the number and density of the NPCs in the nuclear envelope do not change between the myoblast and myotube stages of myogenesis (Asally et al., 2011), during differentiation the NPC undergoes changes in composition and in post-translational modifications. Steady state transcript levels of half the NPC components change with differentiation of the C2C12 muscle cell line (Asally et al., 2011) and protein levels of Nup210 (D'Angelo et al., 2012) and Nup358 (Asally et al., 2011) differ between myoblasts and myotubes. In each case expression of the Nup is induced with differentiation. However, while the increased level of these Nups is necessary for proper differentiation, their depletion does not alter nucleocytoplasmic transport. Indeed, the effect of Nup210 on differentiation is independent of incorporation of the protein into the NPC (Gomez-Cavazos and Hetzer, 2015). Thus, while appropriate levels of Nups are required for myogenesis, changes in NPC composition likely do not account for the differences we observed in nuclear import. Post-translational modification of Nups is more likely to regulate the temporally dynamic alterations in nuclear import during differentiation. Interestingly, C2C12 cells experience a global decrease in O-GlcNAc modification with differentiation from myoblasts to myotubes and pharmacological inhibition of this O-GlcNAc removal blocks myoblast fusion and results in decreased expression of myogenic regulatory factors (Ogawa et al., 2012). In HeLa cells, increased NPC O-GlcNAc

modification decreases nuclear export factors association with the NPC resulting in decreased nuclear export (Crampton et al., 2009). Together these findings suggest that decreased O-GlcNAc modification of the NPC could affect nuclear transport and be important for myoblast differentiation. Many NPC proteins undergo differentiation-dependent phosphorylation with the general trend of reduced phosphorylation as differentiation progresses (Rigbolt et al., 2011). Determining if these NPC modifications regulate differentiation associated changes in nuclear import could provide a way to modulate myogenesis.

Understanding how individual nuclei within a single multinucleated muscle cell behave differently has broader implications than skeletal muscle biology. While the majority of eukaryotic cells have a single nucleus, some specialized cells are multinucleated. Ranging from single celled organisms, to fungi, to differentiated mammalian cells, cells with multiple nuclei present an intriguing biological system. Not only must gene expression be regulated in multiple nuclei in a coordinated fashion to achieve the necessary cellular protein levels, but also in many cases nuclei within these multinucleated cells differ from one another. *Tetrahymena*, a binucleated single cellular organism, contains a germline micronucleus and a non-germline macronucleus which are structurally and functionally distinct (Orias et al., 2011). The NPCs of the two *Tetrahymena* nuclei differ in composition and when Nups specific to one nucleus are targeted to the other nucleus, cargo proteins are inappropriately localized to the wrong nucleus (Iwamoto et al., 2009). Five different syncytial fungi are multinucleated. These fungi grow by mitosis uncoupled from cytokinesis and, in contrast to the *Drosophila* embryo, nuclei can divide independently of one another. Nuclei as close as 1 μm from each other are in different

stages of mitosis despite the concentrations of cyclins not varying among nuclei (Gladfelter et al., 2006). However, sister nuclei have similar lag times between mitoses even as they move separately through different cellular regions (Anderson et al., 2013), suggesting that the difference in mitotic entry among nuclei could be nuclear-intrinsic. Mammalian osteoclasts contain approximately 20 nuclei which differ from one another in chromatin structure and markers of transcriptional activity (Youn et al., 2010). The nuclei of the syncytial trophoblast in placental mammals differ from one another in chromatin arrangement and transcriptional activity (Ellery et al., 2009). These examples of multinucleated cells from several different phyla highlight the unique biology of multinucleated cells that allows nuclei exposed to the same cytoplasm to behave differently from each other. The mechanisms governing variation in myonuclei may be more generally applicable to these other cell types and could represent evolutionarily conserved mechanisms for coordinating activity among nuclei sharing a single cytoplasm.

In summary, we defined that both cNLS and non-cNLS nuclear import activity varies among nuclei in a multinucleated muscle cell. Such variation in nuclear import may be a mechanism for achieving differences in transcript production among myonuclei leading to functional specialization in myofibers. The biochemical and signaling mechanisms that modulate nuclear import and target NPCs in individual myonuclei in a common cytoplasm remain unclear and the focus of future studies. Future studies could also include defining whether physiologic changes such as aging, disease or regeneration spatially or temporally alter nuclear import or the ratio between cNLS and non-cNLS nuclear import in myofibers. A better understanding of the biochemical and signaling mechanisms driving differences in nuclear import among nuclei in a skeletal muscle cell

will also provide further insight into the biology of other mammalian and non-mammalian syncytial cells.

2.5 Methods

In vitro *myogenesis*

Primary myoblasts were isolated from hindlimb muscles of 3-month-old male C57BL/6 mice as described previously with the exception of the Percoll gradient (Bondesen, Mills et al. 2004). Myoblasts were cultured on bovine collagen I (Gibco, Gaithersburg MD) -coated dishes in growth media (Ham's F10, 20% fetal bovine serum (FBS), 100U/mL penicillin, 100µg/mL streptomycin, and 5ng/ml fibroblast growth factor at 37°C and 5% CO_2. For import assays, differentiation was induced by plating 2 $x10^5$ myoblasts on elastin, collagen, laminin (ECL) (Gibco) -coated 18mm diameter coverslips in differentiation media (Dulbecco's modified Eagle's medium, 10mg/L insulin, 5.5 mg/L transferrin, and 6.7µg/L selenium (Gibco), 100U/ml penicillin, 100µg/mL streptomycin) for 18 hours for myocytes or 48 hours for myotubes. To analyze nuclear import in myoblasts, myoblasts were similarly plated on ECL-coated coverslips and cultured in growth media for 18-24 hours.

Fluorescent dextran

Myotubes were differentiated on glass coverslips as described above. Coverslips were placed on ice for 5 minutes and the media was gently aspirated. The cells were washed once with transport buffer (20mM HEPES, 110 mM potassium acetate, 2mM magnesium acetate, 1mM EGTA, 2mM DTT) and then permeabilized on ice with 25 µM digitonin in

transport buffer for 5 minutes. Permeabilized myotubes were stained with DAPI to identify nuclei and then incubated with 10 kDa or 70 kDa Texas red-conjugated dextran for 15 minutes at room temperature (Sigma-Aldrich, St. Louis, MO). The 10kDa dextran enters all nuclei without blocked NPCs. The 70 kDa dextran is excluded from nuclei with intact nuclear envelopes and NPCs (D'Angelo, Raices et al. 2009). After incubation with the fluorescent dextran cells were imaged.

In vitro *nuclear import assay*

The *in vitro* nuclear import assay was modified from previously established protocols (Moore and Schwoebel, 2001, Adam, 2016). Myoblasts, myocytes, and myotubes were generated as described above. Coverslips were placed on ice for 5 minutes and the media was gently aspirated. The cells were washed once with transport buffer and then permeabilized on ice with 25 µM digitonin in transport buffer for 5 minutes. After permeabilization, cells were gently washed with transport buffer. Cells were than incubated at 30°C for 15 minutes in either transport buffer or transport buffer containing 5.6mM wheat germ agglutinin (WGA) (Vector Laboratories, Burlingame, CA). Coverslips were then placed inverted on 100 µL import cocktail (2% bovine serum albumin (BSA), 20% rabbit reticulocyte lysate (Promega, Madison, WI), 4mM, 0.1mM GTP, 7.6mM creatine phosphate, 15U/ml creatine phosphokinase, 1mM ATP, 20mM HEPES, 110 mM potassium acetate, 2mM magnesium acetate, 1mM EGTA, 2mM DTT). Fluorescent import reporters used were either purchased (Sigma) or generated in the laboratory by FPLC purification of recombinant proteins. Coverslips were incubated at 30°C in a humidified chamber for 30 minutes. After incubation, coverslips were washed three times with 1%

BSA in transport buffer. Cells were then fixed in 4% paraformaldehyde (PFA) (Electron Microscopy Sciences, Hatfield, PA), 0.1% glutaraldehyde on ice for 15 minutes. After fixation cells were stained with DAPI to identify nuclei.

Labeling of newly synthesized RNA

The Click-iT RNA imaging kit (Molecular probes, Eugene, OR) was used to label newly synthesized RNA. Primary mouse myotubes were generated by 48 hours of differentiation on coverslips. Control coverslips were pretreated with 5µg/ml Actinomycin D (Molecular Probes) for 1 hour at 37C. All coverslips were then treated with 2mM 5-ethynyl uridine (EU) in differentiation media for 30 minutes. Cells were fixed with 3.7% formaldehyde for 15 minutes on ice and further processed per the manufacturer's instructions.

Plasmids used

The pGEX4TH-SV40NLS-EGFP plasmid (Shumaker, Lopez-Soler et al. 2005) (gift from Steven Adam, Northwestern) was used to generate the cNLS-EGFP reporter protein. The mutant cNLS control reporter protein was generated by site-directed mutagenesis. The GST-cNLS-mCherry construct was cloned by ligation following cleavage of the vector backbone and insert by KpnI and NotI. The insert was produced by PCR amplification of the mCherry gene using the following primers forward: 5'-cgactctagaggatccccgggtaccggtcgccaccatggtgagcaagggcgaggaggat reverse: 5'-atcgtcagtcagtcacgatgcggccgctttacttgtacagctcgtccatgccgcc. The GST mutant cNLS EFGP construct and both PTHrP NLS constructs were cloned by the quick change method using

the following primers, for the mutant cNLS forward primer: 5'-cgaaacgtaaagtggaagatggtccgccgcat, reverse primer: 5'-ttttcggcggaccaccttcgagtcgacccggg, for the PTHrP NLS constructs, forward primer: 5'-gcaacccctgaaaacccccggtaagaaaaaaaaaggaaagcctcatgcctgcaggtcgactctagag, reverse primer: 5-'tctttgtaggtttccactttattagtttcctgcgtcaggtagcgttcgagtcgacccgggaattccgg. For Nup53 NLS and hnRNPA1 NLS constructs, gBlocks were purchased from Integrated DNA Technologies and ligated into the vector backbone after cleavage with EcoRI and XbaI. All constructs were sequence verified.

Recombinant protein expression and purification

BL21(DE3) competent *E. coli* were transformed and grown in selective Luria-Bertani broth to 0.5 optical density. Protein expression was induced with 1mM isopropyl β-D-1-thiogalactopyranoside (IPTG) at 30° for 6 hours. Pelleted bacteria were resuspended in lysis buffer (1mM phenylmethylsulfonyl fluoride (PMSF), 20mM Tris pH 8.0, 100mM NaCl, 10% glycerol, 1µM $ZnCl_2$) and lysed by French press. The lysate was passed through a 2µm filter. Recombinant proteins were purified over a 5ml GSTrap FF column (GE Healthcare Life Sciences, Pittsburgh, PA), using a P-500 pump (Pharmacia Biotech, Pittsburgh, PA), and a Controller LCC-501 Plus (Pharmacia Biotech). Purified protein was eluted in a gradient of lysis buffer and lysis buffer containing 10mM glutathione. Fractions were collected using FRAC-100 (Pharmacia Biotech). Proteins were dialyzed against dialysis buffer (20mM Tris pH 8.5,150mM NaCl, 2mM MgAc, 2µM $ZnCl_2$, 2% glycerol) using a 10 kD membrane (Spectrum Laboratories Inc, Rockleigh NJ), tested for purity by gel electrophoresis and Comassie staining, and concentrated using a viva spin 15-30,000

MWCO column (Sartorius Stedim Biotech, Göttingen, Germany). A representative Coomassie stained gel of purified proteins is shows that the reporter proteins are close to the same molecular weight (Fig 2.8). The molecular weights of the purified proteins are cNLS-EGFP 61.2 kDa, cNLS-mCherry 57.3 kDa, mutant cNLS-EGFP 61.2 kDa, mutant cNLS-EGFP 61.2 kDa, hnRNPA1 NLS-EGFP 64.0 kDa, hnRNPA1 NLS-mCherry 60.1 kDa, Nup53 NLS-EGFP 65.2 kDa, Nup53 NLS-mCherry 61.3 kDa, PThrP NLS-EGFP 63.0 kDa, PThrP NLS-mCherry 59.1 kDa.

Myofiber isolation

Gastrocnemius muscles from 6 month old female C57BL/6 mice were dissected, enzymatically digested and further processed as described previously (Pichavant and Pavlath 2014). Briefly, muscles were gently dissected and cut twice longitudinally in order to increase the surface area of the muscle in contact with the enzyme. Muscles were incubated for 80 minutes in a benchtop Enviro-genie (Scientific Industries, Inc., Bohemia, NY) rocking at 26 RPM at 37°C in digestion media (Dulbecco's modified Eagle's medium, 25 mM HEPES, 400 U/ml collagenase type I (Worthington Biochemical, Lakewood, NJ)). All subsequent steps were carried out at room temperature. The samples were washed three times to remove debris and transferred to a Petri dish. Single myofibers were picked using a Pasteur pipette and placed in 8 well chamber coverslips (Ibidi, Martinsried, Germany) precoated with 4% Matrigel (BD Biosciences, San Jose, CA) containing imaging media (Dulbecco's modified Eagle's medium, 20% FBS, 5mM EGTA, 1mM $MgCl_2$). Chamber coverslips were centrifuged at 1100xg for 20 minutes to adhere the myofibers. Myofibers were incubated at 37°C and 5% CO_2 for 1 hour prior to imaging.

Bungarotoxin staining

Isolated myofibers were incubated with 2µg/ml fluorescein conjugated α-Bungarotoxin (Molecular Probes) for 15 minutes at 37°C. Myofibers were then washed three times with PBS and centrifuged into 8 well coverslips as described above.

Immunocytochemistry

In vitro generated myotubes were fixed with 4% PFA (Electron Microscopy Sciences) for 15 minutes at room temperature and permeabilized with 0.5% Triton x-100 (Fisher Scientific) for 5 minutes at room temperature. Cells were then blocked with 1% BSA and 0.1% donkey serum in TBST for 30 minutes at 4°C. Coverslips were incubated overnight with primary antibody: RanGap 1:50 (Santa Cruz Biotechnology), mAb414 1:500 (Abcam, Cambridge, UK), Kapβ1 1:10,000 (Abcam), Nup 358 1:20,000 (gift from Kehlenbach laboratory). Alexa594 conjugated secondary anti mouse or anti rabbit antibodies 1:200 (Jackson Immuno Research Laboratories Incorporated, West Grove, PA) were used to detect primary antibody signal.

Microscopy and image analysis

For quantitative analysis of *in vitro* nuclear import assays, images were obtained using an Axioplan microscope (Carl Zeiss MicroImaging, Oberkochen, Germany) with either a 0.3 NA 10X Plan-Neofluar objective (Carl Zeiss MicroImaging) or a 0.8 NA 25X Plan-Neofluar objective (Carl Zeiss MicroImaging) and recorded with a CCD camera (Carl Zeiss MicroImaging) and Scion Image 1.63 (Scion Corporation, Torrance, CA) software. Images were uniformly processed; myonuclei within myotubes were identified; and fluorescence intensity in DAPI, EGFP, and mCherry channels were measured using an automated CellProfiler version 2.2.0 (Carpenter et al., 2006) pipeline. The automated

processing used DAPI intensity to identify nuclei between 20 and 60 pixel units by adaptive three class Otsu thresholding. Clumped nuclei were distinguished by shape. Mean fluorescence intensity for nuclear import reports or mean edge flourscence intensity for immune cytochemistry staining was measured.

For analysis of multiple focal planes of myonuclei and live cell imaging of FRAP experiments, images were collected using a Nikon A1R confocal microscope (Nikon, Tokyo, Japan) with a CFI Apo TIRF 60x H objective (Nikon) and were recorded with NIS-Elements Microscope Imaging Software (Nikon). FRAP image sets were processed with Fiji Image J2 (Schindelin et al., 2012, Schindelin et al., 2015) to correct for register drift and quantification of fluorescence intensity. For live cell imaging of myofibers, coverslips were maintained at 37°C and 5% CO_2. Nuclei and portions of the cytoplasm were bleached with a 561nm laser at 80% power (34 seconds) and imaged continuously for the first 2 minutes and every 2.5 minutes thereafter for 90 minutes

Barium chloride muscle injury

Mice were anesthetized with intraperitoneal injection of a solution containing 80 mg/kg ketamine HCl/5 mg/kg xylazine. For analgesia, mice were injected subcutaneously with 0.1 mg/kg buprenorphine before and after muscle injury. Injury was induced in the gastrocnemius (GA) muscles of anesthetized mice by injection of 40 μl of 1.2% $BaCl_2$ (Griffin, Kafadar et al. 2009) (Sigma-Aldrich). Muscles were collected either 21 days post injury.

Microscopy and image analysis

For quantitative analysis of *in vitro* nuclear import assays, images were obtained using an Axioplan microscope (Carl Zeiss MicroImaging, Oberkochen, Germany) with either a 0.3 NA 10X Plan-Neofluar objective (Carl Zeiss MicroImaging) or a 0.8 NA 25X Plan-Neofluar objective (Carl Zeiss MicroImaging) and recorded with a CCD camera (Carl Zeiss MicroImaging) and Scion Image 1.63 (Scion Corporation, Torrance, CA) software. Images were uniformly processed; myonuclei within myotubes were identified; and fluorescence intensity in DAPI, EGFP, and mCherry channels were measured using an automated CellProfiler version 2.2.0 (Carpenter, Jones et al. 2006) pipeline.

For analysis of multiple focal planes of myonuclei and live cell imaging of FRAP experiments, images were collected using a Nikon A1R confocal microscope (Nikon, Tokyo, Japan) with a CFI Apo TIRF 60x H objective (Nikon) and were recorded with NIS-Elements Microscope Imaging Software (Nikon). FRAP image sets were processed with Fiji Image J2 (Schindelin, Arganda-Carreras et al. 2012, Schindelin, Rueden et al. 2015) to correct for register drift and quantification of fluorescence intensity. For live cell imaging of myofibers, coverslips were maintained at 37°C and 5% CO_2. Nuclei and portions of the cytoplasm were bleached with a 561nm laser at 80% power (34 seconds) and imaged continuously for the first 2 minutes and every 2.5 minutes thereafter for 90 minutes.

Statistical analysis

Statistical analysis was performed using MATLAB (MathWorks, Natick, MA) to model second order quadratic curve fitting and determination of time to half recovery ($T_{1/2}$). Other statistical tests (t-test, ANOVA, and chi squared analyses) were performed

using GraphPad Prism version 5 (Graphpad Software, San Diego, CA). A p-value of less than 0.05 was considered statistically significant.

2.6 Tables

Table 2.1: NLS sequences and associated nuclear transport receptors

NLS	**NLS sequence**	**Transport receptor**	**Reference**
SV40	GGPPKKKRKVEDGPP	Importin α KPNB1	(Kalderon, Richardson et al. 1984)
Mutant SV40 (**mutated residue**)	GGPPK**T**KRKVEDGPP	-	(Lanford and Butel 1984)
hnRNPA1	GPGYSGGSRGYGSGGQGYG NQGSGYGGSGSYDSYNNGG GGGFGGGSGSN	KPNB2 KPNB2B	(Pollard, Michael et al. 1996, Lee, Cansizoglu et al. 2006)
Nup53	VRNAEFKVSKNSTSFKNPRR LEIKDGRSLFLRNRGKIHSGV LSSIESDL	IPO5	(Marelli, Lusk et al. 2001, Lusk, Makhnevych et al. 2002, Kobayashi and Matsuura 2013, Soniat, Cagatay et al. 2016)
PTHrP	RYLTQETNKVETYKEQPLKT PGKKKKGKP	KPNB1	(Lam, Hu et al. 2001, Cingolani, Bednenko et al. 2002)

2.7 Figures

Figure 2.1: Some but not all nuclei within myotubes import a fluorescent nuclear import reporter. A To perform the *in vitro* import assay, the plasma membrane of myotubes was digitonin permeablized and the cytoplasm washed out. Cells were incubated with reticulocyte lysate, an energy regenerating cocktail, and a fluorescent nuclear import reporter composed of bovine serum albumin (BSA) and multiple copies of the SV40 T-antigen classical nuclear localization sequence (cNLS). After washing and fixation, nuclei were stained with DAPI and imaged. **B** cNLS-positive nuclei (white arrow heads) were only detected when permeabilized cells were incubated with both the energy regenerating system (E) and reticulocyte lysate (lysate) in addition to the import reporter. Nuclear import was blocked by addition of wheat germ agglutinin (WGA) or by low temperature. **C** Within single myotubes both cNLS-positive (white arrowheads) and cNLS-negative (red arrowhead) nuclei were present. **D** All myotube nuclei were permeable to 10 kD fluorescent dextran but appropriately excluded 70 kD dextran. These results indicate that cNLS-import negative nuclei do not simply have blocked NPCs and that the nuclear envelopes have not been damaged by permeabilization. **E** The percentage of nuclei that were cNLS-negative in the middle of a myotube or on the ends of a myotube was compared to the percentage expected assuming random distribution of positive and negative nuclei in a myotube (red dotted line) The two nuclei on either end of myotubes were cNLS-negative more frequently than predicted by random distribution of cNLS-positive and cNLS-negative nuclei (chi squared $p<0.001$ n=450 myotubes from 3 independent cell isolates). Bar=20μm.

Figure 2.2: Nuclear import depends on the NLS. A The *in vitro* import assay was performed on myotubes using purified recombinant protein composed of Glutathione S-transferase (GST), a single cNLS, and enhanced green fluorescent protein (EGFP). **B** With this nuclear import reporter protein, some but not all nuclei were cNLS-positive (arrowheads) similar to that observed with the reporter containing multiple cNLS in Figure 1. A reporter protein containing a mutant cNLS was not imported into nuclei. **C** Each nucleus was determined to be cNLS-positive or -negative based on whether its fluorescence was more or less intense than the mutant cNLS control protein. **D** cNLS-positive (arrowheads) and -negative nuclei were examined using confocal microscopy. cNLS-negative nuclei remained negative regardless of the plane of focus. **E** To examine the general transcriptional activity of nuclei within myotubes, production of RNA was examined by incorporation of the uridine analog EU. Actinomycin treatment effectively prevented EU incorporation. EU signal was readily apparent in the absence of actinomycin. **F** Almost all nuclei (95% of 680 examined) were EU positive, indicating that they were transcriptionally active. The high percentage of EU positive nuclei compared with the relatively low percentage of cNLS-positive nuclei indicates that cNLS-negative nuclei are transcriptionally active. Bar=20μm.

Figure 2.3: A single nucleus with a myotube can import through multiple import pathways, a single import pathway, or no detectable import pathway. A Purified recombinant protein composed of GST fused to an NLS (cNLS, hnRNPA1 NLS, PthrP

NLS, Nup53 NLS, or mutant cNLS) followed by a fluorescent protein (either EGFP or mCherry) was expressed and isolated. The *in vitro* import assay was performed on myotubes using a GST-NLS-EGFP reporter and a distinct GST-NLS-mCherry reporter to compare the relative import of the two selected NLSs. Pairwise comparisons were made both with cNLS in green and non-cNLS in red and with cNLS in red and non-cNLS in green. **B** For each pairwise comparison, some nuclei were import-positive for both reporters (yellow arrowheads), only one reporter (red and green arrowheads) or none. Bar=10μm. **C** The proportion of nuclei in each pair of NLSs examined that were positive for the cNLS only, both the cNLS and non-cNLS, the non-cNLS only, or neither NLS reporter was quantified based on baseline fluorescence of the mutant NLS. The percentage of nuclei that were negative for both cNLS and non-cNLS reports differed significantly between the cNLS-hnRNP pairing and the other two cNLS-non-cNLS pairings. Data are mean ± SE comparisons by ANOVA with Tukey correction for multiple comparisons hnRNP n=4 independent experiments, PthrP and Nup53 n=5 independent experiments. **D** For each pair of NLSs examined, the proportion of nuclei importing the non-cNLS only or both the cNLS and non-cNLS was compared. The findings differed significantly from the percentage of nuclei predicted to be positive for the non-cNLS reporter or positive for both reporters based on random distribution of active NLS pathways. ($p<0.0001$ by chi squared analysis hnRNP n=4 independent experiments, PthrP and Nup53 n=5 impendent experiments).

Figure 2.4 cNLS nuclear import varies among nuclei within single myofibers. A Myofibers isolated from gastrocnemius muscles of mice constitutively expressing nuclear

targeted cNLS-tdTomato exhibit strong nuclear fluorescence and minimal cytoplasmic fluorescence. **B** Schematic representing the cellular parameters that were studied in FRAP experiments: an unbleached nucleus, a partially bleached nucleus, a bleached portion of cytoplasm, and a fully bleached nucleus. **C** Representative images of unbleached nuclei at different times during the course of the imaging. T= minutes. **D** Unbleached nuclei consistently maintained fluorescence throughout the entire period of imaging (n=20, mean ± SE). **E** Regions of bleached cytoplasm rapidly recovered to their initial fluorescence (n=19, mean ± SE). **F** A representative partially bleached nucleus prior to bleaching, immediately after bleaching and after recovery. Red outlines the bleached area. T= minutes. **G** The bleached sections of partially bleached nuclei rapidly recovered to baseline fluorescence (n=11, mean ± SE). **H** Representative bleached nuclei prior to bleaching, immediately after bleaching and after recovery. T= minutes. **I** The time to half recovery ($T_{1/2}$) of four bleached nuclei within a single myofiber differ from one another as calculated by quadratic regression. **J** The median and range of $T_{1/2}$ of nuclei greatly varied among myofibers indicating differences in the rate of cNLS import among nuclei both within a myofiber and among myofibers (4-8 nuclei measured per myofiber). **K** The histogram of $T_{1/2}$ of bleached nuclei reveals a continuous broad population with median $T_{½}$ of 45 min (n=128). Bar=10µm.

Figure 2.5 Rates of cNLS nuclear import can vary between regions of a single myofiber. A FRAP experiments were performed on nuclei within two different myofiber regions (A or B) not near the neuromuscular junction (NMJ) and nuclei directly under the NMJ using myofibers isolated from gastrocnemius muscles of mice constitutively

expressing nuclear targeted cNLS-tdTomato. **B** The neuromuscular junction was identified by FITC-conjugated bungarotoxin staining of acetylcholine receptors. Bar=10μm. **C** Nuclei were bleached, imaged and the $T_{1/2}$ calculated as in Figure 4. $T_{1/2}$ of 4-8 nuclei in disparate non-NMJ regions (A and B in Figure 5A) of a myofiber can vary. Data are median ± interquartile range. **D** $T_{1/2}$ of NMJ (n=15) and non-NMJ (n=58) nuclei were compared. Red line represents median. **E** In uninjured myofibers, nuclei are located at the periphery of the myofiber. After regeneration, nuclei centrally located in injured myofibers. Arrow indicates a non-central nucleus in an injured myofiber. Bar=50μm. **F** Schematic representing the injury experiment: one gastrocnemius muscle was injured by barium chloride injection. After 3 weeks the injured muscle, the contralateral gastrocnemius, and a gastrocnemius of an uninjured littermate were collected. **G** The $T_{1/2}$ of four bleached nuclei within a single myofiber differ from one another as calculated by quadratic regression as in Figure 4I. The recovery of some nuclei plateaus before reaching $T_{1/2}$. **H** The percent of nuclei that plateau before recovering to $T_{1/2}$ was calculated for nuclei in myofibers from uninjured (8% n=69 from 2 mice), contralateral (4% n=52 from 3 mice), and injured (20% n=304 from 3 mice) muscle. Data represent mean ±SD. **I** The $T_{1/2}$ for nuclei in myofibers isolated from uninjured, contralateral, and injured muscles were calculated. The median $T_{1/2}$ of nuclei from contralateral (109 minutes) and injured myofibers (123 minutes) were significantly higher than from uninjured control (65 minutes). The $T_{1/2}$ of contralateral and injured myofibers also differed significantly. ANOVA with Tukey correction for multiple comparisons Uninjured n=63, contralateral n=44, injured n=143. Red line represents median and quartile range.

Figure 2.6 Nuclear import varies during myogenesis *in vitro*. A Pure cultures of myoblasts were differentiated to form myocytes or myotubes and the *in vitro* nuclear import assay was performed. **B** The percentage of cNLS-positive nuclei was high in myoblasts (25%), dropped dramatically to near background levels in myocytes (9%), and then rose again to near pre-differentiation levels in myotubes (21%). (n=3 independent experiments each with ~200 nuclei per differentiation stage). **C** The *in vitro* import assay was performed using cNLS and non-cNLS import reporters to compare the relative import of the cNLS and non-cNLSs at the different stages of myogenesis. For each pair of NLSs examined, the proportion of nuclei importing the non-cNLS only or both the cNLS and non-cNLS was compared as in Figure 3C. The percentage of hnRNP NLS import differed significantly across differentiation. hnRNP reporter displayed relatively low import in the myoblast and myotube stages but relatively high import in the myocyte stage. (Data are mean ± SE comparisons by ANOVA with Tukey correction for multiple comparisons n=3 independent experiments each with ~200 nuclei per differentiation stage).

Figure 2.7 Nuclear number compared to percent import positive nuclei The percent of import positive nuclei was compared to the number of nuclei in each myotube for myotubes with 4-17 nuclei. The analysis showed no correlation between nuclear number and percent import positive nuclei. (analyzed by linear regression R^2= 0.07323, n=215 myotubes)

Figure 2.8 cNLS nuclear import and Nup levels A Representative images of the immunocytochemistry of pan FG Nup, Nup358, Kapβ, and RanGAP in *in vitro* generated

myotubes. Bar=20μm. **B** Intensities of pan FG Nup, Nup358, Kapβ, and RanGAP were measured for nuclei in myotubes. Box and whiskers represent median, quartiles, and 5-95% range. No bimodal distributions were identified. **C** Representative image of the *in vitro* nuclear import of cNLS reporter followed by immunofluorescence detection of Nup358. Bar=20μm. **D** The mean intensity of the cNLS reporter and the mean edge intensity of Nup358 was plotted for each nucleus. No correlation was detected between the two variables (R^2=0.0089).

Figure 2.9 Purity of purified recombinant proteins A gel showing representative purified recombinant proteins indicates that the isolated proteins are similar molecular weight and that the recombinant protein is the predominant species.

Figure 2.1

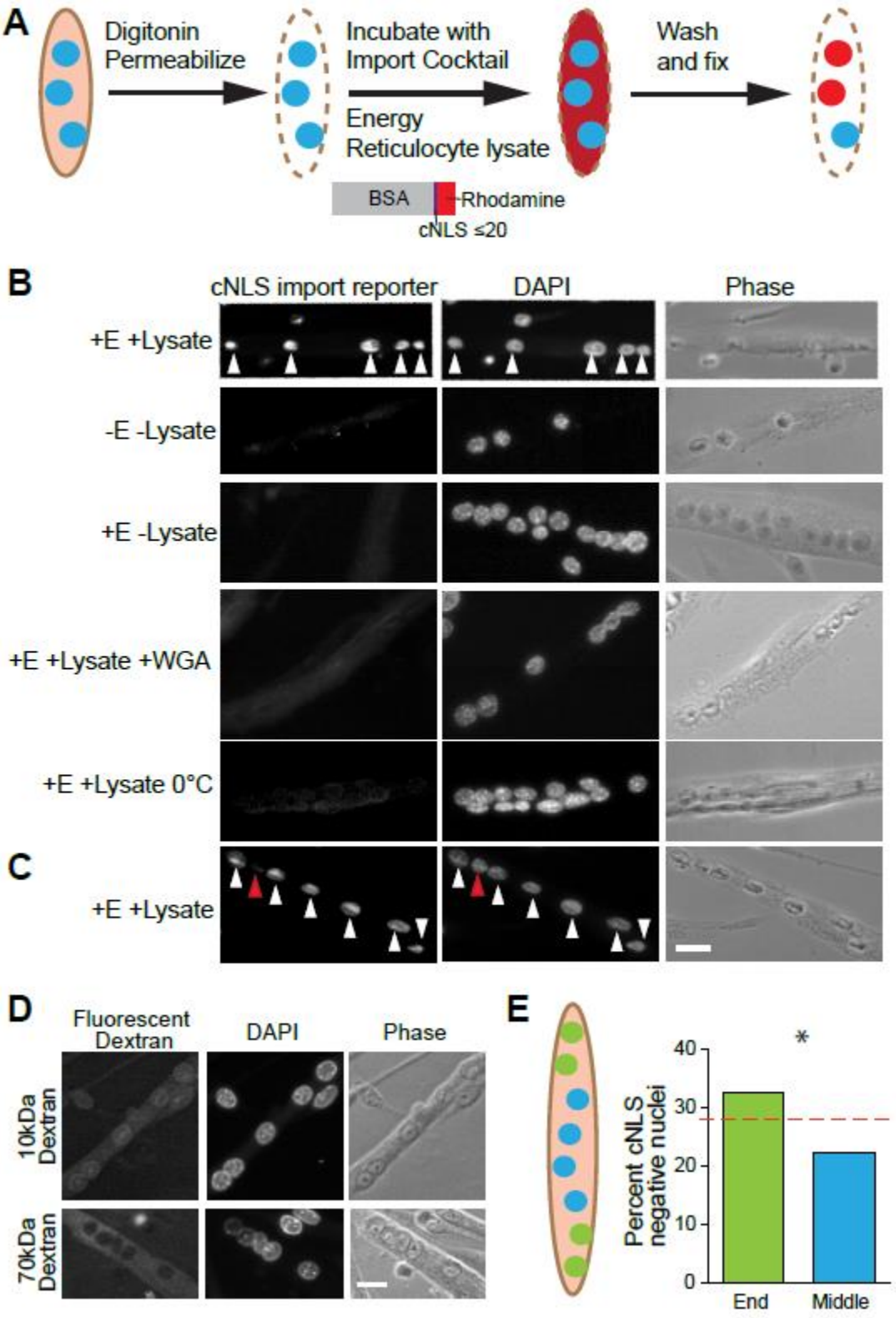
A
Digitonin
Permeabilize
Incubate with
Import Cocktail
Energy
Reticulocyte lysate
Wash
and fix
BSA
Rhodamine
cNLS ≤20
B
cNLS import reporter
DAPI
Phase
+E +Lysate
-E -Lysate
+E -Lysate
+E +Lysate +WGA
+E +Lysate 0°C
C
+E +Lysate
D
Fluorescent
Dextran
DAPI
Phase
10kDa
Dextran
70kDa
Dextran
E
Percent cNLS
negative nuclei
40
30
20
10
0
*
End
Middle

Figure 2.2

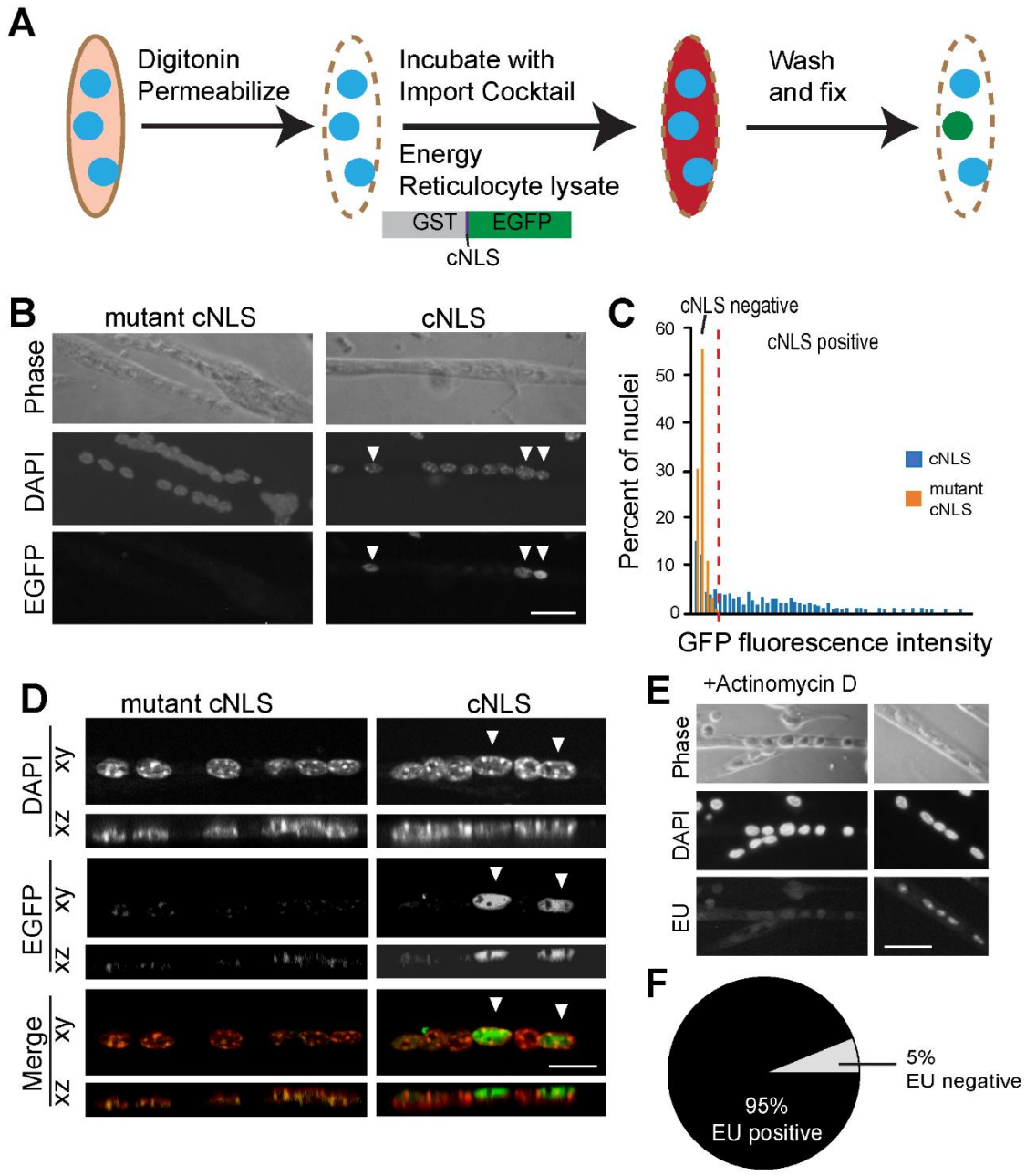
A
Digitonin
Permeabilize
Incubate with
Import Cocktail
Energy
Reticulocyte lysate
Wash
and fix
GST
EGFP
cNLS
B
mutant cNLS
cNLS
Phase
DAPI
EGFP
C
cNLS negative
cNLS positive
Percent of nuclei
60
50
40
30
20
10
0
cNLS
mutant
cNLS
GFP fluorescence intensity
D
mutant cNLS
cNLS
DAPI
EGFP
Merge
xy
xz
E
+Actinomycin D
Phase
DAPI
EU
F
5%
EU negative
95%
EU positive

Figure 2.3

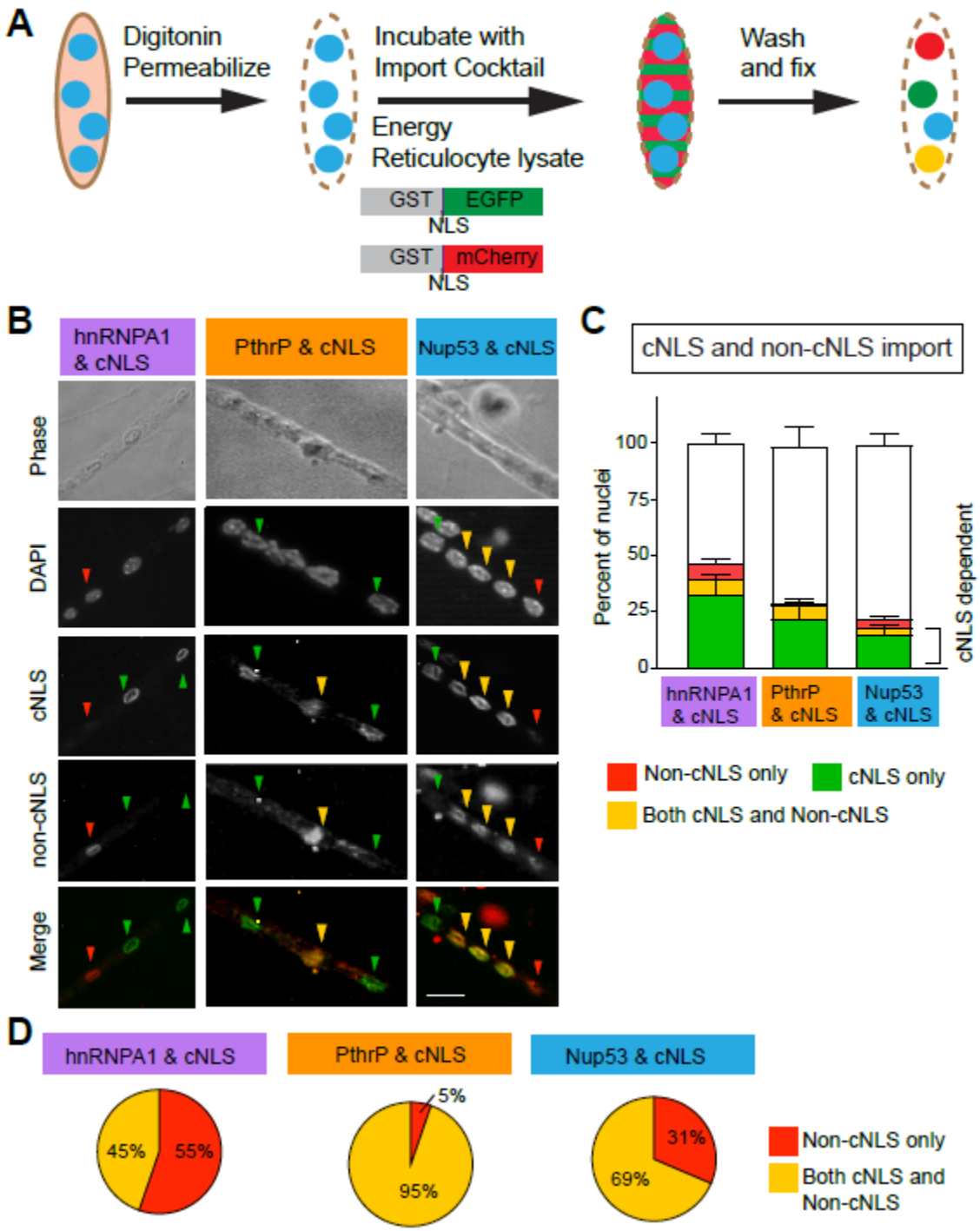
A
Digitonin
Permeabilize
Incubate with
Import Cocktail
Energy
Reticulocyte lysate
Wash
and fix
GST
EGFP
NLS
GST
mCherry
NLS
B
hnRNPA1
& cNLS
PthrP & cNLS
Nup53 & cNLS
Phase
DAPI
cNLS
non-cNLS
Merge
C
cNLS and non-cNLS import
Percent of nuclei
100
75
50
25
0
cNLS dependent
hnRNPA1
& cNLS
PthrP
& cNLS
Nup53
& cNLS
Non-cNLS only
cNLS only
Both cNLS and Non-cNLS
D
hnRNPA1 & cNLS
PthrP & cNLS
Nup53 & cNLS
45%
55%
5%
95%
31%
69%
Non-cNLS only
Both cNLS and
Non-cNLS

Figure 2.4

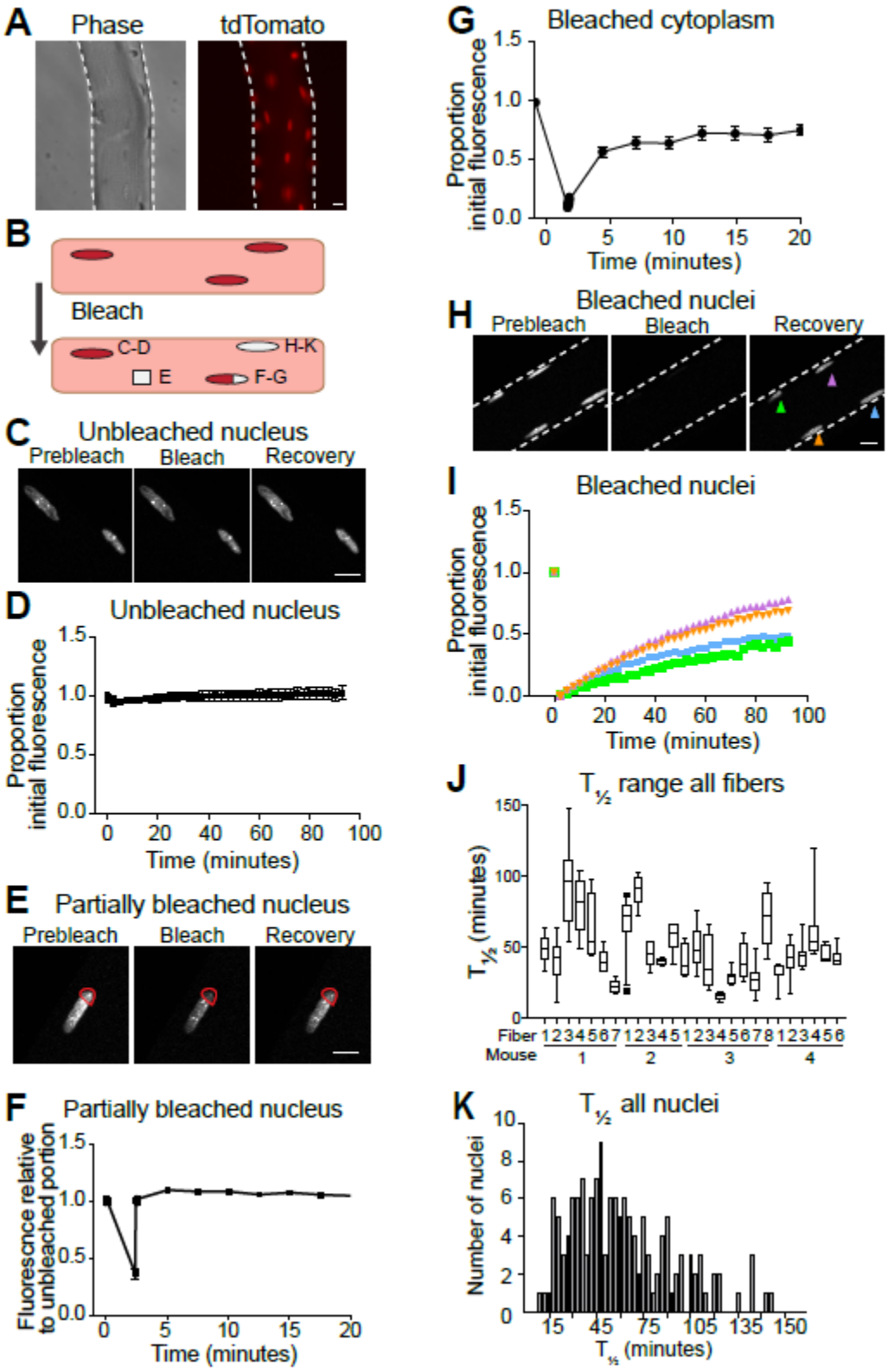
A
Phase
tdTomato
B
Bleach
C-D
H-K
E
F-G
C
Unbleached nucleus
Prebleach
Bleach
Recovery
D
Unbleached nucleus
Proportion initial fluorescence
Time (minutes)
E
Partially bleached nucleus
Prebleach
Bleach
Recovery
F
Partially bleached nucleus
Fluorescnce relative to unbleached portion
Time (minutes)
G
Bleached cytoplasm
Proportion initial fluorescence
Time (minutes)
H
Bleached nuclei
Prebleach
Bleach
Recovery
I
Bleached nuclei
Proportion initial fluorescence
Time (minutes)
J
T½ range all fibers
T½ (minutes)
Fiber
Mouse
K
T½ all nuclei
Number of nuclei
T½ (minutes)

Figure 2.5

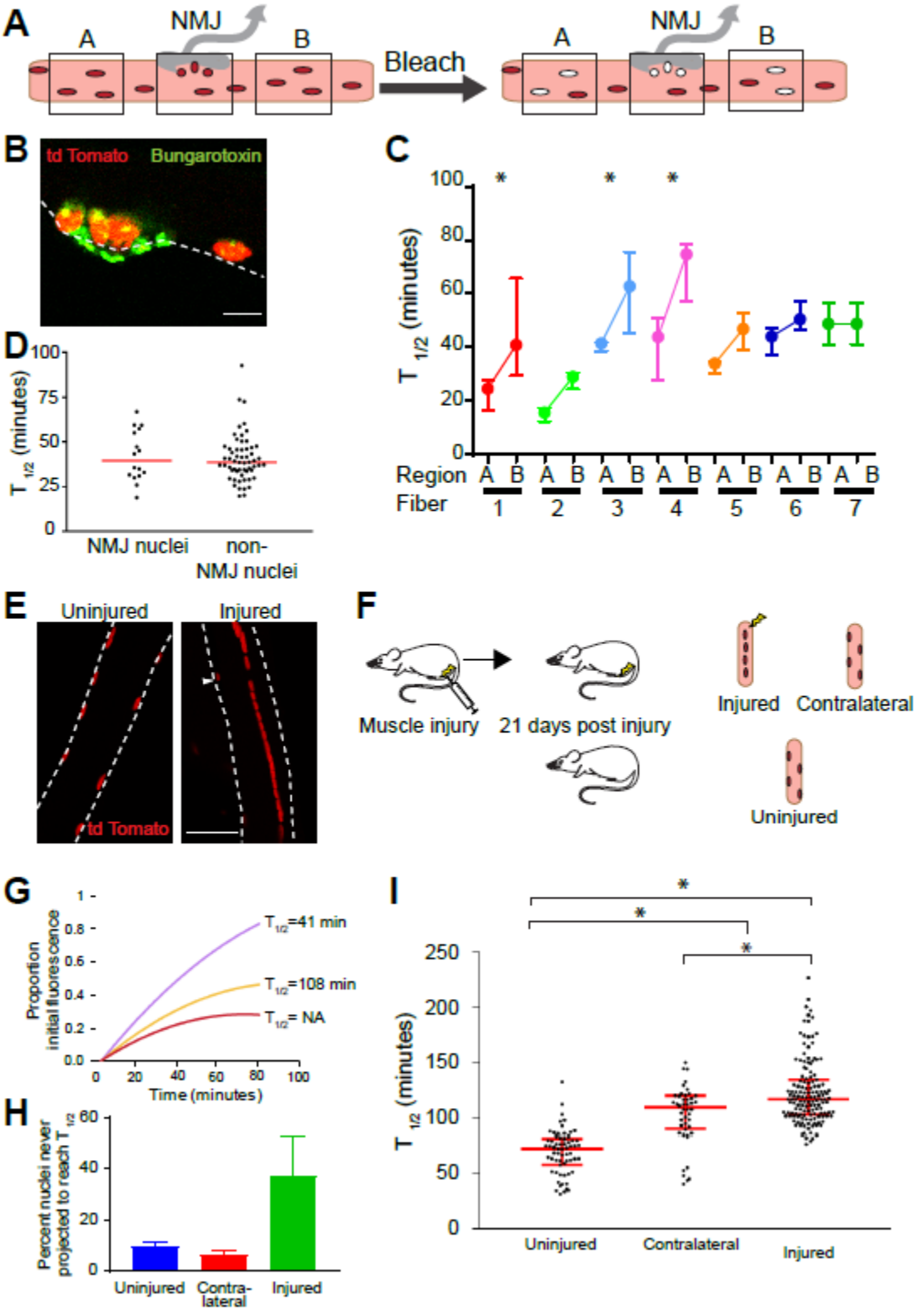
A
NMJ
A
B
Bleach
NMJ
A
B
B
td Tomato
Bungarotoxin
C
100
80
60
40
20
0
T 1/2 (minutes)
Region A B A B A B A B A B A B A B
Fiber 1 2 3 4 5 6 7
D
100
75
50
25
0
T 1/2 (minutes)
NMJ nuclei
non-NMJ nuclei
E
Uninjured
Injured
td Tomato
F
Muscle injury
21 days post injury
Injured
Contralateral
Uninjured
G
Proportion initial fluorescence
1
0.8
0.6
0.4
0.2
0.0
0
20
40
60
80
100
Time (minutes)
T1/2=41 min
T1/2=108 min
T1/2= NA
H
Percent nuclei never projected to reach T 1/2
60
40
20
0
Uninjured
Contra-lateral
Injured
I
250
200
150
100
50
0
T 1/2 (minutes)
Uninjured
Contralateral
Injured

Figure 2.6

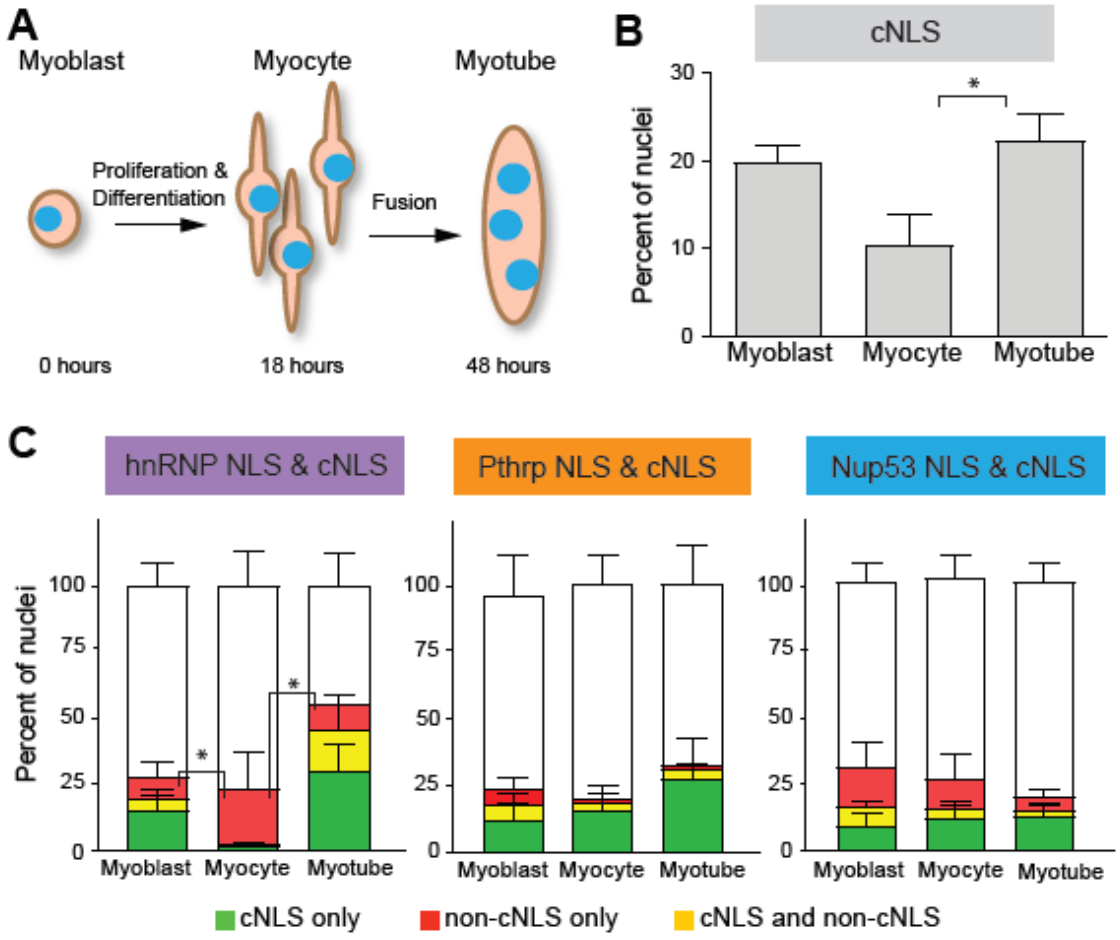
A
Myoblast
Myocyte
Myotube
Proliferation &
Differentiation
Fusion
0 hours
18 hours
48 hours
B
cNLS
Percent of nuclei
30
20
10
0
*
Myoblast
Myocyte
Myotube
C
hnRNP NLS & cNLS
Pthrp NLS & cNLS
Nup53 NLS & cNLS
Percent of nuclei
100
75
50
25
0
*
*
Myoblast
Myocyte
Myotube
cNLS only
non-cNLS only
cNLS and non-cNLS

Figure 2.7

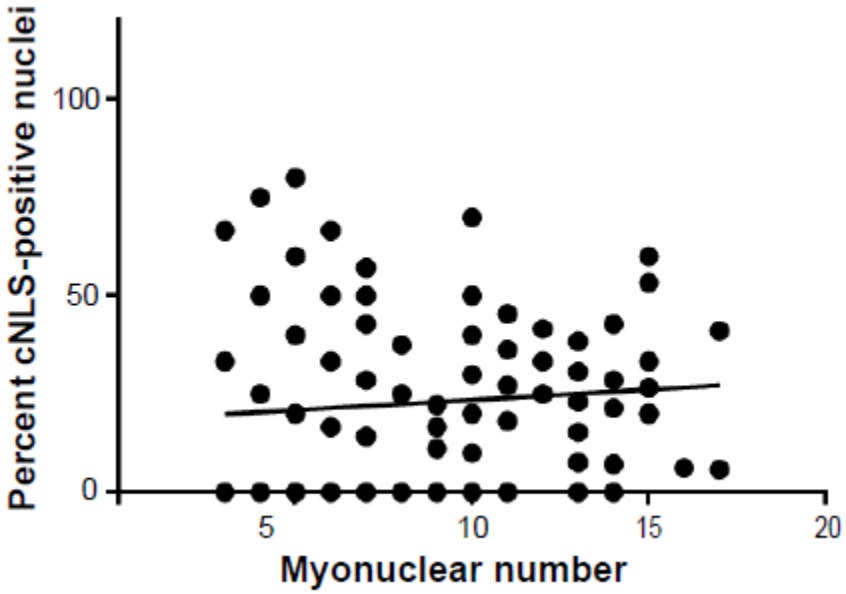
Percent cNLS-positive nuclei
100
50
0
5
10
15
20
Myonuclear number

Figure 2.8

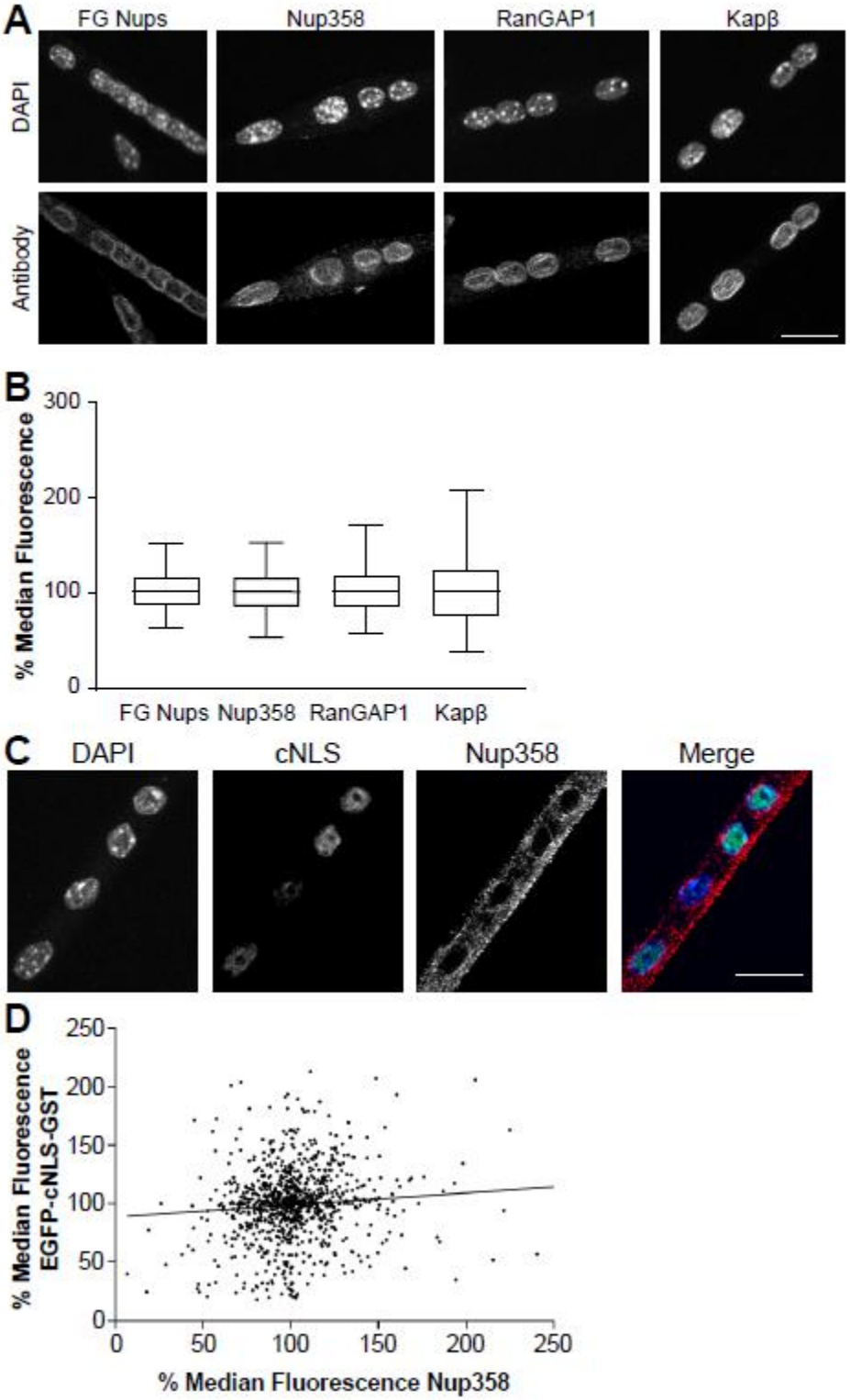
A
FG Nups
Nup358
RanGAP1
Kapβ
DAPI
Antibody
B
% Median Fluorescence
300
200
100
0
FG Nups
Nup358
RanGAP1
Kapβ
C
DAPI
cNLS
Nup358
Merge
D
% Median Fluorescence EGFP-cNLS-GST
250
200
150
100
50
0
0
50
100
150
200
250
% Median Fluorescence Nup358

Figure 2.9

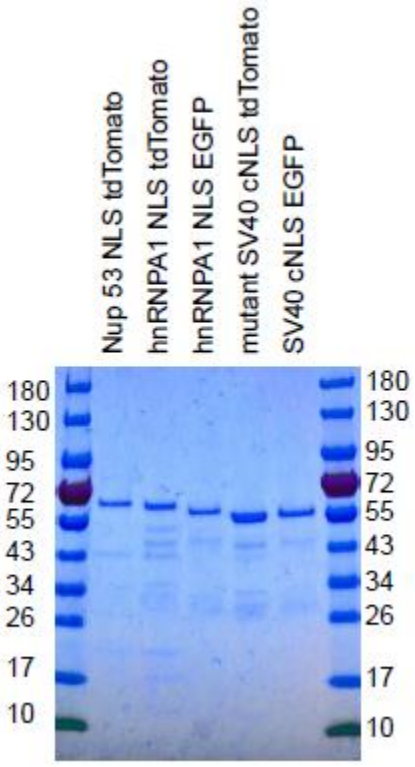
Nup 53 NLS tdTomato
hnRNPA1 NLS tdTomato
hnRNPA1 NLS EGFP
mutant SV40 cNLS tdTomato
SV40 cNLS EGFP
180
130
95
72
55
43
34
26
17
10
180
130
95
72
55
43
34
26
17
10

Chapter 3: Biochemical isolation of myonuclei employed to define changes to the myonuclear proteome that occur with aging

A portion of this chapter is published as:

Cutler, A.A., E.B. Dammer, D.M. Doung, N.T. Seyfried, A.H. Corbett, G.K. Pavlath, *Biochemical isolation of myonuclei employed to define changes to the myonuclear proteome that occur with aging.* Aging Cell (2017) **16**(4): 738-749.

Chapter 3: Biochemical isolation of myonuclei employed to define changes to the myonuclear proteome that occur with aging

3.1 Summary

Skeletal muscle aging is accompanied by loss of muscle mass and strength. Examining changes in myonuclear proteins with age would provide insight into molecular processes which regulate these profound changes in muscle physiology. However, muscle tissue is highly adapted for contraction and thus comprised largely of contractile proteins making the nuclear proteins difficult to identify from whole muscle samples. By developing a method to purify myonuclei from whole skeletal muscle, we were able collect myonuclei for analysis by flow cytometry, biochemistry, and mass spectrometry. Nuclear purification dramatically increased the number and intensity of nuclear proteins detected by mass spectrometry compared to whole tissue. We exploited this increased proteomic depth to investigate age-related changes to the myonuclear proteome. Nuclear levels of 54 of 779 identified proteins (7%) changed significantly with age; these proteins were primarily involved in chromatin maintenance and RNA processing. To determine if the changes we detected were specific to myonuclei or were common to nuclei of excitatory tissues, we compared aging in myonuclei to aging in brain nuclei. Although several of the same processes were affected by aging in both brain and muscle nuclei, the specific proteins involved in these alterations differed between the two tissues. Isolating myonuclei allowed a deeper view into the myonuclear proteome than previously possible facilitating identification of novel age-related changes in skeletal muscle. Our technique will enable future studies into a heretofore underrepresented compartment of skeletal muscle.

3.2 Introduction

Skeletal muscle, which is essential for critical processes such as movement, swallowing, and breathing, dynamically adapts to the body's needs by altering gene expression to accommodate physiological states such as muscle growth, regeneration, and aging. To date, investigations into molecular mechanisms driving shifts in gene expression have been largely candidate-based. Examining global changes in myonuclear proteins would provide insight into molecular processes regulating large-scale shifts in gene expression that accompany physiologic changes in muscle.

Aging leads to profound changes in skeletal muscle. Starting around age 30 and increasing after age 60, muscle mass and strength decline. The resulting frailty is associated with reduced mobility and greater risk of falls (Demontis, Piccirillo et al. 2013). Global changes in RNA levels with age have been identified (Zahn, Sonu et al. 2006, Kim, Park et al. 2014, Su, Ekman et al. 2015), however, large-scale proteomic analysis has been limited to the most abundant proteins. While many cell types support skeletal muscle function, the tissue is comprised primarily of myofibers, large, multinucleated cells densely packed with contractile proteins necessary for muscle function. Over half of the total protein in a muscle cell is either actin or myosin (Deshmukh, Murgia et al. 2015). This lack of heterogeneity in muscle tissue makes proteomic studies that span a large dynamic range of protein abundances technically challenging.

Limited information exists on the dynamic alterations of myonuclear protein levels during aging or other physiologic states. Myonuclear proteins are difficult to study with an unbiased approach because 1) nuclear proteins make up a small minority of proteins in skeletal muscle tissue due to the high abundance of contractile proteins, 2) myonuclei are

challenging to isolate because skeletal muscle is difficult to disrupt without damaging myonuclei and 3) dense debris co-sediments with nuclei contaminating the nuclear fraction. In addition, muscle tissue is comprised of multiple cell types. Existing approaches do not provide sufficient enrichment to interrogate low abundance nuclear proteins, require large amounts of starting material, or necessitate genetic tagging of specific nuclei and have no mechanism of determining what proportion of isolated nuclei are myonuclei. An approach that would sufficiently enrich myonuclear proteins to allow unbiased interrogation would offer a new avenue to examine the molecular mechanisms regulating physiologic states in skeletal muscle.

By developing a method of purifying myonuclei from relatively small amounts of mouse muscle tissue, we were able to collect myonuclei for analysis by flow cytometry, biochemistry, and proteomics. Purification of myonuclei dramatically increased both the number and intensity of nuclear proteins detected compared to whole muscle tissue. Querying changes to the myonuclear proteome associated with aging revealed that nuclear levels of RNA processing proteins, nuclear transport proteins, and proteins regulating transcription increased with age. When compared to brain nuclei, many of the same processes were affected in both tissues with age, although the individual proteins that change differed between tissues. Our approach of isolating myonuclei will provide a useful tool for future studies of myonuclear changes in different physiologic states of skeletal muscle.

3.3 Results

3.3.1 Isolation of pure intact nuclei

To facilitate biochemical and molecular analyses of myonuclei, we optimized a technique to isolate intact nuclei with high purity from single mouse muscles (Figure 3.1A). To isolate nuclei, the muscle was gently homogenized. After preparation of a crude nuclear fraction by filtration and low speed centrifugation, a purified nuclear fraction was obtained by ultracentrifugation over a discontinuous two-step sucrose gradient. Nuclei collect at the interface between the two sucrose cushions with cytoplasmic material above the first cushion and the denser myofibrils under the second cushion. The nuclear fraction was collected and analyzed by downstream methods. The average time required for preparation of a nuclear sample was 5.5 hours. The average yield from a single mouse gastrocnemius (GA) muscle was $1x10^6$ nuclei, whereas pooling two GA and two rectus femoris (RF) muscles yielded $6x10^6$ nuclei and 8 µg of total protein.

The isolated nuclei were stained by 4',6-diamidino-2-phenylindole (DAPI) and were free of visible debris when examined by light microscopy (Figure 3.1B). The nuclear envelope must remain intact to retain nuclear proteins for examination after purification. To determine whether the nuclear envelope was breached in the purification process, we challenged the nuclei with FITC-conjugated 500 kDa dextran, which is excluded from nuclei with intact envelopes (D'Angelo, Raices et al. 2009). Nuclei were incubated with the dextran and analyzed by fluorescence microscopy. We found that 93% of isolated nuclei excluded the fluorescent dextran and thus had intact nuclear envelopes (Figure 3.1C). To further examine whether soluble nuclear proteins were retained during isolation, and to determine the enrichment of nuclear proteins and depletion of proteins from other

cellular organelles in the nuclear fractions, we immunoblotted total muscle tissue, as well as cytoplasmic and nuclear fractions (Figure 3.1D, for full blots see Fig. S1). Proteins from various nuclear compartments were enriched in the nuclear fraction including the nuclear envelope (Nup 214, a nuclear pore protein), the soluble fraction (RNA binding protein HuR) and chromatin (Histone H3). Immunoblotting for markers of mitochondrial, endoplasmic reticulum (ER), and cytoplasmic compartments, revealed that nuclear fractions were free of mitochondrial (Porin) and cytoplasmic (Tubulin) markers and depleted for the ER marker Calnexin, though calnexin depletion was variable. Together, these results indicate that nuclei isolated using this method retain nuclear proteins, are depleted of other organelles, and have intact nuclear envelopes.

3.3.2 Isolated nuclei are predominantly myonuclei

As muscle tissue contains multiple cell types, we assessed what percentage of nuclei purified from muscle tissue were myonuclei by performing flow cytometry using myonuclear-specific markers. TMEM38A is an outer nuclear envelope transmembrane protein expressed in excitatory cells with highest levels in myofibers (Bleunven, 2008). We took advantage of this property to use TMEM38A as a marker of myonuclei. Immunofluorescence analysis of isolated nuclei revealed that while all intact nuclei were labeled with a marker of the nuclear pore complex (mAb414), not all nuclei examined were positive for TMEM38A (Figure 3.2A). Subsequently, we analyzed immunostained nuclei by flow cytometry. Singlet nuclei were identified by DAPI labeling and side scatter (SSC) and were gated for further analysis (Figure 3.2B). To determine what percentage of intact nuclei was TMEM38A positive ($TMEM38A^{+}$), we gated on mAb414 positive ($mAb414^{+}$)

nuclei. Of this mAb414^{+} population of nuclei, 96.4% ± 3.2 SE were TMEM38A^{+} (Fig 2C). While a bright and a dim population of TMEM38A^{+} nuclei were observed, both populations were distinct from nuclei labeled with control IgG (inset Figure 3.2C). As TMEM38A localizes both to the nucleus and the sarcoplasmic reticulum (SR), the bright and dim populations of TMEM38A^{+} nuclei are likely the result of variable amounts of SR associated with isolated nuclei.

To confirm that the TMEM38A antibody specifically labels myonuclei, we took advantage of genetic labeling using the nTnG mouse model which contains a transgene with nuclear targeted tdTomato and eGFP (Prigge, Wiley et al. 2013). As illustrated in Figure 3.2D, the transgene is composed of a floxed nuclear localization signal (NLS)-containing tdTomato gene followed by a stop codon; outside the floxed region is an NLS-containing eGFP gene. Prior to Cre-mediated recombination, the ubiquitously expressed tdTomato labels all nuclei. Upon recombination, the tdTomato gene and stop codons are excised and eGFP labels the nuclei of recombined cells. We bred these nTnG mice to mice expressing Cre recombinase under control of the muscle creatine kinase promoter (*Ckmm*)(Bruning, Michael et al. 1998). In the offspring of this cross, myonuclei are eGFP positive (eGFP^{+}) while all other nuclei are tdTomato positive (tdTomato^{+}). To confirm the specificity of myonuclear labeling in these offspring, we isolated single myofibers from GA muscles and visualized by fluorescence microscopy (Figure 3.2E). All myonuclei within single myofibers were eGFP^{+} with only a few tdTomato^{+} cells on each myofiber. The fluorescent labels were retained during nuclear purification (Figure 3.2F), making them reliable markers for subsequent flow cytometry analyses.

To compare the specificity of the two myonuclear markers, nuclei were isolated from the muscles of Cre^+ nTnG mice and wild type mice, immunostained for TMEM38A or control IgG, and analyzed by flow cytometry (Figure 3.2G). On average, 85.5% ± 5.2 SE of total nuclei were positive for both TMEM38A and eGFP, indicating that the vast majority of purified nuclei were myonuclei. As previously observed (Figure 3.2C), both bright and dim populations of TMEM38A were distinct from the control IgG-labeled wild type nuclei (inset Figure 3.2G). To rule out the possibility that a subset of non-myonuclei were labeled with TMEM38A, we further analyzed the $TMEM38A^+$ nuclei and found that 99.7% ± 0.03 SE were $eGFP^+$, indicating that TMEM38A labels myonuclei (Figure 3.2H). Taken together these results indicate that nuclei isolated by this method from skeletal muscle tissue are at least 85.5% ± 5.2 SE myonuclei.

3.3.3 Increased depth of proteomic detection in myonuclear proteome

We next compared the proteomes of whole muscle tissue samples and isolated nuclear samples using mass spectrometry. Nuclei were purified from GA and RF muscles pooled from three mice. Of 1771 proteins detected in purified nuclear samples, 906 were not detected in whole muscle samples; similarly, 921 of 1786 proteins detected in the whole muscle samples were not detected in isolated myonuclei. We compared the average peptide LC peak intensity area for biological duplicates of nuclear and whole muscle samples and determined that nuclear samples were distinct from whole muscle samples (Figure 3.3A). The most enriched proteins in purified nuclei clustered predominately to Kyoto Encyclopedia of Genes and Genomes (KEGG) pathways in RNA processing while the most depleted proteins clustered to KEGG pathways were involved in metabolism (Figure

3.3B). Of proteins detected in the isolated nuclei samples, 59% were classified as nuclear by gene ontology (GO) analysis using the Database for Annotation, Visualization and Integrated Discovery (DAVID). This is nearly double the 36% classified as nuclear in whole muscle tissue samples where sarcomeric and mitochondrial proteins were the most abundant proteins detected (for a full list of identified proteins, see Table S1). As illustrated in Figure 3C, nuclear proteins were dramatically enriched in nuclei samples compared to whole muscle tissue, even among relatively low enriched proteins, while proteins from other cellular compartments were depleted in all but the highest percentiles for that compartment. The cytoplasmic proteins enriched in the 90^{th} percentile were predominately keratins, which could have been introduced due to handling of the purified nuclei samples. These results establish the compatibility of the nuclear isolation procedure with downstream analysis by mass spectrometry, highlight the increased proteomic depth of nuclear proteins afforded by nuclear isolation, and represent a detailed myonuclear proteome.

3.3.4 The myonuclear proteome changes with age

Given the impact that aging has on skeletal muscle function (Demontis, Piccirillo et al. 2013) and gene expression (Zahn, Sonu et al. 2006) and confident in our ability to isolate high purity myonuclei in quantifiable amounts, we applied this approach to investigate changes in the myonuclear proteome with aging. We isolated nuclei from GA and RF muscles of young (3 month) and old (24 month) mice and analyzed the samples by mass spectrometry. Muscles were pooled from two mice and five replicates were analyzed for each age. After imputation and correction for batch effect, samples were compared

based on p-value and mean fold change. As in the previous experiment, 60% of the proteins detected were classified as nuclear by GO.

The levels of 54 of 779 identified proteins (7%) changed significantly with age (Figure 3.4A, full list in Table S2). Because the samples are fractionated, we cannot distinguish overall changes in steady state protein levels from a change in nuclear distribution. Of the significantly changed proteins ($p<0.05$, fold change >1.5), 43 were more abundant in nuclei from old muscle, 1.5-7 fold higher than young muscle levels, and 11 were less abundant, 1.5-4.5 fold lower than young muscle levels (Table 3.1). The two categories with the most changed proteins were chromatin maintenance and RNA processing (Figure 3.4B). The changes, both increases and decreases, in levels of proteins related to chromatin maintenance suggest general epigenetic changes with aging. In addition to age-related increases in levels of RNA processing proteins, levels of proteins associated with transcriptional regulation increased, suggesting overall changes in transcript production and/or processing. Nuclear transport protein levels also increased, potentially indicating alterations in nuclear transport and potentially consequential mislocalization of proteins. Ribosomal protein levels also increased with age, which could be related to changes in ribosome assembly and/or altered nuclear transport or increased rough ER contribution to the aged nuclei fraction. Of the changed proteins from non-nuclear cellular compartments, most proteins were classified as plasma membrane proteins and mitochondrial proteins. That these proteins change could reflect age-related changes in the overall protein abundance or a differential association with young and old myonuclei. These data show that nuclear levels of markers of diverse nuclear processes including

chromatin organization, RNA processing, and nuclear transport, are altered during aging of mouse skeletal muscles.

3.3.5 Myonuclei share common aging pathways with brain nuclei

To investigate whether the changes to the myonuclear proteome reflect general age-related changes or muscle-specific changes, we compared the age-related changes in myonuclei to those observed in brain nuclei, another excitatory, long lived, post-mitotic tissue. We isolated and processed brain nuclei from young (3 month) and old (24 month) mice as described above for myonuclei. By immunoblotting, isolated brain nuclei were free of contamination from mitochondrial and cytoplasmic compartments (Fig S2). Similar to the myonuclear samples, 61% of the proteins identified from brain nuclei were classified as nuclear by GO. Analysis revealed that levels of 32 of 845 identified proteins (4%) changed significantly ($p<0.05$, >1.5 fold change) between young and old brain nuclei (Figure 3.5A). Of the changed proteins, 21 were increased in abundance in aged brain nuclei, 1.5-3 fold compared to young brain levels, while 11 decreased, 1.5-10 fold compared to young brain levels (Table 3.2). Similar to the changes detected in myonuclei with age, the majority of these proteins were related to chromatin maintenance and RNA processing (Figure 3.5B).

Several cellular processes changed with age in nuclei from both brain and muscle (Figure 3.5C). Brain and muscle nuclei shared increases in markers of transcription, and RNA processing with age as well as overall changes in chromatin maintenance markers, supporting the concept that these are common pathways affected in aging. Two pathways were uniquely changed in nuclei from aged muscle versus brain. Nuclear lamin levels

increased in aged brain nuclei but not myonuclei, while ribosomal proteins increased with age in myonuclei, but not brain nuclei. Despite the similarity in changed processes, the only protein significantly changed with age in both tissues was RCC1 (Figure 3.5D), which increased more than 2 fold in aged nuclei in both tissues. RCC1 is the major guanine nucleotide exchange factor for Ran, helping to establish the Ran GTP gradient, which is the driving force in nucleocytoplasmic transport (Izaurralde, Kutay et al. 1997). This increase in RCC1 in both aged brain and muscle nuclei may suggest age-related changes in nuclear transport (Figure 3.5C) in both tissues.

While some of the same processes were affected by aging in both brain and muscle nuclei, the specific proteins that changed differed between the two tissues. Most of the proteins that changed in the nuclei of either tissue were detected in both tissues but only changed in one (Figure 3.5D): 49 of 54 proteins (91%) that changed in muscle were detected in brain nuclei and 24 of 32 proteins (75%) that changed in brain nuclei were detected in myonuclei. Indeed, when examining the proteins that significantly change with aging in each tissue, it is clear that in individual proteins change with age quite differently in brain than in muscle (Figure 3.5E). The increase in protein levels of Ylpm1, Kpnb1, and RCC1 were verified by western blot of young and old myonuclear lysates (Figures 3.5F, G). Taken together, comparison of the nuclear proteomes of muscle and brain suggest that tissue specific, as well as common pathways, such as epigenetic regulation, RNA processing, and nuclear transport, are altered with age.

3.4 Discussion

In this study, we present a method optimized to yield high purity myonuclei from relatively small samples for downstream analysis by flow cytometry, biochemistry, and mass spectrometry. We exploited this approach to interrogate the myonuclear proteome and investigate changes to the myonuclear proteome that occur with age.

Isolating nuclei from skeletal muscle has historically been difficult. Several researchers have developed approaches to isolate nuclei from skeletal muscle, each technique optimized for a downstream application like ChIP (Ohkawa, Mallappa et al. 2012), analysis of nuclear envelopes (Wilkie and Schirmer 2008), or comparison of multiple cellular compartments (Dimauro, Pearson et al. 2012). Our goal was to develop an isolation technique compatible with downstream analysis by flow cytometry and mass spectrometry using relatively small sample sizes to preserve biological variability. Our approach results in high purity myonuclei isolated from a single GA or RF muscle sufficient for analysis by flow cytometry and pooled GA and RF muscles from two mice sufficient for analysis by mass spectrometry. The isolated nuclei are impermeable to large dextrans, indicating that the nuclear envelopes remain intact, and soluble nuclear proteins such as transcription factors and RNA processing enzymes are readily detectable. Both results indicate that the nuclei do not undergo major loss of protein during purification.

Genetic labeling approaches could complement our biochemical fractionation strategy. Fluorescent labeling using nTnG transgenic mice as used here combined with fluorescent activated nuclear sorting or a recently developed approach termed Isolation of Nuclei Tagged in specific Cell Types (INTACT) (Deal and Henikoff 2011, Jankowska, Latosinska et al. 2016) could increase purity of isolated myonuclei. However, both methods

require generation of new mouse strains for each cell type of interest. Thus, our biochemical isolation has the advantage of isolating a high percentage of myonuclei without genetic labeling.

Using biochemical fractionation, we dramatically enriched the nuclear proteome from skeletal muscle. In many tissues, nuclear proteins are readily detectable by proteomics in unfractionated tissue. Nuclear proteins in skeletal muscle are underrepresented because they comprise a small percentage of the overall muscle proteome (Table S3). Consistent with a previous report (Deshmukh, Murgia et al. 2015), we find that >60% of the proteins identified by mass spectrometry of whole muscle tissue are contractile proteins. Others have employed various approaches to increase proteomic detection of non-contractile proteins in skeletal muscle including depletion of contractile proteins (Carberry, Zweyer et al. 2014, Gueugneau, Coudy-Gandilhon et al. 2014) and enriching less detected proteins (Gannon and Ohlendieck 2012). While these approaches have enriched some non-contractile proteins, they identified few nuclear proteins. Our study offers the first systematic examination of the myonuclear proteome, identifying 535 annotated nuclear proteins by GO, and provides tools for others to interrogate changes in this important cellular compartment.

As muscles age, muscle mass and function decrease and myofibers undergo fiber type switching. Proteomic studies of aging muscle have described alterations in the most abundant proteins in muscle: contractile and metabolic proteins (Baraibar, Gueugneau et al. 2013). Microarray and RNAseq experiments have identified major shifts in transcript levels as muscles age (Zahn, Sonu et al. 2006, Kim, Park et al. 2014, Su, Ekman et al. 2015). To investigate how aging affects myonuclei at the protein level, we compared the

myonuclear proteomes of young and old mice. Some of the changes we detected in protein levels mirror changes in transcript levels: transcript levels of RNA binding proteins Hnrnpr (Welle, Brooks et al. 2003), Srsf5, Paf1, and Ddx41 (Su, Ekman et al. 2015), a chromatin maintenance protein Ssrp1 (Su, Ekman et al. 2015), and a nuclear transport protein Kpnb1 (Swindell 2009) increase with age consistent with changes we observed in protein levels. Protein levels of the RNA binding protein Khdrbs1 also increase with age (Laohavinij 2015). In addition to these specific proteins, transcript levels for RNA processing machinery genes in general increase with age (Gheorghe, Snoeck et al. 2014). Similarly, we identified an increase in RNA binding protein levels within the nucleus with age. Our data showed an increase in ribosomal proteins in myonuclei with age. Others have characterized increases in transcript levels of ribosomal proteins (Calura, Cagnin et al. 2008, Fedorov, Goropashnaya et al. 2014) and decreased ribosome biogenesis (Kirby, Lee et al. 2015) with age. While our results could reflect increased ER contribution to the nuclear fraction from older mice, they could also support abnormalities in ribosome biogenesis or export. With our method of enriching nuclear proteins, we were able to investigate the myonuclear proteome at greater depth than previously possible and identify novel myonuclear age-related changes.

To determine whether the age-related changes we detected in the myonuclear proteome were common to nuclei of other excitatory post-mitotic tissues, we compared aging in brain and muscle nuclei. Previous comparisons of transcript levels from whole skeletal muscle and neuronal tissues with aging predominantly identified common changes in metabolism (Capitanio, Vasso et al. 2009, Gheorghe, Snoeck et al. 2014), chromatin maintenance, and RNA processing (Gheorghe, Snoeck et al. 2014, Su, Ekman et al. 2015).

We likewise detected age-related changes in proteins involved in chromatin maintenance and RNA processing in nuclei from both brain and muscle. In addition, we identified changes in transcription. While the same processes were affected in nuclei from both tissues, Rcc1 was the only protein that increased with age in nuclei from both tissues. RCC1 helps establish the Ran GTP gradient necessary for nucleocyotoplasmic transport (Izaurralde, Kutay et al. 1997). Increased Rcc1 activity increases DNA damage repair and reduces senescence, suggesting a role in aging (Cekan, Hasegawa et al. 2016). While pathways were shared between nuclei from both tissues, the individual proteins that changed differed, which is consistent with a previous study in which aging affected the same pathways in two hind-limb muscles but via different proteins (Chaves, Carvalho et al. 2013).

In summary, our approach to isolating myonuclei allowed a deeper view into the myonuclear proteome than previously possible. Muscle-specific changes that occur with aging in nuclear proteins could offer new insight into processes contributing to age-related muscle loss. Isolating and interrogating myonuclei will also allow investigation into nuclear processes involved in muscle growth, regeneration, and response to disease. In addition to examining changes in the proteome, one could isolate myonuclei to interrogate the nascent transcriptome and other nuclear processes difficult to detect over cytoplasmic background. Our technique will enable future studies into a heretofore underrepresented compartment of skeletal muscle.

3.5 Experimental Procedures

Mice

Wild type C57BL6 mice were obtained from Charles River laboratories (Willmington, MA) and the National Institute of Aging. nTnG mice containing an allele for nuclear targeted tdTomato and eGFP reporter proteins (B6N.129S6-Gt(ROSA)26Sor$^{tm1(CAG-tdTomato*,-EGFP*)Ees}$/J) (Prigge, Wiley et al. 2013) were purchased from Jackson Laboratory (Bar Harbour, ME). These mice were bred to mice expressing Cre recombinase under control of the muscle creatine kinase promoter (B6.FVB(129S4)-Tg(Ckmm-cre)5Khn/J) (Bruning, Michael et al. 1998), also purchased from Jackson Laboratory. The genotype of the offspring was determined using PCR protocols available on the Jackson Laboratory website.

All experiments were performed using tissues from 3-24 month-old male C57BL6 mice or 3-6 month-old male mice homozygous for the nTnG transgene and heterozygous for Cre recombinase. Experiments were performed in accordance with approved guidelines and ethical approval from Emory University's Institutional Animal Care and Use Committee and in compliance with the National Institutes of Health.

Nuclear isolation

The procedure described below was extensively modified from (Wilkie and Schirmer 2008) to achieve sufficient sample quantity and quality for analysis by flow cytometry (a single mouse GA or RF) and mass spectrometry (pooled GA and RF from 2-3 mice). All steps were carried out at 4°C.

Whole brain or GA and RF muscles were dissected, minced, and suspended in 10 ml homogenization buffer 1 (10 mM HEPES, 60 mM KCL, 0.5 mM spermidine, 0.15 mM spermine, 2 mM EDTA, 0.5 mM EGTA, 300 mM sucrose, 5 mM $MgCl_2$, 2 mM dithiothreitol (DTT), 5% complete mini protease inhibitors (CMP) (Roche Diagnostics, Risch-Rotkreuz, Switzerland)). Subsequently, muscles were homogenized with 20-25 strokes using a 15 ml PTFE tissue grinder with clearance 0.15-0.25 mm (VWR, Radnor, PA). The homogenate was filtered (40 µm) and centrifuged at 1000xg for 10 minutes, yielding a crude nuclear pellet. The pellet was resuspended in 3 ml 1.7 M sucrose with two strokes of the dounce homogenizer and loaded over a two-step sucrose cushion: 2.8 M sucrose and 2.0 M sucrose in 50 mM HEPES, 25 mM KCl, 5 mM $MgCl_2$. The sample was centrifuged for 3 hours at 33000 RPM in a SW41Ti rotor in a Beckman Optima LE-80k ultracentrifuge. For larger preparations for proteomics, nuclei were isolated with the same gradient but centrifuged with a SW32Ti rotor in a Beckman Optima LE-80k centrifuge at 32000 RPM for 195 minutes and buffers were supplemented with 1x HALT protease and phosphatase inhibitor (Thermo Scientific, Waltham, MA).

After ultracentrifugation, the nuclei concentrated at the interface between the 2.0 M and 2.8 M sucrose layers were collected, diluted 1:15 with resuspension buffer (20 mM HEPES, 10 mM KCl, 1.5 mM $MgCl_2$, 0.5 mM spermidine, 0.15 mM spermine, 0.2 mM EDTA, 5% CMP (Roche Diagnostics)) and mixed thoroughly by inverting. For optimal yield, the nuclear fraction was collected into conical tubes pretreated with 1% bovine serum albumin (BSA) to prevent nuclei sticking to tube walls. The nuclei were pelleted at 3000xg for 15 minutes. The small clear pellet was washed in resuspension buffer and pelleted at

2000xg for 5 minutes. For biochemistry and mass spectrometry, the pellet was washed 2 more times to remove residual BSA.

To assess the integrity of isolated nuclei, a 10 µl aliquot of nuclei was stained with 1 µg/ml DAPI and 60 µg/ml 500kD fluorescein isothiocyanate (FITC)-conjugated dextran (Sigma-Aldrich, St. Louis, MO) and examined by fluorescence microscopy Nuclei were scored for exclusion of the dextran by fluorescence microscopy (D'Angelo, 2009).

Immunoblotting

GA and RF muscles were dissected and either homogenized in homogenization buffer 2 (150 mM NaCl, 1% NP-40, 0.5% sodium deoxycholate, 0.1% sodium dodecyl sulfate, 50 mM Tris pH8, 5% CMP (Roche Diagnostics) or processed to isolate nuclei as described above. The cytoplasmic fraction was retained after the first centrifugation step. Equal protein content (Bradford 1976) was resolved by SDS-PAGE electrophoresis. Proteins were transferred to nitrocellulose membranes and detected with antibodies (Table S4) and enhanced chemiluminescence.

Single myofiber isolation

GA muscles were dissected and processed as described previously (Pichavant and Pavlath 2014). Briefly, muscles were enzymatically digested, single myofibers transferred to multi-well plates and fixed with paraformaldehyde.

Flow cytometry

Isolated nuclei were incubated with antibodies (see Table S4 for antibodies and dilutions) or appropriate isotype controls for 30 minutes on ice, then washed and incubated with secondary antibodies for 30 minutes on ice. Nuclei were stained with 1 µg/ml DAPI immediately before analysis. After gating on $DAPI^+$ nuclei, 20000 nuclear events from each sample were analyzed for Texas Red, AF647, and eGFP fluorescence using a BD LSRII flow cytometer. Analyses of flow cytometry data were performed using FlowJo (version X 10.0.7r2).

LC-MS/MS analysis

Samples were processed following established protocols (Wang, 2016). For a detailed description see supplemental methods. Briefly, 50 µg from each sample was subjected to in-solution trypsin digest (Herskowitz, Seyfried et al. 2010). Peptide mixtures were separated by a NanoAcquity UHPLC (Waters, Milford, FA) and monitored on a Orbitrap Fusion mass spectrometer (ThermoFisher Scientific, San Jose, CA). The mass spectrometer cycle was programmed for "top speed acquisition" with a cycle time of 3 seconds.

Label-free proteomic quantification

For a detailed description of quantification, see supplemental methods. Briefly, for analysis of purified myonuclei compared to whole muscle samples, raw files were searched against the mouse UniPort reference database using SEQUEST algorithm through Proteome Discoverer 2.0 platform (Thermo Scientific, Bremen, Germany). The embedded

Percolator algorithm (Kall, Storey et al. 2008) was used to filter the peptide spectral matches to achieve a false discovery rate (FDR) of < 1%. For analysis of age-related proteomic changes in myonuclei and brain nuclei, data were analyzed using MaxQuant v1.5.2.8 with Thermo Foundation 2.0 for RAW file reading capability. The search engine Andromeda was used to build and search a concatenated target-decoy mouse UniProt Knowledgebase (UniProtKB) (53,289 target sequences downloaded April 2015 for Andromeda search within MaxQuant (Cox, Michalski et al. 2011). The label free quantitation (LFQ) algorithm in MaxQuant (Luber, Cox et al. 2010, Cox, Hein et al. 2014) was used for protein quantitation. Imputation of missing values using Perseus (Tyanova, Temu et al. 2016) was followed by batch effect correction using ComBat (Johnson, Li et al. 2007). After calculating fold change and p-value for each protein, data were analyzed by GO term using DAVID (Huang da, Sherman et al. 2009, Huang da, Sherman et al. 2009) or KEGG pathway by GO-elite v1.2.5 (Zambon, Gaj et al. 2012).

Image acquisition

For analysis of isolated nuclei, images were obtained using an Axioplan microscope (Carl Zeiss MicroImaging, Oberkochen, Germany) with either a 0.3 NA 10X Plan-Neofluar objective (Carl Zeiss MicroImaging) or a 0.8 NA 25X Plan-Neofluar objective (Carl Zeiss MicroImaging) and were recorded with a camera (Carl Zeiss MicroImaging) and Scion Image 1.63 (Scion Corporation, Torrance, CA) software. For analysis of single myofibers, images were obtained using a Nikon Eclipse TE2000-U confocal microscope (Nikon, Tokyo, Japan) with a 0.50 NA Plan Fluor 20x objective (Nikon) and were recorded with a SensiCam QE (Cooke, Campbell, CA) with IPlab 4.0 (Scanalytics, Fairfax, VA)

software. All images were assembled and equally processed using Adobe Photoshop CS4 version 11.0.2 (Adobe, San Jose, CA).

Statistical Analysis

Data were analyzed for statistical significance based on fold change, p-value, or z-score. z-score enrichment was determined using GOelite (Zambon, Gaj et al. 2012). A p-value of <0.05 or z-score of >1.96 was considered statistically significant. Relevant changes were considered greater than 1.5 fold.

Supporting Information is available through the journal Aging Cell.

3.6 Tables

Table 3.1 Myonuclear proteins that change significantly with age

log2 fold change	P-value	Uniprot ID	Gene Symbol	Protein name	Role
-2.19	0.009	P43276	*Hist1h1b*	Histone H1.5	Chromatin maintenance
-2.12	0.014	Q70IV5-2	*Synm*	Synemin	Cytoskeletal
-1.73	0.019	Q6PIC6	*Atp1a3*	Sodium/potassium-transporting ATPase subunit alpha-3	Membrane ion pump
-1.67	0.040	O54941	*Smarce1*	SWI/SNF-related matrix-associated actin-dependent regulator of chromatin subfamily E member 1	Chromatin maintenance
-1.46	0.018	Q91XV3	*Basp1*	Brain acid soluble protein 1	Transcription
-1.40	0.047	P49813	*Tmod1*	Tropomodulin-1	Sarcomeric
-1.38	0.036	Q9D6R2-2	*Idh3a*	Isocitrate dehydrogenase [NAD] subunit alpha, mitochondrial	Metabolism
-1.24	0.039	P62242	*Rps8*	40S ribosomal protein S8	Ribosomal
-1.22	0.032	A2AUC9	*Klhl41*	Kelch-like protein 41	Myofibril assembly
-1.08	0.025	Q9ESU6	*Brd4*	Bromodomain-containing protein 4	Chromatin maintenance
-0.73	0.016	P51637	*Cav3*	Caveolin-3	Membrane protein scaffold
0.69	0.024	Q810A7-2	*Ddx42*	ATP-dependent RNA helicase DDX42	RNA processing
0.70	0.041	G3UX35	*Smarca4*	Isoform of Q3TKT4, Transcription activator BRG1	Chromatin maintenance
0.82	0.031	P62908	*Rps3*	40S ribosomal protein S3	Ribosomal
0.84	0.038	Q8K4Q8	*Colec12*	Collectin-12	Cell signaling
0.84	0.021	Q60865	*Caprin1*	Caprin-1	RNA processing
0.86	0.013	Q64511	*Top2b*	DNA topoisomerase 2-beta	Transcription
0.87	0.046	E9Q7Q3	*Tpm3*	Isoform of P21107, Tropomyosin alpha-3 chain	Sarcomeric
0.93	0.040	Q8K2T8	*Paf1*	RNA polymerase II-associated factor 1 homolog	Transcription

0.97	0.027	Q64522	*Hist2h2ab*	Histone H2A type 2-B	Chromatin maintenance
1.00	0.002	S4R1C4	*Atp2b2*	Isoform of Q9R0K7, Calcium-transporting ATPase	Membrane ion pump
1.03	0.025	P62309	*Snrpg*	Small nuclear ribonucleoprotein G	RNA processing
1.07	0.032	Q8BH74	*Nup107*	Nuclear pore complex protein Nup107	Nuclear Transport
1.13	0.029	Q3UN88	*Mcpt4*	Isoform of P21812, Mast cell protease 4	Cytoplasmic protease
1.26	0.026	Q922P9	*Glyr1*	Putative oxidoreductase GLYR1	Chromatin maintenance
1.35	0.033	G3UZI2	*Syncrip*	Isoform of Q7TMK9, Heterogeneous nuclear ribonucleoprotein Q	RNA processing
1.35	0.049	Q99JY0	*Hadhb*	Trifunctional enzyme subunit beta, mitochondrial	Metabolism
1.36	0.002	P08113	*Hsp90b1*	Endoplasmin	ER chaperone
1.36	0.040	Q8CJF7	*Ahctf1*	Protein ELYS	Nuclear Transport
1.38	0.006	P32067	*Ssb*	Lupus La protein homolog	RNA processing
1.40	0.040	P68040	*Gnb2l1*	Guanine nucleotide-binding protein subunit beta-2-like 1	Cell signaling
1.43	0.025	P47857	*Pfkm*	ATP-dependent 6-phosphofructokinase, muscle type	Metabolism
1.43	0.002	Q91YQ5	*Rpn1*	Dolichyl-diphosphooligosaccharide--protein glycosyltransferase subunit 1	ER glycosylation
1.44	0.048	Q60749	*Khdrbs1*	KH domain-containing, RNA-binding, signal transduction-associated protein 1	RNA processing
1.44	0.023	O08539-2	*Bin1*	Myc box-dependent-interacting protein 1	Apoptotic process
1.46	0.030	Q8QZT1	*Acat1*	Acetyl-CoA acetyltransferase, mitochondrial	Metabolism
1.50	0.016	O35326	*Srsf5*	Serine/arginine-rich splicing factor 5	RNA processing
1.51	0.002	P62858	*Rps28*	40S ribosomal protein S28	Ribosomal
1.52	0.001	P10852	*Slc3a2*	4F2 cell-surface antigen heavy chain	Membrane transporter
1.57	0.025	Q9D8E6	*Rpl4*	60S ribosomal protein L4	Ribosomal
1.59	0.028	O35343	*Kpna4*	Importin subunit alpha-3	Nuclear Transport
1.61	0.016	P42669	*Pura*	Transcriptional activator protein Pur-alpha	Transcription
1.61	0.015	Q99MR6-3	*Srrt*	Serrate RNA effector molecule homolog	RNA processing
1.78	0.004	A2AW05	*Ssrp1*	Isoform of Q08943, FACT complex subunit SSRP1	Transcription

1.78	0.019	E9PYL9	*Gm10036*	Protein Gm10036	RNA processing
1.81	0.008	Q8VHM5	*Hnrnpr*	Heterogeneous nuclear ribonucleoprotein R	RNA processing
1.84	0.002	P30275	*Ckmt1*	Creatine kinase U-type, mitochondrial	Metabolism
1.85	0.046	Q6ZWY9	*Hist1h2bc*	Histone H2B type 1-C/E/G	Chromatin maintenance
1.90	0.047	P70168	*Kpnb1*	Importin subunit beta-1	Nuclear Transport
1.90	0.035	P62315	*Snrpd1*	Small nuclear ribonucleoprotein Sm D1	RNA processing
1.94	0.026	Q9CQF3	*Nudt21*	Cleavage and polyadenylation specificity factor subunit 5	RNA processing
2.05	0.023	D3YWX2	*Ylpm1*	Isoform of Q9R0I7, YLP motif-containing protein 1	RNA processing
2.33	0.013	Q8VE37	*Rcc1*	Regulator of chromosome condensation	Nuclear Transport
2.89	0.005	Q99KK2	*Cmas*	N-acylneuraminate cytidylyltransferase	Metabolism

Table 3.2 Brain nuclear proteins that change significantly with age

log2 fold change	P-value	Uniprot ID	Gene Symbol	Protein name	Role
-3.40	0.001	P10854	*Hist1h2bm*	Histone H2B type 1-M	Chromatin maintenance
-3.19	0.003	P84228	*Hist1h3b*	Histone H3.2	Chromatin maintenance
-2.03	0.005	D3Z7R4	*Syt1*	Isoform of P46096, Synaptotagmin-1	Vesicular trafficking
-1.77	0.024	Q9CWF2	*Tubb2b*	Tubulin beta-2B chain	Cytoskeletal
-1.54	0.008	Q8QZY9	*Sf3b4*	Splicing factor 3B subunit 4	RNA processing
-1.32	0.035	Q9QYG0	*Ndrg2*	Protein NDRG2	Signal transduction
-1.32	0.032	Q9ES97-3	*Rtn3*	Reticulon-3	Beta amyloid regulation
-0.86	0.005	A2AR02	*Ppig*	Peptidyl-prolyl cis-trans isomerase G	Lamin
-0.79	0.024	Q9QYX7-2	*Pclo*	Protein piccolo	Cytoskeletal
-0.70	0.014	P28659-2	*Celf1*	CUGBP Elav-like family member 1	RNA processing
-0.53	0.019	Q0P678	*Zc3h18*	Zinc finger CCCH domain-containing protein 18	RNA processing
0.53	0.023	P0C0S6	*H2afz*	Histone H2A.Z	Chromatin maintenance
0.57	0.026	Q6PDM2	*Srsf1*	Serine/arginine-rich splicing factor 1	RNA processing
0.64	0.011	P21619	*Lmnb2*	Lamin-B2	Lamin
0.69	0.045	Q9CX86	*Hnrnpa0*	Heterogeneous nuclear ribonucleoprotein A0	RNA processing
0.71	0.046	P70372	*Elavl1*	ELAV-like protein 1	RNA processing
0.75	0.013	Q64525	*Hist2h2bb*	Histone H2B type 2-B	Chromatin maintenance
0.75	0.013	A0A087WRG2	*U2surp*	Isoform of Q6NV83, U2 snRNP-associated SURP motif-containing protein	RNA processing
0.80	0.021	P70288	*Hdac2*	Histone deacetylase 2	Chromatin maintenance
0.84	0.048	Q91VR5	*Ddx1*	ATP-dependent RNA helicase DDX1	RNA processing
0.88	0.026	Q9CU62	*Smc1a*	Structural maintenance of chromosomes protein 1A	Chromatin maintenance
0.98	0.039	G3UZ34	*Eftud2*	Isoform of O08810, 116 kDa U5 small nuclear ribonucleoprotein component	RNA processing
1.09	0.036	Q62318	*Trim28*	Transcription intermediary factor 1-beta	Transcription

1.11	0.005	Q9CQI7	*Snrpb2*	U2 small nuclear ribonucleoprotein B"	RNA processing
1.18	0.042	P63158	*Hmgb1*	High mobility group protein B1	Chromatin maintenance
1.27	0.018	P10126	*Eef1a1*	Elongation factor 1-alpha 1	Translation
1.30	0.049	Q61191	*Hcfc1*	Host cell factor 1	Transcription
1.33	0.003	P48678-2	*Lmna*	Prelamin-A/C	Lamin
1.37	0.019	Q8VE37	*Rcc1*	Regulator of chromosome condensation	Nuclear Transport
1.37	0.006	Q6ZPZ3-2	*Zc3h4*	Zinc finger CCCH domain-containing protein 4	RNA processing
1.39	0.037	Q7TNT2-2	*Far2*	Fatty acyl-CoA reductase 2	Metabolism
1.49	0.005	A0A0G2JD95	*Rsbn1*	Isoform of Q80T69, Round spermatid basic protein 1	Transcription

Supplemental Tables are available through the journal Aging Cell.

3.7 Figures

Figure 3.1. Workflow for isolating nuclei from skeletal muscle. (A) Workflow: 1) Skeletal muscle was dissected from mice and then 2) minced and homogenized. 3) The homogenate was filtered and nuclei pelleted at low speed. 4) The crude nuclear fraction was resuspended, layered over sucrose cushions, and 5) ultracentrifuged. 6) The nuclear fraction was collected, diluted, and pelleted at low speed. 7) The nuclear pellet was collected for downstream applications. (B) Purified nuclei were stained with DAPI and examined by microscopy. Nuclei were free from visible debris in phase and DAPI channels. Bar=10μm. (C) Nuclei were incubated with FITC-conjugated 500 kDa dextran. Intact nuclear envelopes excluded the large dextran (93%) while envelopes breached during isolation (arrowhead) were permeable to the dextran (7%). Bar=10μm. (D) Nuclei (Nuc) were compared to total (T) and cytoplasmic (Cyto) fractions by immunoblotting. Nuclei were enriched for markers of the nuclear envelope (Nup 214), RNA binding proteins (HuR), and chromatin (Histone 3). Purified nuclei were also enriched in endoplasmic reticulum markers (ER) but depleted of cytoplasmic (Cyto) and mitochondrial (Mito) markers.

Figure 3.2. Isolated nuclei are predominately myonuclei. (A) Purified nuclei were stained with DAPI and immunostained with anti-nuclear pore complex antibody (Mab414) to label all nuclear envelopes, and anti-TMEM38A antibody to label myonuclei. Pictured are representative images of $TMEM38A^+$ and $TMEM38A^-$ nuclei. Bar=10μm. (B) Isolated nuclei were analyzed by flow cytometry by side scatter (SSC) and DAPI; intact $DAPI^+$

singlets were selected for further analysis (red gate). (C) IgG control immunostained nuclei (gray) were compared to experimental nuclei immunostained with Mab414 and TMEM38A antibodies (magenta). Myonuclei were defined to be double positive for Mab414 and TMEM38A (red gate); 96.4% ± 3.2 SE of Mab414^{+} nuclei were also positive for TMEM38A (n=4). Bright and dim TMEM38A populations were distinct from control IgG immunostained nuclei (inset). (D) Transgenic mice with a cassette containing nuclear-targeted tdTomato and eGFP reporter proteins (nTnG) were crossed with mice expressing Cre recombinase from a skeletal muscle-specific promoter (Ckmm) to genetically label myonuclei and non-myonuclei with distinct fluorescent markers in the offspring. All nuclei from wildtype mice (WT) are non-fluorescent. All nuclei from from nTnG^{+} Ckmm Cre^{-} mice (Cre^{-}) are fluorescent red. Myonuclei from nTnG^{+} Ckmm Cre^{+} mice (Cre^{+}) are fluorescent green while non-myonuclei are fluorescent red. (E) Single myofibers were isolated from Cre^{-} and Cre^{+} mice. Arrowheads indicate red non-muscle cells on a myofiber containing green myonuclei. Bar=50μm. (F) Nuclei isolated from Cre^{-} and Cre^{+} mice retained their fluorescent label after isolation. Bar=10μm. (G) DAPI^{+} nuclei isolated from a Cre^{+} mouse (purple) and a WT mouse (gray) were analyzed by TMEM38A and eGFP fluorescence; 85.5% ± 5.2 SE of nuclei from Cre^{+} mice were positive for both TMEM38A and eGFP (n=4). Bright and dim TMEM populations were distinct from WT nuclei immunostained with control IgG (inset). TMEM38A^{+} nuclei were selected for further analysis (red gate). (H) TMEM38A^{+} nuclei were analyzed for eGFP fluorescence; 99.7% ±0.03 SE of TMEM38A^{+} nuclei were eGFP^{+}, confirming that TMEM38A labels myonuclei.

Figure 3.3: Nuclear proteins are enriched in purified nuclei. (A) The log2 of the mean extracted ion chromatogram (XIC) intensity of proteins from purified myonuclei and whole muscle tissue samples are represented in a heat map: blue indicates low intensity ($1.5x10^4$) and red indicates high intensity ($1.5x10^{10}$) (n=2 of each sample type). (B) The top KEGG pathways for the most depleted (purple) or most enriched (blue) proteins from isolated nuclei were plotted by z score significance. The red line indicates significance threshold (z=1.96). (C) Proteins unique for nuclear, cytoplasmic, mitochondrial, sarcomeric, and endoplasmic reticular (ER) compartments were assigned by DAVID. Within each compartment, proteins were binned in deciles from the least enriched to the most enriched in nuclei compared to whole muscle tissue and plotted against the mean log 2 ratio of XIC in purified nuclei and whole muscle samples. This view reveals the consistency of enrichment and depletion within groups of proteins.

Figure 3.4: Aging of the myonuclear proteome. (A) The mean log2 fold change in LFQ (label free quantification) between young (3 month) and old (24 month) mouse myonuclei proteins was plotted against the -log10 p-value for each protein (n=5 at each age). Proteins that significantly changed with age more than 1.5 fold ($p<0.05$) are plotted in red: all others are plotted in gray. (B) Proteins that significantly changed with age in myonuclei were categorized by primary function and depicted as a percentage of total changed proteins.

Figure 3.5: Comparison of age-related alterations in muscle and brain nuclear proteomes. (A) The mean log2 fold change in LFQ between young (3 month) and old (24 month) mouse brain nuclei proteins was plotted against the -log10 p-value for each protein

(n=5 at each age). Proteins that significantly changed with age more than 1.5 fold ($p<0.05$) are plotted in red: all others are plotted in gray. (B) Proteins that changed with age in brain nuclei were categorized by primary function and depicted as a percentage of total changed proteins. (C) The percentage of proteins that changed with age that were assigned to each GO category was compared between brain and muscle samples. (D) The full sets of proteins detected in muscle or brain nuclear samples were compared to the subsets that significantly changed with age. The majority of proteins analyzed were detected in both tissues but the subsets that changed with age differed greatly between tissues. Of 743 proteins detected in muscle nuclei and 811 proteins detected in brain nuclei, 661 were common to both tissues. Of the proteins that changed with age in myonuclei (54) or brain nuclei (32), only 1 was changed in both. (E) Heat map of all proteins that changed significantly with age in either tissue; aging-related changes differ between brain and muscle nuclei. Blue indicates lower levels in old samples and red indicates higher levels in old samples. OM=old muscle; YM=young muscle; OB=old brain; YB=young brain. (F) Representative immunoblot and accompanying Ponceau staining. The immunoblot was probed for target proteins identified as changed with age by mass spectrometry. (G) Quantification of immunoblot by densitometry (n=3-4, error bar=standard error of the mean).

Supplemental Figures are available through the journal Aging Cell.

Figure 3.1

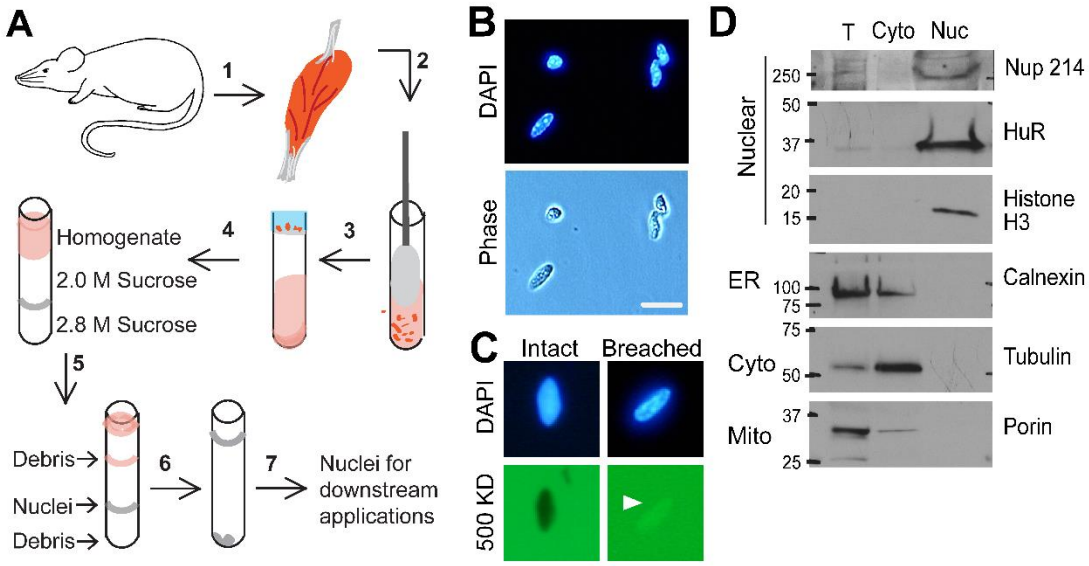
A
1
2
3
4
5
6
7
Homogenate
2.0 M Sucrose
2.8 M Sucrose
Debris
Nuclei
Debris
Nuclei for downstream applications
B
DAPI
Phase
C
Intact
Breached
DAPI
500 KD
D
T
Cyto
Nuc
Nuclear
250
50
37
20
15
Nup 214
HuR
Histone H3
ER
100
75
Calnexin
75
Cyto
50
Tubulin
37
Mito
25
Porin

Figure 3.2

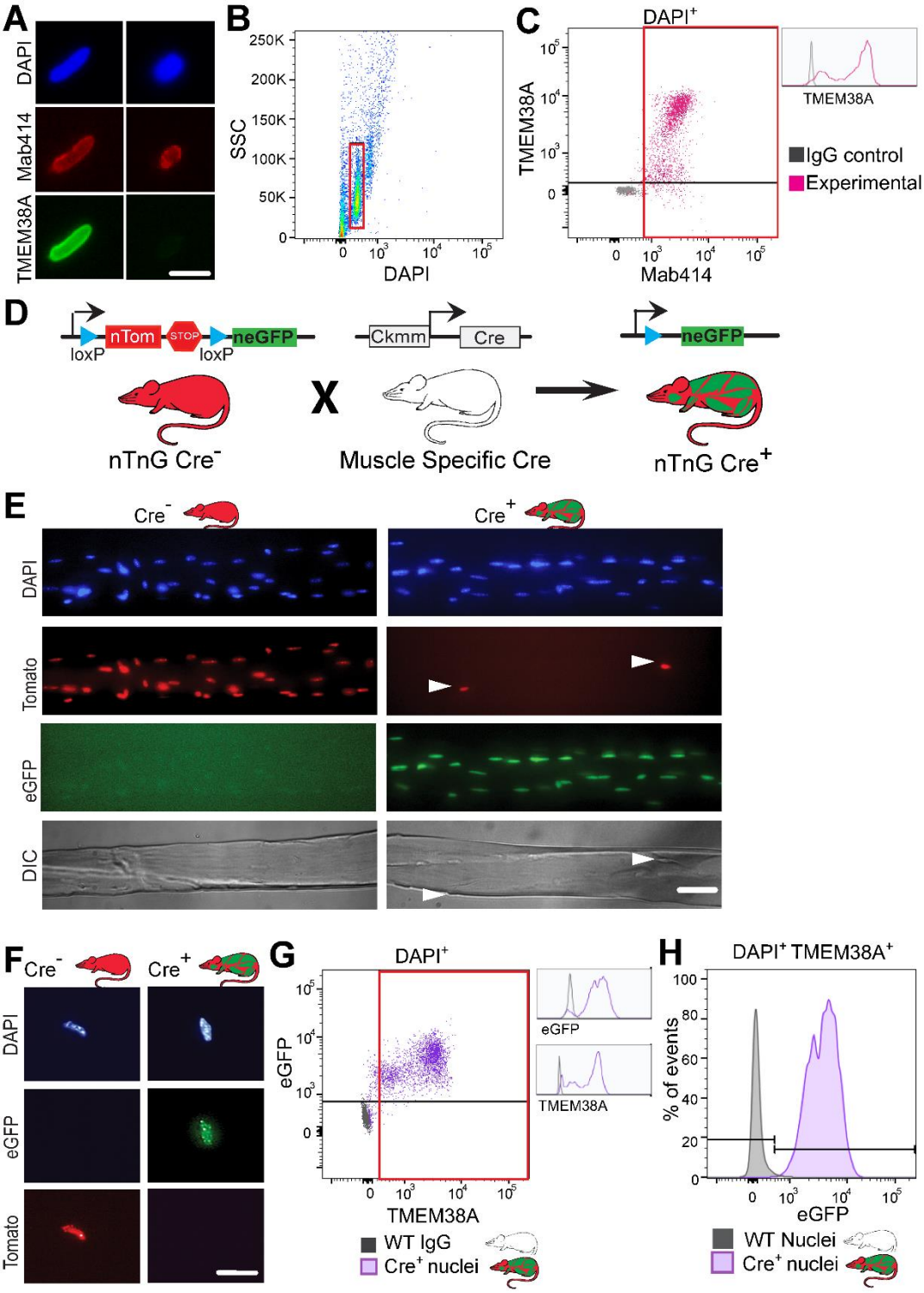
A
DAPI
Mab414
TMEM38A
B
SSC
DAPI
C
DAPI+
TMEM38A
Mab414
IgG control
Experimental
D
loxP
nTom
STOP
loxP
neGFP
Ckmm
Cre
neGFP
nTnG Cre-
X
Muscle Specific Cre
nTnG Cre+
E
Cre-
Cre+
DAPI
Tomato
eGFP
DIC
F
Cre-
Cre+
DAPI
eGFP
Tomato
G
DAPI+
eGFP
TMEM38A
WT IgG
Cre+ nuclei
H
DAPI+ TMEM38A+
% of events
eGFP
WT Nuclei
Cre+ nuclei

Figure 3.3

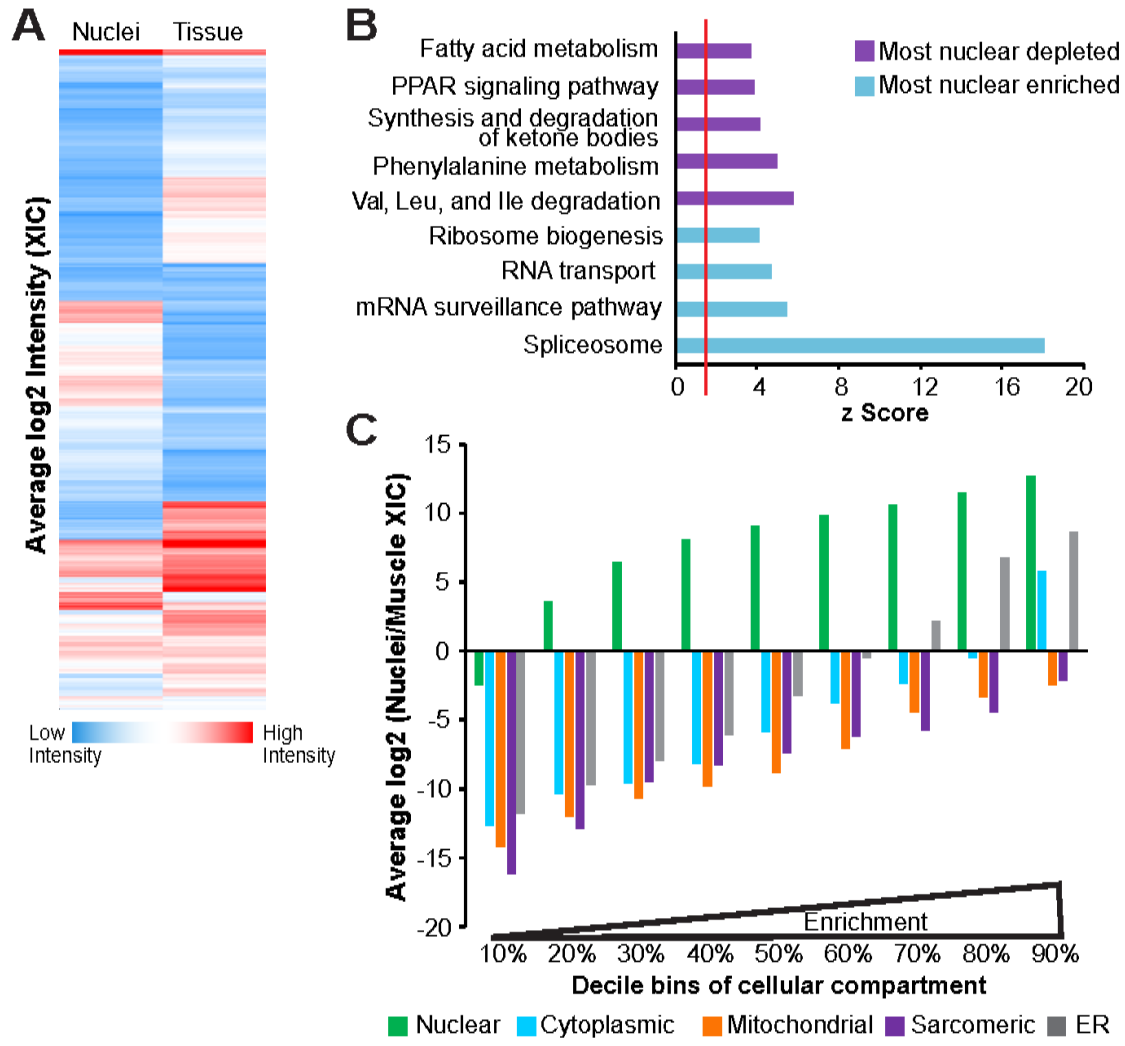
A
Nuclei
Tissue
Average log2 Intensity (XIC)
Low Intensity
High Intensity
B
Fatty acid metabolism
PPAR signaling pathway
Synthesis and degradation of ketone bodies
Phenylalanine metabolism
Val, Leu, and Ile degradation
Ribosome biogenesis
RNA transport
mRNA surveillance pathway
Spliceosome
Most nuclear depleted
Most nuclear enriched
0
4
8
12
16
20
z Score
C
Average log2 (Nuclei/Muscle XIC)
15
10
5
0
-5
-10
-15
-20
Enrichment
10%
20%
30%
40%
50%
60%
70%
80%
90%
Decile bins of cellular compartment
Nuclear
Cytoplasmic
Mitochondrial
Sarcomeric
ER

Figure 3.4

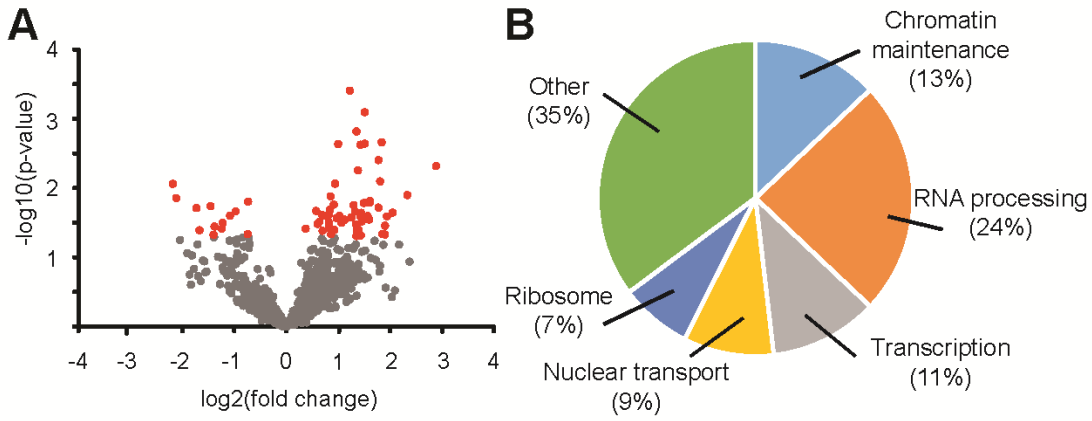
A
-log10(p-value)
4
3
2
1
-4
-3
-2
-1
0
1
2
3
4
log2(fold change)
B
Chromatin maintenance (13%)
RNA processing (24%)
Transcription (11%)
Nuclear transport (9%)
Ribosome (7%)
Other (35%)

Figure 3.5

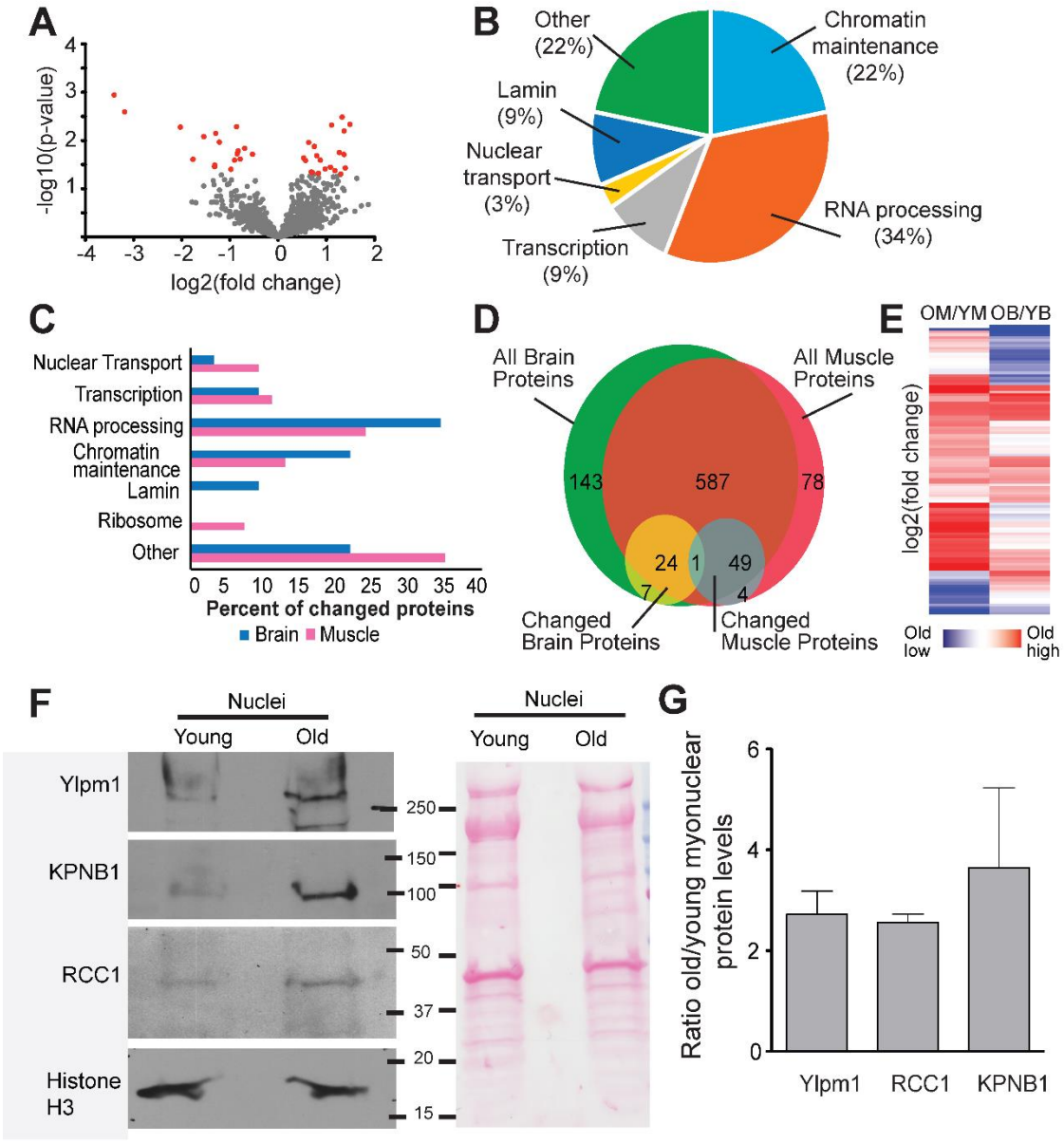
A
-log10(p-value)
log2(fold change)
B
Other (22%)
Chromatin maintenance (22%)
Lamin (9%)
Nuclear transport (3%)
RNA processing (34%)
Transcription (9%)
C
Nuclear Transport
Transcription
RNA processing
Chromatin maintenance
Lamin
Ribosome
Other
Percent of changed proteins
Brain Muscle
D
All Brain Proteins
All Muscle Proteins
143
587
78
24
1
49
7
4
Changed Brain Proteins
Changed Muscle Proteins
E
OM/YM OB/YB
log2(fold change)
Old low
Old high
F
Nuclei
Young
Old
Ylpm1
KPNB1
RCC1
Histone H3
250
150
100
50
37
20
15
G
Ratio old/young myonuclear protein levels
Ylpm1
RCC1
KPNB1

Chapter 4: Discussion and future directions

Chapter 4: Discussion and future directions

Unlike most eukaryotic cells, multinucleated cells contain multiple nuclei sharing a single cytoplasm. Individual nuclei within a single cell can differ morphologically (Huppertz and Gauster 2011) and functionally (Dix and Eisenberg 1990, Newlands, Rustin et al. 1996, Ellery, Cindrova-Davies et al. 2009, Youn, Takada et al. 2010). Whether nuclear activity in syncytial cells is coordinated among nuclei and how differences among nuclei are established remain open questions. While some mechanisms regulating individual nuclei have been established in ciliates and slime molds, individual nuclei of multinucleated cells in multicellular organisms remain largely unexamined. The findings presented in this dissertation are the first step toward clarifying the fundamental biology of individually regulating syncytial nuclei in multicellular organisms. Future studies will determine specific mechanisms and could provide insight into novel potential therapeutic avenues for treating diseases with multinucleated cell involvement.

Despite being primarily responsible for regulating gene expression, relatively little is known about the myonuclear proteome and global nuclear activity in myofibers. Prior to our studies, the myonuclear proteome had never been examined in detail, in part due to technical challenges of detecting nuclear proteins. Our approach to selectively isolate myonuclei (Cutler, Dammer et al. 2017) opens exciting possibilities to examine the transcriptome, epigenome, and proteome in a myonuclear-specific manner from whole skeletal muscle tissue. Additionally, our work lays the foundation for elucidating these nuclear characteristics on the level of individual nuclei. When myonuclear activity has been assayed previously, the experiments were carried out on a population of nuclei including both myonuclei and nuclei from other cell types. In addition to not distinguishing nuclei

from multiple cell types, these analyses make no distinction between nuclei from different myofibers. Myofibers can contain thousands of nuclei all sharing a common cytoplasm. Our work and previous studies have described differences among myonuclei within the a single myofiber (Fontaine and Changeux 1989, Abbott, Friday et al. 1998, Newlands, Levitt et al. 1998). This heterogeneity of myonuclei represents a previously underappreciated characteristic of skeletal muscle biology and highlights the limitations of assaying nuclear activity based on populations of nuclei. Natural extensions of our work will seek to identify characteristics of individual myonuclei, the biochemical and signaling mechanisms regulating differences among myonuclei, and how myonuclear activity is coordinated within a myofiber. In order to achieve these goals, new techniques and reagents to interrogate nuclear activity and nuclear content on a single nucleus level must be developed and optimized for use in skeletal muscle. The principles and mechanisms governing myonuclear independence will have broad implications for understanding individual regulation of nuclei in other multinucleated cells.

Previous work examining the changes to the skeletal muscle transcriptome and epigenome have been carried out on whole muscle tissue or on cultured muscle cells. The resulting findings have propelled the field forward but are also limited by the constraints of the respective systems. Substantial studies have been carried out on general changes that occur to the muscle epigenome and transcriptome in myogenesis, exercise, aging, and other physiological states. A major shift in chromatin modification and mRNA transcripts produced occurs as myoblasts differentiate to form myofibers. Histone deacetylases (HDAC) reverse histone acetylation. In proliferative myoblasts HDACs are highly active, preventing expression of muscle differentiation genes (Dressel, Bailey et al. 2001). As

differentiation begins HDACs are displaced by proteins like p300/CBP associated protein (PCAF) (Puri, Sartorelli et al. 1997) and relocalized the cytoplasm (McKinsey, Zhang et al. 2001). Histone acetyl transferases (HAT) are targeted to the chromatin around muscle differentiation genes by proteins like Rnpj (Bjornson, Cheung et al. 2012). This results in acetylation of the histones, promoting expression of the myogenesis genetic program (Castel, Mourikis et al. 2013). Similarly, exercise results in relocalization of HDACs from the nucleus to the cytoplasm (McKinsey, Zhang et al. 2001, McGee, Fairlie et al. 2009) and recruitment of HATs to the chromatin surrounding myogenic loci in satellite cells (Serra, Palacios et al. 2007, Fujimaki, Hidaka et al. 2014). Consistent exercise over extended time causes DNA methylation of metabolism associated genes (Reviewed in (Sharples, Stewart et al. 2016)). In contrast, as muscle ages HDAC levels increase in the muscle and there is progressive methylation of myogenesis genes in satellite cells (Jin, Jiang et al. 2014, Zykovich, Hubbard et al. 2014) resulting in impaired myogenesis. Although the levels of the majority of transcripts do not change with age (Weindruch, Kayo et al. 2001), mRNA levels of metabolic proteins, sarcomeric components, and chromatin proteins differ significantly between young and old mouse muscle (Su, Ekman et al. 2015) contributing to muscle aging phenotypes. Similar characterization of chromatin and mRNA levels in dietary restriction, cachexia, and various muscular dystrophies have also been undertaken. These examples demonstrate that the skeletal muscle transcriptome and epigenome change in response to physiological conditions and highlight specific markers that vary with the state of the muscle.

While the findings of these studies advanced our understanding of signaling important in muscle's homeostatic response and have identified some therapeutic targets,

they also are subject to the limitations of impure starting material, *in vitro* conditions, or limited targets. These studies were carried out on either cultured cells, which are a pure population but do not fully recapitulate the intact tissue, or mixed nuclei from all cell types present in skeletal muscle tissue. Selectively examining myonuclei could identify key molecular players regulating muscle activity in these states. Studies which do examine nuclear changes specifically in myonuclei are limited by the nature of transgenic experiments to a small number of specific candidates and thus are afforded only a small glimpse into the complexity of the nuclear compartment. Our approach to selectively isolate myonuclei combined with a battery of studies focusing on epigenetics, transcriptomics, and proteomics could provide a complete illustration of myonuclear activity and profiles in different physiological states. These findings would advance understanding of myofiber biology and could provide potential therapeutic targets to modulate both physiologic and pathophysiologic responses to environmental stressors. As the technology matures single nucleus proteomics and transcriptomics would inform our understanding of the heterogeneity of nuclei in a myofiber and the significance of that heterogeneity.

The findings presented in Chapter 2 demonstrate that nuclear import varies among myonuclei sharing a common cytoplasm and that nuclear import is responsive to muscle injury. We proposed that differential nuclear import could be a mechanism by which individual nuclei differ in protein accumulation (McPherron, Lawler et al. 1997, Abbott, Friday et al. 1998, Artaza, Bhasin et al. 2002, Salamon, Millino et al. 2003, Ishido, Kami et al. 2004, O'Connor, Mills et al. 2007, Yamamoto, Csikasz et al. 2008, Ferri, Barbieri et al. 2009) and gene expression (Newlands, Levitt et al. 1998, Artaza, Bhasin et al. 2002).

While the findings presented in Chapter 2 represent an important first step in characterizing the mechanisms regulating differences among myonuclei, more work is needed to establish the biochemical mechanisms and signaling pathways responsible and the specific effects of differences in myonuclear import.

Identifying the biochemical mechanisms for differences in nuclear import among myonuclei is technically challenging because individual nuclei are difficult to isolate and yield very little material to analyze. The most probable biochemical causes of differences in nuclear import among myonuclei include post-translational modifications of NPC components (Crampton, Kodiha et al. 2009, Kodiha, Tran et al. 2009, Regot, de Nadal et al. 2013), differences in Nup incorporation at the NPCs (Gustin and Sarnow 2001, Gustin and Sarnow 2002, Crampton, Kodiha et al. 2009), or differences in the RanGTP gradient (Lyman, Guan et al. 2002, Snow, Dar et al. 2013). Identifying these biochemical differences among nuclei would require separating nuclei based on nuclear import activity or analyzing individual nuclei. Additionally, each nucleus contains thousands of NPCs (Asally, Yasuda et al. 2011) which may differ in Nup incorporation or in post-translational modification (Kinoshita, Kalir et al. 2012). Thus, the causative changes are small and potentially only affect a subset of a protein population in each nucleus. For this reason, standard biochemical approaches are insufficient to identify the causative modifications and instead technical advances and production of new reagents will be required.

Candidate-based and discovery-based approaches could be effective in identifying the biochemical mechanisms regulating differences among nuclei. The first step for either approach would be to separate nuclei based on specific properties. Nuclei could be separated by fluorescence nuclear sorting (Dammer, Duong et al. 2013) or by specific

affinity based isolation (Deal and Henikoff 2011). The approach outlined in Chapter 3 could be employed to isolate nuclei, however subsequent separation will require expanding markers for nuclei of interest, which could include nuclei in specialized regions of the myofiber, nuclei with specific gene expression or protein accumulation, and newly fused nuclei. Some nuclear markers currently available include markers of NMJ nuclei and a subset of proteins and transcripts that differentially accumulate in some but not all myonuclei in a fiber. The nuclear envelope protein Syne-1 is present on nuclei of the NMJ but not other myonuclei (Apel, Lewis et al. 2000), however no markers are known for nuclei of the myotendinous junction or the body of the myofiber. Some proteins and transcripts differentially localize among myonuclei (McPherron, Lawler et al. 1997, Abbott, Friday et al. 1998, Newlands, Levitt et al. 1998, Artaza, Bhasin et al. 2002, Salamon, Millino et al. 2003, Ishido, Kami et al. 2004, O'Connor, Mills et al. 2007, Yamamoto, Csikasz et al. 2008, Ferri, Barbieri et al. 2009). Unfortunately, these markers are suboptimal for sorting nuclei because they are internal rather than surface markers and so would require fixation and permeabilization of the nuclear sample, which limits downstream analysis. There are currently no markers available for newly incorporated myonuclei.

In addition to limited markers of nuclei of interest, reagents to detect the candidate biochemical modifications responsible for differences in nuclear import are also limiting. Examining differences in Nup stoichiometry at the nuclear pore is complicated by lack of specific antibodies to NPC component proteins. Similarly, examination of post-translational modifications of Nups is dependent on antibody availability. Currently, modification specific antibodies have been limited those Nup modifications relevant to

kinetochore assembly and activity. Detecting and correlating multiple markers of nuclear activity, nuclear content, NPC composition, and NPC modification will require a system with high capacity and low cross detection. Mass cytometry (CyTOF) has been a powerful tool in interrogating signaling pathways on the cellular level (Hawley, Ding et al. 2017, Porpiglia, Samusik et al. 2017). Once the relevant reagents are available for candidate proteins and modifications, CyTOF could also be effectively deployed to answer questions of signaling in individual nuclei. Alternatively, discovery based analysis (like mass spectrometry, RNA seq, or ChIP seq) of different groups of myonuclei could identify additional proteins and modifications involved in differentially regulating individual nuclei. Any technique employed to examine the mechanistic biochemical differences among nuclei must have very high sensitivity as heterogeneity in modification status and incorporation into the NPC exists even among proteins within a single nucleus.

Before myonuclei are biochemical modified to alter their activity, signaling events will define which nuclei in the common cytoplasm should be modified. These signaling events could result from intrinsic nuclear maturation, nuclear position in a cell, or extracellular cues. The data presented in Chapters 2 and 3 support contribution of all three sources of signaling on nuclear import. Future work will determine the effect of each of these potential signaling sources. Disentangling the signaling pathways at work will require identifying the biochemical changes involved in regulating nuclear transport to identify candidate enzymes in the pathways. It is worth noting that signaling events conveying information of nuclear age, nuclear position and extracellular cues are likely stem from different intersecting signaling pathways.

The relative effects of nuclear age and nuclear position could be dissected by combining nuclear import experiments with lineage tracing. In growth, new nuclei are added predominantly to the ends of myofibers (Zhang and McLennan 1995). Comparison of newly added nuclei at the ends of a myofiber to new nuclei in the middle of a myofiber would reveal if position has a differential effect on nuclear activity. Signaling related to nuclear position could also be examined by investigating the properties of specialized myofiber regions. In addition to the well-established NMJ and MTJ regions, our findings in conjunction with those of Newlands et al. (Newlands, Levitt et al. 1998) suggest that, in addition to regions easily identified by anatomical land marks, other subtler myofiber regions may exist. If characterized, these regions could present a new fundamental aspect of skeletal muscle cells. This discovery would be an important advancement in the basic cellular biology of skeletal muscle cells. However, determining the effect of these hypothetical regions will first require that the regions and their boundaries be identified and characterized. Finally, examining the impact of the age of a nucleus in a myofiber could be achieved by separately analyzing newly added, middle aged, and very old nuclei. The results presented in Chapter 2 that nuclear import is affected in regeneration and the findings described in Chapter 3 that aging changes the levels of proteins present in myonuclei support a correlation between age of a myonucleus in a cell and nuclear activity. Myonuclei are exceptionally long-lived, with an average half-life of 14 years in human muscle. Understanding how nuclear age affects nuclear activity could provide insight into some root causes of reduced muscle function with aging.

In addition to cell intrinsic signaling, systemic signaling events also play a role in regulating myonuclear activity. As presented in Chapter 2, the rate of nuclear import

decreases in response to muscle injury on the contralateral side, indicating that circulating factors, or coordination mediated by another system like the nervous system, regulate nuclear import in locations distal to an insult. The finding that nuclear import is responsive to contralateral injury suggests that nuclear import could be also be affected by many different physiological states including aging, development, exercise, fasting, and disease. Research on the skeletal muscle impact of these states has focused on the effects of these factors on satellite cells or myofiber metabolism and sarcomere function (Lee, Allison et al. 2002, O'Connell, Gannon et al. 2007, Middelbos, Vester et al. 2009, Baraibar, Gueugneau et al. 2013, Kwon, Kim et al. 2014, Capitanio, Vasso et al. 2016). Understanding how the changes in the organism affect myonuclei could provide new insights into way of modifying the muscle's response. Nuclear transport has been proposed as a therapeutic target for treating cancer (Turner and Sullivan 2008), HIV (Newlands, Rustin et al. 1996, Chahine and Pierce 2009), and chronic inflammation (Faustino, Nelson et al. 2007). Similarly, pharmacologically regulating nuclear transport in skeletal muscle could represent a novel therapeutic avenue to treat disease and aging related symptoms. Isolating the circulating factor responsible for the effect on nuclear transport described in Chapter 2 could provide a way of exogenously regulating nuclear import and thus general nuclear activity in myonuclei and nuclei of other cells. Further work examining the signaling events regulating nuclear transport will inform our understanding of differences among myonuclei as well as coordinated, systemic responses to stimuli affecting the whole organism.

The significance of differences among nuclei is clear in the case of specialized myofiber regions but the biological purpose of differences among nuclei in unspecialized

regions remains unclear. Nuclei within the body of the myofiber, where there is no readily discernable regionalization, differ in nuclear import, gene expression, and protein accumulation. These differences could be important in coordinating nuclear activity among the nuclei in the myofiber, represent waves of nuclear activity pulsing through a fiber, or be indications of specialized regions not bound by easily identifiable anatomical borders. Identifying the impact of these differences among myonuclei will require understanding the biochemical mechanism responsible as well as advances in detection of low abundance nuclear proteins. Characterization of cargos specific to non-cNLS import pathways and identification of new non-cNLS pathways will provide candidate proteins which may be selectively localized to some but not all myonuclei. Alternatively, by separating myonuclei based on import activity, transcript production, or protein accumulation, advancements in proteomics and transcriptomics would enable comparison of nuclear protein and RNA contents. This would reveal the functional effects of differences in nuclear import. The specific differences identified could shed light on ways myofibers regulated expression or repression of specific gene programs

As described in Chapter 1, nuclei in multinucleated cells in which nuclear properties of individual nuclei have been examined differ (Lehmann and Nüsslein-Volhard 1986, Fontaine and Changeux 1989, Gladfelter, Hungerbuehler et al. 2006, Etxebeste, Ni et al. 2008, Ellery, Cindrova-Davies et al. 2009, Shalakhmetova, Umbayev et al. 2009, Youn, Takada et al. 2010, Orias, Cervantes et al. 2011). Advancements in describing mechanisms regulating differences among syncytial nuclei informs studies in other multinucleated cell types. Our findings that nuclear import differs among myonuclei in a single cell and that nuclear activity is responsive to circulating factors could be of particular

interest to the researchers studying osteoclasts and the syncytiotrophoblast. Osteoclasts are multinucleated cells containing 10-20 nuclei and are responsible for bone breakdown (Youn, Takada et al. 2010). In osteoporosis, overactivity of osteoclasts in relation to bone depositing cells (osteoblasts), results in dangerously decreased bone density. Osteoporotic bone is fragile and individuals with osteoporosis are frail and have increased at risk of serious injury and death following a fall (Khosla and Hofbauer 2017). As bone resorption activity of an osteoclast positively correlates with nuclear number (Youn, Takada et al. 2010), modulating nuclear activity could also modulate bone resorption. Examining nuclear import in osteoclasts could reveal a therapeutic target to reduce nuclear activity in osteoclasts thereby reducing bone resorption and ameliorating the effects of osteoporosis.

The synctiotrophoblast is an embryonically derived portion of the placenta that contains thousands of nuclei that vary in morphology and transcriptional activity. The trophoblast directly interacts with the maternal portion of the placenta, the myometrium, and is the site of exchange of nutrients, gases and waste between the maternal and fetal bloodstreams (Huppertz and Gauster 2011). Several pregnancy complications, including eclampsia, are associated with abnormalities in the syctiotrophoblast (Ellery, Cindrova-Davies et al. 2009). Examination of placentas from patients with eclampsia revealed an increased abundance of morphologically abnormal, transcriptionally inactive nuclei. Applying techniques presented in this dissertation the normal and abnormal nuclei of the syctiotrophoblast could be examined to determine the mechanisms by which the trophoblast nuclei sharing a common cytoplasm differ and the biochemical mechanism that inactivates the nuclei. Modulating nuclear activity could be a potential therapeutic avenue for ameliorating the symptoms of eclampsia.

Here we have presented nuclear import as one mechanism contributing to establishing differences among myonuclei and the first detailed examination of the myonuclear proteome. We have also developed a technique to isolate myonuclei for downstream quantitative analysis. Our work lays the foundation for further studies into skeletal muscle function on the level of individual nuclei. Future work will continue to establish the importance of the myonuclear compartment in maintaining proper muscle function and coordinating systemic responses to stress. Studies based on this work will inform our understanding of myofiber physiology and cell biology of multinucleated cells in general.

Appendix 1: Biochemical isolation of myonuclei from mouse skeletal muscle tissue

A portion of this chapter has been submitted for publication as:

Cutler, A.A., A.H. Corbett, G.K. Pavlath, *Biochemical isolation of myonuclei from mouse skeletal muscle tissue.* Bio-protocol (2017).

Appendix 1.1 Abstract

Skeletal muscle provides the contractile force necessary for movement, swallowing, and breathing and, consequently, is necessary for survival. Skeletal muscle cells are unique in that they are extremely large cells containing thousands of nuclei. These nuclei must all work in concert to maintain skeletal muscle function and thereby maintain life. The nucleus is a major site of signaling integration and gene expression regulation. However, examining nuclear processes in skeletal muscle can be difficult because myonuclei are challenging to isolate. We optimized a protocol to purify myonuclei from whole muscle tissue using ultracentrifugation over a discontinuous sucrose gradient to separate the nuclear fraction. We used these purified nuclei for downstream applications including flow cytometry and mass spectrometry. We used this method to compare the myonuclear proteome of young and old mouse hindlimb muscles (Cutler *et al*., 2017). This protocol may be applied to isolating myonuclei for a variety of downstream analyses such as flow cytometry, microscopy, Western blot, and proteomics.

Appendix 1.2 Background

Proper skeletal muscle function must be maintained for survival. One component of this maintenance is adjustments in gene expression in response to cellular needs and environmental cues. Nuclear processes modulating gene expression are a critical component in regulating cellular composition and behavior. However, myonuclear proteins involved in these processes are difficult to study because of four technical limitations. First, skeletal muscle is dense, tightly packed with contractile proteins that make up more than 60% of proteins in the tissue (Deshmukh *et al*., 2015; Cutler *et al*., 2017). These high abundance contractile proteins eclipse the far less abundant nuclear proteins. Second, the dense fibrous structure of skeletal muscle makes it difficult to dissociate without damaging nuclei, making nuclei difficult to isolate. Third, after centrifugation dense debris cosediments with nuclei, compounding the difficulty of isolating nuclei from the tissue. Fourth, skeletal muscle is comprised of multiple cell types, so nuclei isolated and nuclear proteins detected may be from myonuclei or nuclei of other cell types.

Several approaches have been optimized to enrich myonuclei from different organisms for various downstream applications. Ohkawa *et al*. presented a detailed protocol for isolating myonuclei from mouse tissue that was developed to maximize access of cross-linking reagent for Chromatin Immunoprecipitation (ChIP) analysis (Ohkawa *et al*., 2012). Wilkie and Shrimer developed a procedure to isolate the myonuclear envelope and sarcoplasmic reticulum for proteomic comparison (Wilkie and Schirmer, 2008). An approach optimized by Dimauro *et al*. simultaneously collected mitochondrial, nuclear, and cytoplasmic fractions to compare protein localization among different cellular compartments (Dimauro *et al*., 2012). While each of these approaches to enrich nuclei from skeletal muscle tissue was effective for the intended subsequent analysis, they did not prioritize isolating intact nuclei and do not distinguish between myonuclei and nuclei from other cell types. An affinity based method to selectively isolate nuclei from specific cell types was developed in *Arabadopsis thaliana* (Deal and Henikoff, 2011) and is now available for mice (Jankowska *et al*., 2016). However, this affinity based approach requires genetic labeling of the cell types of interest, which makes it prohibitively cumbersome to examine myonuclei from multiple mouse models. We optimized an ultracentrifugation sucrose gradient-based fractionation approach that requires relatively small sample sizes, no genetic labeling, and is compatible with downstream analysis by flow cytometry and mass spectrometry. The isolated nuclei are intact, biochemically depleted of proteins from non-nuclear organelles, and 85% of nuclei are myonuclei. To isolate myonuclei more quickly we also optimized affinity based purification using a myonuclear-specific nuclear envelope protein, Transmembrane Protein 38A (TMEM38A) (Bleunven *et al*., 2008; Cutler *et al*., 2017), and magnetic beads. This approach is more rapid and yields nuclei with comparable population purity to nuclear isolation by ultracentrifugation but with lower biochemical purity. These nuclear isolation techniques can be used to purify myonuclei from any mouse model for diverse downstream analyses.

Appendix 1.3 Materials and Reagents

A. Materials

1. 10 ml round bottom polypropylene tubes (Fisher Scientific, catalog number: 14-959-11B)
2. 40 µm nylon mesh cell strainer (BioExpress, catalog number: C-4700-1)
3. 50 ml conical polypropylene tubes (BioExpress, catalog number: C-3394-4)
4. 30 ml ultraclear ultracentrifuge tubes (Beckman Coulter, catalog number: 344058)
5. 1.7 ml low-adhesion hydrophobic tubes (BioExpress, catalog number: C-3302-1)
6. 5 ml conical polystyrene tube with cell strainer cap (Corning, catalog number: 352235)
7. 15 cm glass Pasteur pipets (Fisher Scientific, catalog number: 13-678-20A)
8. 0.45 µm polypropylene syringe filters (Thermo Fisher Scientific, catalog number: F2500-9)
9. 20-gauge needle (Fisher Scientific, catalog number: 14-826-5C)
10. 10 ml syringe (Fisher Scientific, catalog number: 14-823-2A)

B. Reagents

1. Sucrose (Fisher Scientific, catalog number: BP220)
2. HEPES (Fisher Scientific, catalog number: BP310)
3. Potassium chloride (KCl) (Fisher Scientific, catalog number: P217)
4. Magnesium chloride ($MgCl_2$) (Fisher Scientific, catalog number: M33)
5. Sodium hydroxide (NaOH) (Fisher Scientific, catalog number: S318)
6. Spermidine (Sigma-Aldrich, catalog number: 85558)
7. Spermine tetrahydrochloride (Sigma-Aldrich, catalog number: S2876)
8. Dithiothreitol (DTT) (US Biological, catalog number: D8070)
9. cOmplete mini protease inhibitors (Roche Diagnostic, catalog number: 11836153001)
10. Bovine serum albumin (BSA) (Sigma-Aldrich, catalog number: A2153)
11. 1x phosphate buffered saline (Fisher Scientific, catalog number: 21-600-069)
12. 4,6-Diamidino-2-phenylindole (DAPI) (Sigma-Aldrich, catalog number: D9542)
13. Protein A-conjugated magnetic beads (Thermo Fisher Scientific, catalog number: 10001D)

14. Anti-TMEM38A antibody (EMD Millipore Corportation, catalog number: 06-1005)
15. Ethylenediaminetetraacetic acid (EDTA) (Fisher Scientific, catalog number: BP120)
16. Ethylene glycol-bis(β-aminoethylether)-N,N,N’,N’-tetraacetic acid (EGTA) (Sigma-Aldrich, catalog number: E3889)
17. 100 mM EDTA (see Recipes)
18. 100 mM EGTA (see Recipes)
19. 2.1 M sucrose solution (see Recipes)
20. 2.8 M sucrose solution (see Recipes)
21. Homogenization buffer (see Recipes)
22. 1% BSA homogenization buffer (see Recipes)
23. Resuspension buffer (see Recipes)
24. 1% BSA resuspension buffer (see Recipes)

Appendix 1.4 Equipment

1. Dissection equipment
    a. Pins (Carolina Biological Supply Company, catalog number: 629122)
    b. 4.5 inch pointed dissection scissors (Fisher Scientific, catalog number: 08-940)
    c. Hemostat (Graham-Field Health Products Incorporated, catalog number: 2675)
2. 15 ml Dounce homogenizer with PTFE serrated plunger (Cole-Parmer Instrument Company, catalog numbers: 44468-07 and 44468-16)
3. UV lamp (optional) (Spectroline, catalog number: ENF-240C)
4. Centrifuge (Eppendorf, model: 5702)
5. Microcentrifuge (International Equipment Company, model: 3590F1917)
6. Ultracentrifuge (Beckman Coulter, model: Optima LE-80K LLE7)
7. SW 32 Ti swing bucket rotor (Beckman Coulter, model: SW 32 Ti, catalog number: 369650)
8. UltraRocker rocking platform (Bio-Rad Laboratories, catalog number: 1660709EDU)

9. Magnet (optional) (Thermo Fisher Scientific, catalog number: 12320D)
10. Round ended microspatula (Fisher Scientific, catalog number: 21-401-5)

Appendix 1.5 Procedure

Note: All solutions should be chilled to 4 °C and all steps performed at 4 °C to reduce enzyme activity and preserve sample integrity.

1. Prepare 2.8 M and 2.1 M sucrose solutions (see Recipes) and buffers.
   Note: It is easiest to prepare the sucrose gradient if 8 ml of the 2.8 M sucrose solution is added to the bottom of the 30 ml ultracentrifuge tubes before it is chilled to 4 °C.
2. Prepare dissection equipment by washing thoroughly with ethanol
3. Dissect gastrocnemius and rectus femoris muscles from mouse (Figure A1) and place up to 4 muscles in 10 ml round bottom tube.
   Notes:

a. The soleus often adheres to the gastrocnemius during dissection. Remove the soleus from the gastrocnemius before proceeding to process the gastrocnemius.

b. The rectus femoris is one of four muscles that make up the quadriceps.

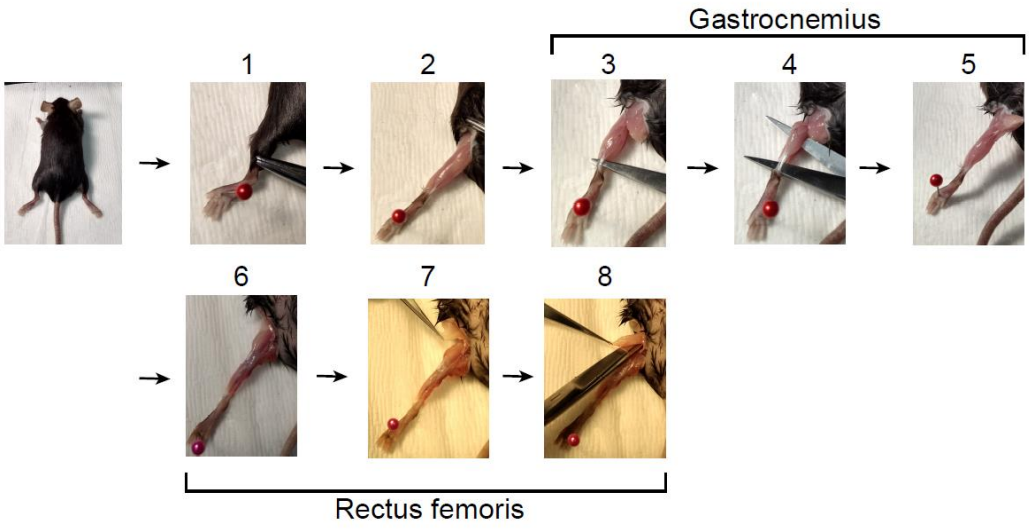

Figure A1. Muscle dissection. **1.** Starting with the mouse lying on its ventral side, use hemostats to retract skin from ankle to hip. **2.** Remove the fat pad over the back of the knee. **3.** Insert scissors behind Achilles tendon. **4.** Open scissors to separate gastrocnemius muscle from underlying tissue. **5.** Cut Achilles tendon and the head of the gastrocnemius. If the soleus is still attached to the gastrocnemius, remove it. **6.** Turn the mouse over so it is lying on its back. **7.** Remove the fat pad over the hip. **8.** With scissors parallel to the femur cut the tendon connecting the rectus femoris to the acetabulum (knee) and continue lengthwise to the hip. Finally, with scissors perpendicular to the femur cut the tendon connecting the muscle to the iliac spine and collect the rectus femoris muscle.

4. Mince muscles with scissors.
5. Add 5 ml of chilled homogenization buffer (see Recipes) for 1-2 muscles or 10 ml of chilled homogenization buffer for 3-4 muscles to the minced muscles.
6. Homogenize muscles with dounce homogenizer on ice about 50 strokes (until all large chunks of muscle have been forced from the bottom of the homogenizer to the top of the plunger) (Figure A2).

   Notes:

   a. *Warning: a vacuum may form between the plunger and the surface of the homogenization buffer. If the plunger rapidly collides the buffer this can shatter the homogenizer.*
   b. *If you are pooling homogenate from more than 4 muscles, homogenize them separately and then pool the homogenate prior to step 7.*
   c. *Aged or regenerating muscle samples may take longer to homogenize*
   d. *Homogenizer and dissection equipment should be cleaned with ethanol and water*.

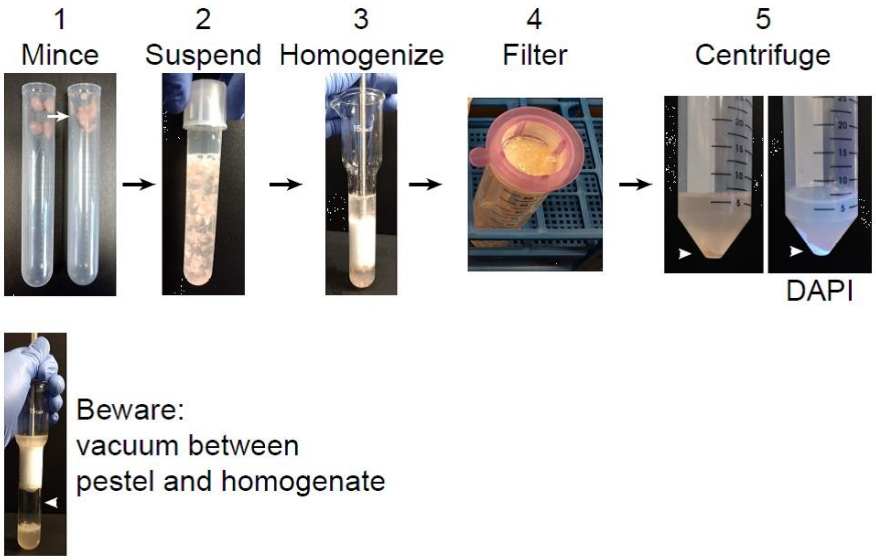

Figure A2. Pre-ultracentrifugation preparation. 1. Using scissors mince collected muscles in the tube. Intact muscles are shown on the left and minced muscles on the right. **2.** Suspend the minced muscles in 10 ml homogenization buffer. **3.** Homogenize muscle using a dounce homogenizer. **4.** Pass homogenate through a 40 µm filter into a 50 ml conical tube. Incompletely disrupted tissue and large debris will remain in the filter. **5.** Centrifuge the filtrate to obtain a crude nuclear pellet (arrowhead). DAPI clearly labels the nuclear pellet under UV light. **Warning:** when homogenizing a vacuum may form between the pestle and homogenate. If the pestle is sucked down into the homogenizer, it can strike with sufficient force to shatter the homogenizer.

7. Rinse a 40 µm filter with 1-2 ml of homogenization buffer. Pass the homogenate over this filter into a 50 ml conical.

   Note: Fibrous material that cannot pass through the filter may clog the filter. Gently scrape the filter with a round ended microspatula to help the filtrate pass through.

8. Rinse the filter with 5 ml homogenization buffer.
9. Centrifuge the filtrate at 1,000 *x g* for 10 min at 4 °C to obtain a crude nuclear pellet.
10. During the centrifugation, carefully layer 12 ml of the 2.1 M sucrose solution over the 2.8 M sucrose cushion in the 30 ml ultracentrifuge tube.

11. After the centrifugation is completed, discard the cytoplasmic supernatant and resuspend the crude nuclear pellet in 8 ml homogenization buffer. Carefully layer the resuspended lysate on the top of the sucrose gradient.

    Notes:

    a. *If DAPI is added at a final concentration of 1 µg/ml to the homogenate at this step, the position of the nuclei in the sucrose gradient can be visualized.*
    b. *The cytoplasmic fraction can be saved for subsequent biochemical or proteomic analysis. If it will be used immediately the cytoplasmic fraction should be kept on ice. For longer term storage the cytoplasmic fraction should be aliquoted and stored at -80°C.*

12. Balance the ultracentrifuge tubes by weight.
13. Centrifuge the samples at 186,712 max G (32,000 rpm in SW 32 Ti Beckman swing bucket rotor) for 3:20 at 4 °C.
14. During the centrifugation, coat a 50 ml conical tube with BSA by incubating it with 20 ml 1% BSA resuspension buffer (see Recipes) for at least 30 min at 4 °C with low speed rocking on a standard laboratory rocker.

    Note: Removing the top of a glove box allows the tubes to roll on the rocker resulting in even BSA coating of up to 6 tubes (Figure 3).

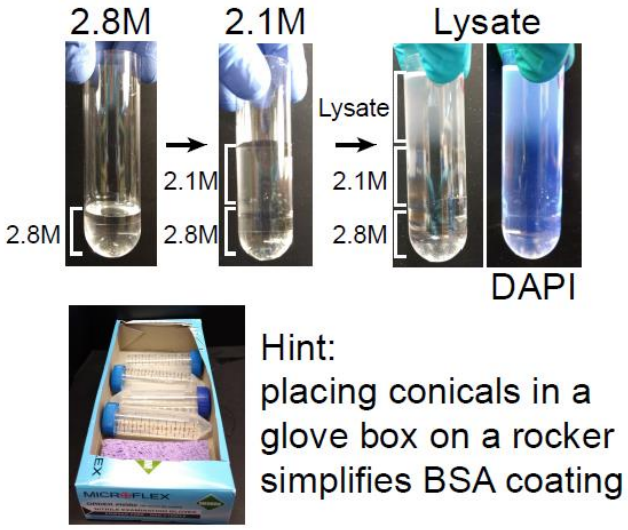

Figure A3. Loading ultracentrifuge tubes. Before beginning the protocol, 2.8 M sucrose should be layered into the bottom of the ultracentrifuge tube and chilled. During 1,000 *x g* centrifugation step of the muscle homogenate, layer chilled 2.1 M sucrose solution over the 2.8 M solution. When the centrifugation of the muscle homogenate is completed, resuspend the crude nuclear pellet in homogenization buffer and carefully layer it over the 2.1 M solution. DAPI labels the nuclei in the lysate. During the ultracentrifugation step coat 50 ml conical tubes with BSA, which is simplified by allowing the tubes to roll in a box on the rocker.

15. After the ultracentrifugation is complete, aspirate the upper layers of the sucrose gradient to within a centimeter of the 2.1 M and 2.8 M boundary. Collect the 2.1 M/2.8 M interface into the BSA-coated 50 ml conical tubes using glass Pasteur pipettes (Figure A4 steps 1-4).

    Notes:

    a. *If the overlying layers have been correctly removed there is little danger of contaminating the nuclear fraction with material from another interface. Thus collecting 1 cm above and 1 cm below the interface will increase yield of nuclei without endangering the purity of the fraction.*
    b. *If DAPI has been added to the homogenate, the position of the nuclei in the gradient can be visualized with UV light. DAPI fluorescence under UV light can be used to confirm that the entire interface containing the nuclei has been collected (Figure A4 step 4).*
    c. *Nuclei can be collected by puncturing the side of the ultracentrifugation tube with a 20-gauge needle and 10 ml syringe. However, nuclei are sheared passing through the needle and the high viscosity of the sucrose makes collection difficult. Similarly, collection of fractions beginning with the bottom of the gradient is difficult because of the high viscosity of the 2.8 M sucrose.*

16. Dilute the collected interface in the 50 ml conical tube 1:10 with resuspension buffer (see Recipes). Mix by inverting 5-10 times (Figure A4 step 5).

Note: The collected interface is much denser than the resuspension buffer. Be careful to completely mix the interface and resuspension buffer.

17. Centrifuge the diluted interface in the 50 ml conical tube at 1,000 *x g* for 10 min at 4 °C (Figure A4 step 6).
18. Discard the supernatant and resuspend the nuclear pellet in 1 ml resuspension buffer and transfer to a 1.7 ml tube.

    Note: For flow cytometry and microscopy, resuspend the nuclei in chilled resuspension buffer with 1% BSA.

19. Centrifuge the resuspended nuclei at 800 *x g* for 10 min at 4 °C (Figure A4 step 8).
20. Discard the supernatant and resuspend the nuclear pellet in appropriate buffer (See Figure A5A for representative images of isolated nuclei).

    Notes:

    a. *For flow cytometry, resuspend the nuclear pellet in 500 µl resuspension buffer with 1% BSA and pass through a 35 µm cell strainer into a 5 ml polystyrene tube before analyzing.*
    b. *For microscopy, resuspend the nuclear pellet in 1-3 ml resuspension buffer with 1% BSA.*
    c. *For western blot or mass spectrometry, wash the nuclear pellet two more times with resuspension buffer to remove residual BSA, then resuspend in an appropriate denaturing buffer.*

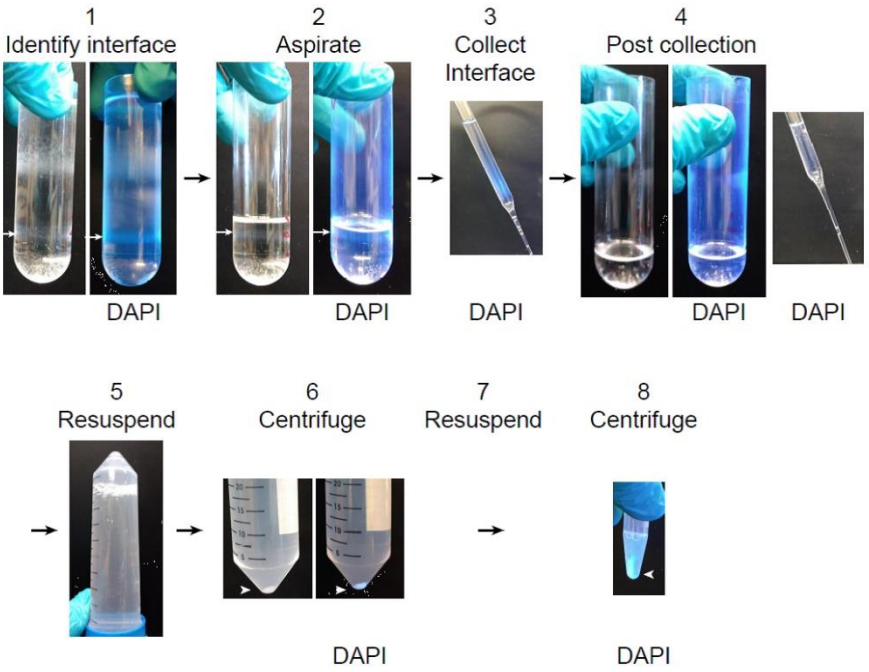

Figure A4. Unloading ultracentrifuge tubes. 1. Identify the interface between the 2.8 M and 2.1 M sucrose solutions which contains the nuclear fraction (white arrow). It is easy to identify by DAPI fluorescence under UV light. **2.** Aspirate the overlying layers to a centimeter above the nuclear fraction (white arrow). **3.** Collect the nuclear fraction into the BSA-coated 50 ml conical tube. Nuclei in the fraction can be observed by DAPI fluorescence. **4.** After collecting the nuclear fraction, the thin gray band of nuclei will no longer be visible and no DAPI fluorescence will be detectable in the ultracentrifuge tube or sucrose collected from the surface of the remaining solution. **5.** Resuspend the collected nuclear fraction 1:10 in resuspension buffer by inverting the BSA-coated 50 ml conical tube several times. **6.** Pellet the purified nuclei by centrifugation. The nuclear pellet is easy to see both with and without DAPI labeling. **7.** Remove the supernatant and resuspend the pellet in 1.5 ml resuspension buffer. **8.** Pellet the nuclei by centrifugation. Nuclei can be resuspended for imaging or washed 2 more times for biochemical and proteomic analyses.

Appendix 1.6 Optional alternative approach

If biochemical purity is not critical, nuclei can be isolated more rapidly by affinity purification. Nuclei isolated by affinity purification are depleted for mitochondrial and cytoplasmic markers but retain substantial amounts of endoplasmic reticulum markers. If specific nuclear markers are known affinity based purification can be easily applied to other cell types (Deal and Henikoff, 2011).

Note: All solutions should be chilled to 4 °C and all steps performed at 4 °C.

1. Wash 1.5 mg Protein A-conjugated magnetic beads by incubating with 500 µl homogenization buffer in a 1.7 ml microcentrifuge tube for 5 min with rocking. Then place the tube in a magnetic separation rack and wait 20 sec for the beads to accumulate on the side of the tube and aspirate the buffer. Repeat 2 times.
2. Add 5 µg anti-TMEM38A antibody and 200 µl homogenization buffer with 1% BSA to the washed beads. Incubate at 4 °C with low speed rocking for 30 min.
   Note: Magnetic beads rather than agarose or sepharose beads must be used because debris will cosediment with the agarose or sepharose beads but can be separated from magnetic beads which accumulate on the side of the tube where the magnet is placed.
3. Process samples as described above for steps 2-8.
4. After centrifugation to obtain a crude nuclear pellet (described in step 8 above), discard the supernatant and resuspend the pellet in 1 ml chilled homogenization buffer with 1% BSA.
5. Incubate the magnetic beads with the resuspended nuclei from up to 4 muscles at 4 °C for 30 min with gentle rocking.
6. Place the tubes containing the beads in a magnetic separation rack and wait 20 sec for the beads to accumulate on the side of the tube. Aspirate the buffer and debris at the bottom of the tube.
7. Wash the magnetic beads once with 500 µl chilled homogenization buffer with 1% BSA (see Recipes).
8. Resuspend the beads in an appropriate buffer for the downstream application (See Figure 5B for representative images of isolated nuclei).

Notes:

a. *For flow cytometry, resuspend the nuclei in 500 µl resuspension buffer with 1% BSA and pass through a 35 µm cell strainer into a 5 ml polystyrene tube before analyzing.*
b. *For microscopy, resuspend the nuclei in resuspension buffer with 1% BSA.*
c. *For Western blot or mass spectrometry, wash the nuclei twice with PBS to remove residual BSA and resuspend in the appropriate denaturing buffer for downstream application.*

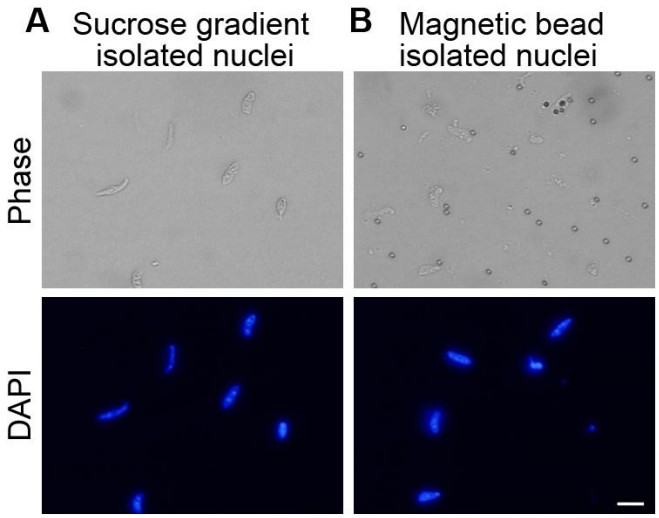

Figure A5. Purified myonuclei. A. Nuclei isolated by ultracentrifugation through 2.1 M sucrose. Nuclei are visible in DAPI channel. **B.** Affinity purified nuclei isolated by binding of TMEM38A antibody and magnetic beads to nuclei. Nuclei are visible in DAPI channel. Scale bar = 10 µm.

Appendix 1.7 Data analysis

Data should be processed according to standard practice for the relevant downstream technique. Appropriate downstream analysis can include microscopy, western blot, proteomics, and flow cytometry.

The average yield from a single mouse gastrocnemius muscle is $1x10^6$ nuclei. Pooling two gastrocnemius and two rectus femoris muscles yields $6x10^6$ nuclei and 8 µg of total protein. It should be noted that unless care is taken to thoroughly wash nuclei, residual BSA can artificially inflate measurements of total protein. For this reason, it is recommended to first check purity and yield by microscopy and then measure protein concentration if applicable. The yield and purity are consistent between experiments. The greatest variation in yield resulted from failure to keep samples at 4°C for the duration of the experiment.

For proteomics applications we had the greatest success when both gastrocnemius and rectus femoris muscles from 3 mice were pooled. Proteomics experiments should be completed with at least 5 biological replicates to detect small changes in protein abundance.

For analysis by flow cytometry nuclei isolated from a single gastrocnemius or rectus femoris muscle provided ample starting material. Flow cytometry experiments should include at least three biological replicates.

Appendix 1.8 Notes

1. The biochemical purification of myonuclei requires about 5 h to complete. If a large number of samples are being prepared more time is required. Magnetic bead affinity based preparation requires about 1 h to complete.
2. Endoplasmic reticulum depletion is variable across preparations.

Appendix 1.9 Recipes

1. 100 mM EDTA (50 ml)
   Combine:

   372 mg EDTA

40 ml ultra-pure water

Adjust pH to 7 with NaOH

Adjust final volume to 50 ml with ultra-pure water

Store at room temperature for up to a year

2. 100 mM EGTA (50 ml)
   Combine:

   1.9 g EGTA

   40 ml ultra-pure water

   Adjust to pH 8 with NaOH

   Adjust final volume to 50 ml with ultra-pure water

   Store at room temperature for up to a year

3. 2.1 M sucrose solution (50 ml)
   Combine the following over high heat with medium stirring:

   35.9 g sucrose

   2.5 ml HEPES (1 M)

   1.25 ml KCl (1 M)

   2.5 ml $MgCl_2$ (100 mM)

   Ultra-pure water to 50 ml

   Note: Because the solution is made over heat, some of the fluid will boil off. Adjust the final volume after the solution has been removed from heat.

   Store at 4 °C for up to 1 week

4. 2.8 M sucrose solution (25 ml)
   Combine the following over high heat with medium stirring:

   24 g sucrose

1.25 ml HEPES (1 M)

625 µl KCl (1 M)

1.25 ml $MgCl_2$ (100 mM)

Ultra-pure water to 25 ml

Note: Because the solution is made over heat, some of the fluid will boil off. Adjust the final volume after the solution has been removed from heat.

Prepare fresh for each use

5. Homogenization buffer (50 ml)
   Combine the following:

   500 µl HEPES (1 M)

   3 ml KCl (1 M)

   250 µl spermidine (100 mM)

   750 µl spermine tetrahydrochloride (10 mM)

   10 ml EDTA (10 mM)

   250 µl EGTA (100 mM)

   2.5 ml $MgCl_2$ (100 mM)

   5.13 g sucrose

   Ultra-pure water to 50 ml

   Filter sterilize and store at 4 °C for up to 1 month

   Immediately prior to use add:

   100 µl DTT (1M)

   5 Roche cOmplete mini protease inhibitor tablets

6. 1% BSA homogenization buffer (50ml)

Combine the following:

500 mg	BSA
50 ml	homogenization buffer

Prepare fresh for each use

7. Resuspension buffer (50 ml)

   Combine the following:

1 ml	HEPES (1 M)
750 µl	$MgCl_2$ (100 mM)
500 µl	KCl (1 M)
250 µl	spermidine (100 mM)
750 µl	spermine tetrahydrochloride (10 mM)
1 ml	EDTA (10 mM)
45.75 ml	ultra-pure water

   Store at 4 °C for up to 1 month

8. 1% BSA resuspension buffer (50 ml)

   Combine the following:

500 mg	BSA
50 ml	resuspension buffer

   Prepare fresh for each use

Acknowledgments

This work was supported by grants to GKP (AR062483), to AAC (AR067645), and a training grant (T32GM008367) from the National Institutes of Health. The described protocol was adapted from the work of Wilkie *et al*. (Wilkie and Schirmer, 2008)).

References

Abbott, K. L., B. B. Friday, D. Thaloor, T. J. Murphy and G. K. Pavlath (1998). "Activation and cellular localization of the cyclosporine A-sensitive transcription factor NF-AT in skeletal muscle cells." Mol Biol Cell **9**(10): 2905-2916.

Adam, S. A. (2016). "Nuclear Protein Transport in Digitonin Permeabilized Cells." Methods Mol Biol **1411**: 479-487.

Adam, S. A., R. S. Marr and L. Gerace (1990). "Nuclear protein import in permeabilized mammalian cells requires soluble cytoplasmic factors." J Cell Biol **111**(3): 807-816.

Anderson, C. A., U. Eser, T. Korndorf, M. E. Borsuk, J. M. Skotheim and A. S. Gladfelter (2013). "Nuclear repulsion enables division autonomy in a single cytoplasm." Curr Biol **23**(20): 1999-2010.

Anderson, J. M., A. Rodriguez and D. T. Chang (2008). "Foreign body reaction to biomaterials." Semin Immunol **20**(2): 86-100.

Anderson, K. V. and C. Nusslein-Volhard (1984). "Information for the dorsal--ventral pattern of the Drosophila embryo is stored as maternal mRNA." Nature **311**(5983): 223-227.

Andres-Hernando, A., M. A. Lanaspa, C. J. Rivard and T. Berl (2008). "Nucleoporin 88 (Nup88) is regulated by hypertonic stress in kidney cells to retain the transcription factor tonicity enhancer-binding protein (TonEBP) in the nucleus." J Biol Chem **283**(36): 25082-25090.

Apel, E. D., R. M. Lewis, R. M. Grady and J. R. Sanes (2000). "Syne-1, a dystrophin- and Klarsicht-related protein associated with synaptic nuclei at the neuromuscular junction." J Biol Chem **275**(41): 31986-31995.

Ariizumi, T., A. Ogose, H. Kawashima, T. Hotta, H. Umezu and N. Endo (2009). "Multinucleation followed by an acytokinetic cell division in myxofibrosarcoma with giant cell proliferation." J Exp Clin Cancer Res **28**: 44.

Artaza, J. N., S. Bhasin, C. Mallidis, W. Taylor, K. Ma and N. F. Gonzalez-Cadavid (2002). "Endogenous expression and localization of myostatin and its relation to myosin heavy chain distribution in C2C12 skeletal muscle cells." J Cell Physiol **190**(2): 170-179.

Asally, M., Y. Yasuda, M. Oka, S. Otsuka, S. H. Yoshimura, K. Takeyasu and Y. Yoneda (2011). "Nup358, a nucleoporin, functions as a key determinant of the nuclear pore complex structure remodeling during skeletal myogenesis." Febs j **278**(4): 610-621.

Baraibar, M. A., M. Gueugneau, S. Duguez, G. Butler-Browne, D. Bechet and B. Friguet (2013). "Expression and modification proteomics during skeletal muscle ageing." Biogerontology **14**(3): 339-352.

Bassey, E. J. (1998). "Longitudinal changes in selected physical capabilities: muscle strength, flexibility and body size." Age Ageing **27 Suppl 3**: 12-16.

Bergmann, O., R. D. Bhardwaj, S. Bernard, S. Zdunek, F. Barnabe-Heider, S. Walsh, J. Zupicich, K. Alkass, B. A. Buchholz, H. Druid, S. Jovinge and J. Frisen (2009). "Evidence for cardiomyocyte renewal in humans." Science **324**(5923): 98-102.

Bianchi, E., K. Boekelheide, M. Sigman, S. J. Hall and K. Hwang (2017). "Ghrelin modulates testicular damage in a cryptorchid mouse model." PLoS One **12**(5): e0177995.

Biolo, G., X. J. Zhang and R. R. Wolfe (1995). "Role of membrane transport in interorgan amino acid flow between muscle and small intestine." Metabolism **44**(6): 719-724.

Bjornson, C. R., T. H. Cheung, L. Liu, P. V. Tripathi, K. M. Steeper and T. A. Rando (2012). "Notch signaling is necessary to maintain quiescence in adult muscle stem cells." Stem Cells **30**(2): 232-242.

Boissy, P., F. Saltel, C. Bouniol, P. Jurdic and I. Machuca-Gayet (2002). "Transcriptional activity of nuclei in multinucleated osteoclasts and its modulation by calcitonin." Endocrinology **143**(5): 1913-1921.

Bondesen, B. A., S. T. Mills, K. M. Kegley and G. K. Pavlath (2004). "The COX-2 pathway is essential during early stages of skeletal muscle regeneration." Am J Physiol Cell Physiol **287**(2): C475-483.

Boruc, J., A. H. Griffis, T. Rodrigo-Peiris, X. Zhou, B. Tilford, D. Van Damme and I. Meier (2015). "GAP Activity, but Not Subcellular Targeting, Is Required for Arabidopsis RanGAP Cellular and Developmental Functions." Plant Cell **27**(7): 1985-1998.

Bradford, M. M. (1976). "A rapid and sensitive method for the quantitation of microgram quantities of protein utilizing the principle of protein-dye binding." Anal Biochem **72**: 248-254.

Brenner, H. R., V. Witzemann and B. Sakmann (1990). "Imprinting of acetylcholine receptor messenger RNA accumulation in mammalian neuromuscular synapses." Nature **344**(6266): 544-547.

Bruning, J. C., M. D. Michael, J. N. Winnay, T. Hayashi, D. Horsch, D. Accili, L. J. Goodyear and C. R. Kahn (1998). "A muscle-specific insulin receptor knockout exhibits features of the metabolic syndrome of NIDDM without altering glucose tolerance." Mol Cell **2**(5): 559-569.

Bruusgaard, J. C., K. Liestøl, M. Ekmark, K. Kollstad and K. Gundersen (2003). "Number and spatial distribution of nuclei in the muscle fibres of normal mice studied in vivo." The Journal of Physiology **551**(Pt 2): 467-478.

Buchwalter, A. L., Y. Liang and M. W. Hetzer (2014). "Nup50 is required for cell differentiation and exhibits transcription-dependent dynamics." Mol Biol Cell **25**(16): 2472-2484.

Buckingham, M. (1992). "Making muscle in mammals." Trends Genet **8**(4): 144-148.

Buckingham, M., L. Bajard, T. Chang, P. Daubas, J. Hadchouel, S. Meilhac, D. Montarras, D. Rocancourt and F. Relaix (2003). "The formation of skeletal muscle: from somite to limb." Journal of Anatomy **202**(1): 59-68.

Butel, J. S., M. J. Guentzel and F. Rapp (1969). "Variants of defective simian papovavirus 40 (PARA) characterized by cytoplasmic localization of simian papovavirus 40 tumor antigen." J Virol **4**(5): 632-641.

Cahill, G. F., Jr. (1970). "Starvation in man." N Engl J Med **282**(12): 668-675.

Calderaro, J., G. Couchy, S. Imbeaud, G. Amaddeo, E. Letouze, J. F. Blanc, C. Laurent, Y. Hajji, D. Azoulay, P. Bioulac-Sage, J. C. Nault and J. Zucman-Rossi (2017). "Histological subtypes of hepatocellular carcinoma are related to gene mutations and molecular tumour classification." J Hepatol.

Calura, E., S. Cagnin, A. Raffaello, P. Laveder, G. Lanfranchi and C. Romualdi (2008). "Meta-analysis of expression signatures of muscle atrophy: gene interaction networks in early and late stages." BMC Genomics **9**(1): 1-20.

Campbell, M., A. McComas and F. Petito (1973). "Physiological changes in ageing muscles." Journal of Neurology, Neurosurgery & Psychiatry **36**(2): 174-182.

Capitanio, D., M. Vasso, S. De Palma, C. Fania, E. Torretta, F. P. Cammarata, V. Magnaghi, P. Procacci and C. Gelfi (2016). "Specific protein changes contribute to the differential muscle mass loss during ageing." Proteomics **16**(4): 645-656.

Capitanio, D., M. Vasso, C. Fania, M. Moriggi, A. Vigano, P. Procacci, V. Magnaghi and C. Gelfi (2009). "Comparative proteomic profile of rat sciatic nerve and gastrocnemius muscle tissues in ageing by 2-D DIGE." Proteomics **9**(7): 2004-2020.

Carberry, S., M. Zweyer, D. Swandulla and K. Ohlendieck (2014). "Comparative proteomic analysis of the contractile-protein-depleted fraction from normal versus dystrophic skeletal muscle." Analytical Biochemistry **446**: 108-115.

Carpenter, A. E., T. R. Jones, M. R. Lamprecht, C. Clarke, I. H. Kang, O. Friman, D. A. Guertin, J. H. Chang, R. A. Lindquist, J. Moffat, P. Golland and D. M. Sabatini (2006). "CellProfiler: image analysis software for identifying and quantifying cell phenotypes." Genome Biology **7**(10): R100.

Castel, D., P. Mourikis, S. J. Bartels, A. B. Brinkman, S. Tajbakhsh and H. G. Stunnenberg (2013). "Dynamic binding of RBPJ is determined by Notch signaling status." Genes Dev **27**(9): 1059-1071.

Cekan, P., K. Hasegawa, Y. Pan, E. Tubman, D. Odde, J. Q. Chen, M. A. Herrmann, S. Kumar and P. Kalab (2016). "RCC1-dependent activation of Ran accelerates cell cycle and DNA repair, inhibiting DNA damage-induced cell senescence." Mol Biol Cell **27**(8): 1346-1357.

Cesari, M., S. B. Kritchevsky, B. W. H. J. Penninx, B. J. Nicklas, E. M. Simonsick, A. B. Newman, F. A. Tylavsky, J. S. Brach, S. Satterfield, D. C. Bauer, M. Visser, S. M. Rubin, T. B. Harris and M. Pahor (2005). "Prognostic Value of Usual Gait Speed in Well-Functioning Older People—Results from the Health, Aging and Body Composition Study." Journal of the American Geriatrics Society **53**(10): 1675-1680.

Chahine, M. N. and G. N. Pierce (2009). "Therapeutic targeting of nuclear protein import in pathological cell conditions." Pharmacol Rev **61**(3): 358-372.

Chaves, D. F., P. C. Carvalho, D. B. Lima, H. Nicastro, F. M. Lorenzeti, M. Siqueira-Filho, S. M. Hirabara, P. H. Alves, J. J. Moresco, J. R. Yates, 3rd and A. H. Lancha, Jr. (2013). "Comparative proteomic analysis of the aging soleus and extensor digitorum longus rat muscles using TMT labeling and mass spectrometry." J Proteome Res **12**(10): 4532-4546.

Chen, X. and L. Xu (2010). "Specific nucleoporin requirement for Smad nuclear translocation." Mol Cell Biol **30**(16): 4022-4034.

Chook, Y. M. and K. E. Suel (2011). "Nuclear import by karyopherin-betas: recognition and inhibition." Biochim Biophys Acta **1813**(9): 1593-1606.

Chook, Y. M. and K. E. Süel (2011). "Nuclear import by Karyopherin-βs: recognition and inhibition." Biochimica et biophysica acta **1813**(9): 1593-1606.

Cingolani, G., J. Bednenko, M. T. Gillespie and L. Gerace (2002). "Molecular basis for the recognition of a nonclassical nuclear localization signal by importin beta." Mol Cell **10**(6): 1345-1353.

Cohen, P. R., T. Paravar and R. A. Lee (2014). "Epidermal multinucleated giant cells are not always a histopathologic clue to a herpes virus infection: multinucleated epithelial giant cells in the epidermis of lesional skin biopsies from patients with acantholytic dermatoses can histologically mimic a herpes virus infection." Dermatology Practical & Conceptual **4**(4): 21-27.

Cooper, K. E., E. Preston and W. L. Veale (1976). "Effects of atropine, injected into a lateral cerebral ventricle of the rabbit, on fevers due to intravenous leucocyte pyrogen and hypothalamic and intraventricular injections of prostaglandin E1." J Physiol **254**(3): 729-741.

Copes, N., C. Edwards, D. Chaput, M. Saifee, I. Barjuca, D. Nelson, A. Paraggio, P. Saad, D. Lipps, S. M. Stevens, Jr. and P. C. Bradshaw (2015). "Metabolome and proteome changes with aging in Caenorhabditis elegans." Exp Gerontol **72**: 67-84.

Corbett, A. H. and P. A. Silver (1996). "The NTF2 gene encodes an essential, highly conserved protein that functions in nuclear transport in vivo." J Biol Chem **271**(31): 18477-18484.

Couteaux, R. and M. Pecot-Dechavassine (1973). "[Ultrastructural and cytochemical data on the mechanism of acetylcholine release in synaptic transmission]]." Arch Ital Biol **111**(3-4): 231-262.

Cox, J., M. Y. Hein, C. A. Luber, I. Paron, N. Nagaraj and M. Mann (2014). "Accurate Proteome-wide Label-free Quantification by Delayed Normalization and Maximal Peptide Ratio Extraction, Termed MaxLFQ." Molecular & Cellular Proteomics : MCP **13**(9): 2513-2526.

Cox, J., A. Michalski and M. Mann (2011). "Software lock mass by two-dimensional minimization of peptide mass errors." J Am Soc Mass Spectrom **22**(8): 1373-1380.

Cozzolino, I., G. Ciancia, G. Limite, R. Di Micco, V. Varone, A. Cortese, A. Vatrella, V. Di Crescenzo and P. Zeppa (2014). "Neuroendocrine differentiation in breast carcinoma with osteoclast-like giant cells. Report of a case and review of the literature." Int J Surg **12 Suppl 2**: S8-11.

Crampton, N., M. Kodiha, S. Shrivastava, R. Umar and U. Stochaj (2009). "Oxidative stress inhibits nuclear protein export by multiple mechanisms that target FG nucleoporins and Crm1." Mol Biol Cell **20**(24): 5106-5116.

Cutler, A. A., E. B. Dammer, D. M. Doung, N. T. Seyfried, A. H. Corbett and G. K. Pavlath (2017). "Biochemical isolation of myonuclei employed to define changes to the myonuclear proteome that occur with aging." Aging Cell **16**(4): 738-749.

D'Angelo, M. A., J. S. Gomez-Cavazos, A. Mei, D. H. Lackner and M. W. Hetzer (2012). "A change in nuclear pore complex composition regulates cell differentiation." Dev Cell **22**(2): 446-458.

D'Angelo, M. A., M. Raices, S. H. Panowski and M. W. Hetzer (2009). "Age-dependent deterioration of nuclear pore complexes causes a loss of nuclear integrity in postmitotic cells." Cell **136**(2): 284-295.

D'Angelo, M. A., M. Raices, S. H. Panowski and M. W. Hetzer (2009). "Age-dependent deterioration of nuclear pore complexes causes a loss of nuclear integrity in post-mitotic cells." Cell **136**(2): 284-295.

Dammer, E. B., D. M. Duong, I. Diner, M. Gearing, Y. Feng, J. J. Lah, A. I. Levey and N. T. Seyfried (2013). "Neuron enriched nuclear proteome isolated from human brain." J Proteome Res **12**(7): 3193-3206.

Dargent, J. L., L. Lespagnard, A. Kornreich, P. Hermans, N. Clumeck and A. Verhest (2000). "HIV-associated multinucleated giant cells in lymphoid tissue of the Waldeyer's ring: a detailed study." Mod Pathol **13**(12): 1293-1299.

Deal, R. B. and S. Henikoff (2011). "The INTACT method for cell type-specific gene expression and chromatin profiling in Arabidopsis thaliana." Nat Protoc **6**(1): 56-68.

Demontis, F., R. Piccirillo, A. L. Goldberg and N. Perrimon (2013). " Mechanisms of skeletal muscle aging: insights from Drosophila and mammalian models ." Disease Models & Mechanisms **6**(6): 1339-1352.

Deshmukh, A. S., M. Murgia, N. Nagaraj, J. T. Treebak, J. Cox and M. Mann (2015). "Deep proteomics of mouse skeletal muscle enables quantitation of protein isoforms, metabolic pathways, and transcription factors." Mol Cell Proteomics **14**(4): 841-853.

Dimauro, I., T. Pearson, D. Caporossi and M. J. Jackson (2012). "A simple protocol for the subcellular fractionation of skeletal muscle cells and tissue." BMC Research Notes **5**: 513-513.

Divisato, G., F. S. di Carlo, L. Pazzaglia, R. Rizzo, D. A. Coviello, M. S. Benassi, P. Picci, T. Esposito and F. Gianfrancesco (2017). "The distinct clinical features of giant cell tumor of bone in pagetic and non-pagetic patients are associated with genetic, biochemical and histological differences." Oncotarget.

Dix, D. J. and B. R. Eisenberg (1990). "Myosin mRNA accumulation and myofibrillogenesis at the myotendinous junction of stretched muscle fibers." J Cell Biol **111**(5 Pt 1): 1885-1894.

Draeger, A., A. G. Weeds and R. B. Fitzsimons (1987). "Primary, secondary and tertiary myotubes in developing skeletal muscle: a new approach to the analysis of human myogenesis." J Neurol Sci **81**(1): 19-43.

Dressel, U., P. J. Bailey, S. C. Wang, M. Downes, R. M. Evans and G. E. Muscat (2001). "A dynamic role for HDAC7 in MEF2-mediated muscle differentiation." J Biol Chem **276**(20): 17007-17013.

Dufour, A. B., M. T. Hannan, J. M. Murabito, D. P. Kiel and R. R. McLean (2013). "Sarcopenia definitions considering body size and fat mass are associated with mobility limitations: the Framingham Study." J Gerontol A Biol Sci Med Sci **68**(2): 168-174.

Dupont-Versteegden, E. E., B. A. Strotman, C. M. Gurley, D. Gaddy, M. Knox, J. D. Fluckey and C. A. Peterson (2006). "Nuclear translocation of EndoG at the initiation of disuse muscle atrophy and apoptosis is specific to myonuclei." Am J Physiol Regul Integr Comp Physiol **291**(6): R1730-1740.

Ellery, P. M., T. Cindrova-Davies, E. Jauniaux, A. C. Ferguson-Smith and G. J. Burton (2009). "Evidence for transcriptional activity in the syncytiotrophoblast of the human placenta." Placenta **30**(4): 329-334.

Erenpreisa, J., K. Salmina, A. Huna, E. A. Kosmacek, M. S. Cragg, F. Ianzini and A. P. Anisimov (2011). "Polyploid tumour cells elicit paradiploid progeny through depolyploidizing divisions and regulated autophagic degradation." Cell Biol Int **35**(7): 687-695.

Etxebeste, O., M. Ni, A. Garzia, N. J. Kwon, R. Fischer, J. H. Yu, E. A. Espeso and U. Ugalde (2008). "Basic-zipper-type transcription factor FlbB controls asexual development in Aspergillus nidulans." Eukaryot Cell **7**(1): 38-48.

Faria, A. M., A. Levay, Y. Wang, A. O. Kamphorst, M. L. Rosa, D. R. Nussenzveig, W. Balkan, Y. M. Chook, D. E. Levy and B. M. Fontoura (2006). "The nucleoporin Nup96 is required for proper expression of interferon-regulated proteins and functions." Immunity **24**(3): 295-304.

Faustino, R. S., T. J. Nelson, A. Terzic and C. Perez-Terzic (2007). "Nuclear transport: target for therapy." Clin Pharmacol Ther **81**(6): 880-886.

Fedorov, V. B., A. V. Goropashnaya, N. C. Stewart, Ø. Tøien, C. Chang, H. Wang, J. Yan, L. C. Showe, M. K. Showe and B. M. Barnes (2014). "Comparative functional genomics of adaptation to muscular disuse in hibernating mammals." Molecular ecology **23**(22): 5524-5537.

Ferri, P., E. Barbieri, S. Burattini, M. Guescini, A. D'Emilio, L. Biagiotti, P. Del Grande, A. De Luca, V. Stocchi and E. Falcieri (2009). "Expression and subcellular localization of myogenic regulatory factors during the differentiation of skeletal muscle C2C12 myoblasts." J Cell Biochem **108**(6): 1302-1317.

Finlay, D. R., D. D. Newmeyer, T. M. Price and D. J. Forbes (1987). "Inhibition of in vitro nuclear transport by a lectin that binds to nuclear pores." J Cell Biol **104**(2): 189-200.

Fogarty, N. M. E., A. C. Ferguson-Smith and G. J. Burton "Syncytial Knots (Tenney-Parker Changes) in the Human Placenta." The American Journal of Pathology **183**(1): 144-152.

Fontaine, B. and J. P. Changeux (1989). "Localization of nicotinic acetylcholine receptor alpha-subunit transcripts during myogenesis and motor endplate development in the chick." J Cell Biol **108**(3): 1025-1037.

Fontoura, B. M., G. Blobel and N. R. Yaseen (2000). "The nucleoporin Nup98 is a site for GDP/GTP exchange on ran and termination of karyopherin beta 2-mediated nuclear import." J Biol Chem **275**(40): 31289-31296.

Franz, C., R. Walczak, S. Yavuz, R. Santarella, M. Gentzel, P. Askjaer, V. Galy, M. Hetzer, I. W. Mattaj and W. Antonin (2007). "MEL-28/ELYS is required for the recruitment of nucleoporins to chromatin and postmitotic nuclear pore complex assembly." EMBO Rep **8**(2): 165-172.

Frescas, D., M. Mavrakis, H. Lorenz, R. Delotto and J. Lippincott-Schwartz (2006). "The secretory membrane system in the Drosophila syncytial blastoderm embryo exists as functionally compartmentalized units around individual nuclei." J Cell Biol **173**(2): 219-230.

Frontera, W. R., V. A. Hughes, R. A. Fielding, M. A. Fiatarone, W. J. Evans and R. Roubenoff (2000). "Aging of skeletal muscle: a 12-yr longitudinal study." J Appl Physiol (1985) **88**(4): 1321-1326.

Fujimaki, S., R. Hidaka, M. Asashima, T. Takemasa and T. Kuwabara (2014). "Wnt protein-mediated satellite cell conversion in adult and aged mice following voluntary wheel running." J Biol Chem **289**(11): 7399-7412.

Gannon, J. and K. Ohlendieck (2012). "Subproteomic analysis of basic proteins in aged skeletal muscle following offgel pre-fractionation." Mol Med Rep **5**(4): 993-1000.

Gheorghe, M., M. Snoeck, M. Emmerich, T. Bäck, J. J. Goeman and V. Raz (2014). "Major aging-associated RNA expressions change at two distinct age-positions." BMC Genomics **15**(1): 1-12.

Gladfelter, A. S., A. K. Hungerbuehler and P. Philippsen (2006). "Asynchronous nuclear division cycles in multinucleated cells." J Cell Biol **172**(3): 347-362.

Gomez-Cavazos, J. S. and M. W. Hetzer (2015). "The nucleoporin gp210/Nup210 controls muscle differentiation by regulating nuclear envelope/ER homeostasis." J Cell Biol **208**(6): 671-681.

Griffin, C. A., K. A. Kafadar and G. K. Pavlath (2009). "MOR23 promotes muscle regeneration and regulates cell adhesion and migration." Developmental cell **17**(5): 649-661.

Guan, T., R. H. Kehlenbach, E. C. Schirmer, A. Kehlenbach, F. Fan, B. E. Clurman, N. Arnheim and L. Gerace (2000). "Nup50, a nucleoplasmically oriented nucleoporin with a role in nuclear protein export." Mol Cell Biol **20**(15): 5619-5630.

Gueugneau, M., C. Coudy-Gandilhon, O. Gourbeyre, C. Chambon, L. Combaret, C. Polge, D. Taillandier, D. Attaix, B. Friguet, A. B. Maier, G. Butler-Browne and D. Bechet (2014). "Proteomics of muscle chronological ageing in post-menopausal women." BMC Genomics **15**: 1165.

Guidotti, J. E., O. Bregerie, A. Robert, P. Debey, C. Brechot and C. Desdouets (2003). "Liver cell polyploidization: a pivotal role for binuclear hepatocytes." J Biol Chem **278**(21): 19095-19101.

Gupta, G., S. B. Athanikar, V. V. Pai and K. N. Naveen (2014). "Giant Cells in Dermatology." Indian Journal of Dermatology **59**(5): 481-484.

Gustin, K. E. and P. Sarnow (2001). "Effects of poliovirus infection on nucleo-cytoplasmic trafficking and nuclear pore complex composition." Embo j **20**(1-2): 240-249.

Gustin, K. E. and P. Sarnow (2002). "Inhibition of nuclear import and alteration of nuclear pore complex composition by rhinovirus." J Virol **76**(17): 8787-8796.

Hanover, J. A., C. K. Cohen, M. C. Willingham and M. K. Park (1987). "O-linked N-acetylglucosamine is attached to proteins of the nuclear pore. Evidence for cytoplasmic and nucleoplasmic glycoproteins." J Biol Chem **262**(20): 9887-9894.

Harris, A. J., M. J. Duxson, R. B. Fitzsimons and F. Rieger (1989). "Myonuclear birthdates distinguish the origins of primary and secondary myotubes in embryonic mammalian skeletal muscles." Development **107**(4): 771-784.

Hawley, D., J. Ding, S. Thotakura, S. Haskett, H. Aluri, C. Kublin, A. Michel, L. Clapisson, M. Mingueneau and D. Zoukhri (2017). "RNA-Seq and CyTOF immuno-profiling of regenerating lacrimal glands identifies a novel subset of cells expressing muscle-related proteins." PLoS One **12**(6): e0179385.

Heazell, A. E., S. J. Moll, C. J. Jones, P. N. Baker and I. P. Crocker (2007). "Formation of syncytial knots is increased by hyperoxia, hypoxia and reactive oxygen species." Placenta **28 Suppl A**: S33-40.

Herskowitz, J. H., N. T. Seyfried, D. M. Duong, Q. Xia, H. D. Rees, M. Gearing, J. Peng, J. J. Lah and A. I. Levey (2010). "Phosphoproteomic analysis reveals site-specific changes in GFAP and NDRG2 phosphorylation in frontotemporal lobar degeneration." J Proteome Res **9**(12): 6368-6379.

Hetzer, M. W. and S. R. Wente (2009). "Border Control at the Nucleus: Biogenesis and Organization of the Nuclear Membrane and Pore Complexes." Developmental cell **17**(5): 606-616.

Hixon, M. L., C. Obejero-Paz, C. Muro-Cacho, M. W. Wagner, E. Millie, J. Nagy, T. J. Hassold and A. Gualberto (2000). "Cks1 mediates vascular smooth muscle cell polyploidization." J Biol Chem **275**(51): 40434-40442.

Holland, A., P. Dowling and K. Ohlendieck (2014). "New pathobiochemical insights into dystrophinopathy from the proteomics of senescent mdx mouse muscle." Front Aging Neurosci **6**: 109.

Huang da, W., B. T. Sherman and R. A. Lempicki (2009). "Bioinformatics enrichment tools: paths toward the comprehensive functional analysis of large gene lists." Nucleic Acids Res **37**(1): 1-13.

Huang da, W., B. T. Sherman and R. A. Lempicki (2009). "Systematic and integrative analysis of large gene lists using DAVID bioinformatics resources." Nat Protoc **4**(1): 44-57.

Huber, J., U. Cronshagen, M. Kadokura, C. Marshallsay, T. Wada, M. Sekine and R. Luhrmann (1998). "Snurportin1, an m3G-cap-specific nuclear import receptor with a novel domain structure." Embo j **17**(14): 4114-4126.

Hulsmann, B. B., A. A. Labokha and D. Gorlich (2012). "The permeability of reconstituted nuclear pores provides direct evidence for the selective phase model." Cell **150**(4): 738-751.

Hülsmann, Bastian B., Aksana A. Labokha and D. Görlich (2012). "The Permeability of Reconstituted Nuclear Pores Provides Direct Evidence for the Selective Phase Model." Cell **150**(4): 738-751.

Hung, M. C. and W. Link (2011). "Protein localization in disease and therapy." J Cell Sci **124**(Pt 20): 3381-3392.

Huppertz, B. and M. Gauster (2011). Trophoblast Fusion. Cell Fusion in Health and Disease. T. Dittmar and K. S. Zänker. Dordrecht, Springer Netherlands**:** 81-95.

Hutten, S., A. Flotho, F. Melchior and R. H. Kehlenbach (2008). "The Nup358-RanGAP complex is required for efficient importin alpha/beta-dependent nuclear import." Mol Biol Cell **19**(5): 2300-2310.

Illmensee, K. and A. P. Mahowald (1974). "Transplantation of posterior polar plasm in Drosophila. Induction of germ cells at the anterior pole of the egg." Proc Natl Acad Sci U S A **71**(4): 1016-1020.

Ishido, M., K. Kami and M. Masuhara (2004). "Localization of MyoD, myogenin and cell cycle regulatory factors in hypertrophying rat skeletal muscles." Acta Physiol Scand **180**(3): 281-289.

Iwamoto, M., C. Mori, T. Kojidani, F. Bunai, T. Hori, T. Fukagawa, Y. Hiraoka and T. Haraguchi (2009). "Two distinct repeat sequences of Nup98 nucleoporins characterize dual nuclei in the binucleated ciliate tetrahymena." Curr Biol **19**(10): 843-847.

Izaurralde, E., U. Kutay, C. von Kobbe, I. W. Mattaj and D. Gorlich (1997). "The asymmetric distribution of the constituents of the Ran system is essential for transport into and out of the nucleus." Embo j **16**(21): 6535-6547.

Jakel, S. and D. Gorlich (1998). "Importin beta, transportin, RanBP5 and RanBP7 mediate nuclear import of ribosomal proteins in mammalian cells." Embo j **17**(15): 4491-4502.

Jankowska, U., A. Latosinska, B. Skupien-Rabian, B. Swiderska, M. Dziedzicka-Wasylewska and S. Kedracka-Krok (2016). "Optimized procedure of extraction, purification and proteomic analysis of nuclear proteins from mouse brain." Journal of Neuroscience Methods **261**: 1-9.

Jasmin, B. J., R. K. Lee and R. L. Rotundo (1993). "Compartmentalization of acetylcholinesterase mRNA and enzyme at the vertebrate neuromuscular junction." Neuron **11**(3): 467-477.

Jin, L., Z. Jiang, Y. Xia, P. Lou, L. Chen, H. Wang, L. Bai, Y. Xie, Y. Liu, W. Li, B. Zhong, J. Shen, A. Jiang, L. Zhu, J. Wang, X. Li and M. Li (2014). "Genome-wide DNA methylation changes in skeletal muscle between young and middle-aged pigs." BMC Genomics **15**: 653.

Joe, A. W. B., L. Yi, A. Natarajan, F. Le Grand, L. So, J. Wang, M. A. Rudnicki and F. M. V. Rossi (2010). "Muscle injury activates resident fibro/adipogenic progenitors that facilitate myogenesis." Nature cell biology **12**(2): 153-163.

Johnson, W. E., C. Li and A. Rabinovic (2007). "Adjusting batch effects in microarray expression data using empirical Bayes methods." Biostatistics **8**(1): 118-127.

Jubrias, S. A., N. K. Vollestad, R. K. Gronka and M. J. Kushmerick (2008). "Contraction coupling efficiency of human first dorsal interosseous muscle." J Physiol **586**(7): 1993-2002.

Kalderon, D., W. D. Richardson, A. F. Markham and A. E. Smith (1984). "Sequence requirements for nuclear location of simian virus 40 large-T antigen." Nature **311**(5981): 33-38.

Kall, L., J. D. Storey, M. J. MacCoss and W. S. Noble (2008). "Assigning significance to peptides identified by tandem mass spectrometry using decoy databases." J Proteome Res **7**(1): 29-34.

Kaur, E., J. Rajendra, S. Jadhav, E. Shridhar, J. S. Goda, A. Moiyadi and S. Dutt (2015). "Radiation-induced homotypic cell fusions of innately resistant glioblastoma cells mediate their sustained survival and recurrence." Carcinogenesis **36**(6): 685-695.

Kawaguchi, H., N. Manabe, C. Miyaura, H. Chikuda, K. Nakamura and M. Kuro-o (1999). "Independent impairment of osteoblast and osteoclast differentiation in klotho mouse exhibiting low-turnover osteopenia." J Clin Invest **104**(3): 229-237.

Kehlenbach, R. H. and L. Gerace (2000). "Phosphorylation of the nuclear transport machinery down-regulates nuclear protein import in vitro." J Biol Chem **275**(23): 17848-17856.

Khosla, S. and L. C. Hofbauer (2017). "Osteoporosis treatment: recent developments and ongoing challenges." The Lancet Diabetes & Endocrinology.

Kim, J. Y., Y.-K. Park, K.-P. Lee, S.-M. Lee, T.-W. Kang, H.-J. Kim, S. H. Dho, S.-Y. Kim and K.-S. Kwon (2014). "Genome-wide profiling of the microRNA-mRNA regulatory network in skeletal muscle with aging." Aging (Albany NY) **6**(7): 524-544.

Kinoshita, Y., T. Kalir, P. Dottino and D. S. Kohtz (2012). "Nuclear Distributions of NUP62 and NUP214 Suggest Architectural Diversity and Spatial Patterning among Nuclear Pore Complexes." PLoS ONE **7**(4): e36137.

Kirby, T. J., J. D. Lee, J. H. England, T. Chaillou, K. A. Esser and J. J. McCarthy (2015). "Blunted hypertrophic response in aged skeletal muscle is associated with decreased ribosome biogenesis." Journal of Applied Physiology **119**(4): 321-327.

Kirby, T. J., R. M. Patel, T. S. McClintock, E. E. Dupont-Versteegden, C. A. Peterson and J. J. McCarthy (2016). "Myonuclear transcription is responsive to mechanical load and DNA content but uncoupled from cell size during hypertrophy." Molecular Biology of the Cell **27**(5): 788-798.

Kobayashi, J. and Y. Matsuura (2013). "Structural basis for cell-cycle-dependent nuclear import mediated by the karyopherin Kap121p." J Mol Biol **425**(11): 1852-1868.

Kodiha, M., D. Tran, A. Morogan, C. Qian and U. Stochaj (2009). "Dissecting the signaling events that impact classical nuclear import and target nuclear transport factors." PLoS One **4**(12): e8420.

Kodiha, M., D. Tran, C. Qian, A. Morogan, J. F. Presley, C. M. Brown and U. Stochaj (2008). "Oxidative stress mislocalizes and retains transport factor importin-alpha and nucleoporins Nup153 and Nup88 in nuclei where they generate high molecular mass complexes." Biochim Biophys Acta **1783**(3): 405-418.

Kohler, A. and E. Hurt (2007). "Exporting RNA from the nucleus to the cytoplasm." Nat Rev Mol Cell Biol **8**(10): 761-773.

Kosako, H. and N. Imamoto (2010). "Phosphorylation of nucleoporins: Signal transduction-mediated regulation of their interaction with nuclear transport receptors." Nucleus **1**(4): 309-313.

Kosako, H., N. Yamaguchi, C. Aranami, M. Ushiyama, S. Kose, N. Imamoto, H. Taniguchi, E. Nishida and S. Hattori (2009). "Phosphoproteomics reveals new ERK MAP kinase targets and links ERK to nucleoporin-mediated nuclear transport." Nat Struct Mol Biol **16**(10): 1026-1035.

Kuang, S., K. Kuroda, F. Le Grand and M. A. Rudnicki "Asymmetric Self-Renewal and Commitment of Satellite Stem Cells in Muscle." Cell **129**(5): 999-1010.

Kudryavtsev, B. N., M. V. Kudryavtseva, G. A. Sakuta and G. I. Stein (1993). "Human hepatocyte polyploidization kinetics in the course of life cycle." Virchows Arch B Cell Pathol Incl Mol Pathol **64**(6): 387-393.

Kwon, K.-S., J. Y. Kim, S.-M. Lee, K. P. Lee and S.-Y. Kim (2014). "Genome-wide microRNA and mRNA profiling in skeletal muscle aging (1009.5)." The FASEB Journal **28**(1 Supplement).

Lam, M. H., W. Hu, C. Y. Xiao, M. T. Gillespie and D. A. Jans (2001). "Molecular dissection of the importin beta1-recognized nuclear targeting signal of parathyroid hormone-related protein." Biochem Biophys Res Commun **282**(2): 629-634.

Landi, F., R. Liperoti, A. Russo, S. Giovannini, M. Tosato, E. Capoluongo, R. Bernabei and G. Onder (2012). "Sarcopenia as a risk factor for falls in elderly individuals: results from the ilSIRENTE study." Clin Nutr **31**(5): 652-658.

Lanford, R. E. and J. S. Butel (1984). "Construction and characterization of an SV40 mutant defective in nuclear transport of T antigen." Cell **37**(3): 801-813.

Lange, A., L. M. McLane, R. E. Mills, S. E. Devine and A. H. Corbett (2010). "Expanding the definition of the classical bipartite nuclear localization signal." Traffic **11**(3): 311-323.

Laohavinij, W. (2015). "Antiaging phenotype in skeletal muscle after endurance exercise is associated with the oxidative phosphorylation pathway." Asian Biomed **9**(4): 455.

Lee, B. J., A. E. Cansizoglu, K. E. Suel, T. H. Louis, Z. Zhang and Y. M. Chook (2006). "Rules for nuclear localization sequence recognition by karyopherin beta 2." Cell **126**(3): 543-558.

Lee, C., D. B. Allison, J. Brand, R. Weindruch and T. A. Prolla (2002). "Transcriptional profiles associated with aging and middle age-onset caloric restriction in mouse hearts." Proc Natl Acad Sci USA **99**.

Lehmann, R. and C. Nüsslein-Volhard (1986). "Abdominal segmentation, pole cell formation, and embryonic polarity require the localized activity of oskar, a maternal gene in drosophila." Cell **47**(1): 141-152.

Lemos, D. R., F. Babaeijandaghi, M. Low, C. K. Chang, S. T. Lee, D. Fiore, R. H. Zhang, A. Natarajan, S. A. Nedospasov and F. M. Rossi (2015). "Nilotinib reduces muscle fibrosis in chronic muscle injury by promoting TNF-mediated apoptosis of fibro/adipogenic progenitors." Nat Med **21**(7): 786-794.

Lénárt, P., G. Rabut, N. Daigle, A. R. Hand, M. Terasaki and J. Ellenberg (2003). "Nuclear envelope breakdown in starfish oocytes proceeds by partial NPC disassembly followed by a rapidly spreading fenestration of nuclear membranes." The Journal of Cell Biology **160**(7): 1055-1068.

Lott, K. and G. Cingolani (2011). "The Importin β Binding Domain as a Master Regulator of Nucleocytoplasmic Transport." Biochimica et biophysica acta **1813**(9): 1578-1592.

Luber, C. A., J. Cox, H. Lauterbach, B. Fancke, M. Selbach, J. Tschopp, S. Akira, M. Wiegand, H. Hochrein, M. O'Keeffe and M. Mann (2010). "Quantitative proteomics reveals subset-specific viral recognition in dendritic cells." Immunity **32**(2): 279-289.

Lupu, F., A. Alves, K. Anderson, V. Doye and E. Lacy (2008). "Nuclear pore composition regulates neural stem/progenitor cell differentiation in the mouse embryo." Dev Cell **14**(6): 831-842.

Lusk, C. P., T. Makhnevych, M. Marelli, J. D. Aitchison and R. W. Wozniak (2002). "Karyopherins in nuclear pore biogenesis: a role for Kap121p in the assembly of Nup53p into nuclear pore complexes." J Cell Biol **159**(2): 267-278.

Lyman, S. K., T. Guan, J. Bednenko, H. Wodrich and L. Gerace (2002). "Influence of cargo size on Ran and energy requirements for nuclear protein import." J Cell Biol **159**(1): 55-67.

Makhnevych, T., C. P. Lusk, A. M. Anderson, J. D. Aitchison and R. W. Wozniak (2003). "Cell cycle regulated transport controlled by alterations in the nuclear pore complex." Cell **115**(7): 813-823.

Malone, C. D., K. A. Falkowska, A. Y. Li, S. E. Galanti, R. C. Kanuru, E. G. LaMont, K. C. Mazzarella, A. J. Micev, M. M. Osman, N. K. Piotrowski, J. W. Suszko, A. C. Timm, M. M. Xu, L. Liu and D. L. Chalker (2008). "Nucleus-specific importin alpha proteins and nucleoporins regulate protein import and nuclear division in the binucleate Tetrahymena thermophila." Eukaryot Cell **7**(9): 1487-1499.

Marelli, M., C. P. Lusk, H. Chan, J. D. Aitchison and R. W. Wozniak (2001). "A link between the synthesis of nucleoporins and the biogenesis of the nuclear envelope." J Cell Biol **153**(4): 709-724.

Marfori, M., A. Mynott, J. J. Ellis, A. M. Mehdi, N. F. Saunders, P. M. Curmi, J. K. Forwood, M. Boden and B. Kobe (2011). "Molecular basis for specificity of nuclear import and prediction of nuclear localization." Biochim Biophys Acta **1813**(9): 1562-1577.

Mariano, M. and W. G. Spector (1974). "The formation and properties of macrophage polykaryons (inflammatory giant cells)." J Pathol **113**(1): 1-19.

Markina-Inarrairaegui, A., O. Etxebeste, E. Herrero-Garcia, L. Araujo-Bazan, J. Fernandez-Martinez, J. A. Flores, S. A. Osmani and E. A. Espeso (2011). "Nuclear transporters in a multinucleated organism: functional and localization analyses in Aspergillus nidulans." Mol Biol Cell **22**(20): 3874-3886.

Marsh, A. P., W. J. Rejeski, M. A. Espeland, M. E. Miller, T. S. Church, R. A. Fielding, T. M. Gill, J. M. Guralnik, A. B. Newman and M. Pahor (2011). "Muscle strength and BMI as predictors of major mobility disability in the Lifestyle Interventions and Independence for Elders pilot (LIFE-P)." J Gerontol A Biol Sci Med Sci **66**(12): 1376-1383.

Mauro, A. (1961). "Satellite cell of skeletal muscle fibers." J Biophys Biochem Cytol **9**: 493-495.

Mavrakis, M., R. Rikhy and J. Lippincott-Schwartz (2009). "Cells within a cell: Insights into cellular architecture and polarization from the organization of the early fly embryo." Commun Integr Biol **2**(4): 313-314.

Mavrakis, M., R. Rikhy and J. Lippincott-Schwartz (2009). "Plasma membrane polarity and compartmentalization are established before cellularization in the fly embryo." Dev Cell **16**(1): 93-104.

Mayhew, T. M. (2014). "Turnover of human villous trophoblast in normal pregnancy: what do we know and what do we need to know?" Placenta **35**(4): 229-240.

McGee, S. L., E. Fairlie, A. P. Garnham and M. Hargreaves (2009). "Exercise-induced histone modifications in human skeletal muscle." J Physiol **587**(Pt 24): 5951-5958.

McKinsey, T. A., C. L. Zhang and E. N. Olson (2001). "Identification of a signal-responsive nuclear export sequence in class II histone deacetylases." Mol Cell Biol **21**(18): 6312-6321.

McNally, A. K. and J. M. Anderson (2011). "Macrophage fusion and multinucleated giant cells of inflammation." Adv Exp Med Biol **713**: 97-111.

McPherron, A. C., A. M. Lawler and S. J. Lee (1997). "Regulation of skeletal muscle mass in mice by a new TGF-beta superfamily member." Nature **387**(6628): 83-90.

Metter, E. J., R. Conwit, J. Tobin and J. L. Fozard (1997). "Age-associated loss of power and strength in the upper extremities in women and men." J Gerontol A Biol Sci Med Sci **52**(5): B267-276.

Middelbos, I. S., B. M. Vester, L. K. Karr-Lilienthal, L. B. Schook and K. S. Swanson (2009). "Age and Diet Affect Gene Expression Profile in Canine Skeletal Muscle." PLoS ONE **4**(2): e4481.

Miller, M. W., M. R. Caracciolo, W. K. Berlin and J. A. Hanover (1999). "Phosphorylation and glycosylation of nucleoporins." Arch Biochem Biophys **367**(1): 51-60.

Mizuguchi-Hata, C., Y. Ogawa, M. Oka and Y. Yoneda (2013). "Quantitative regulation of nuclear pore complex proteins by O-GlcNAcylation." Biochim Biophys Acta **1833**(12): 2682-2689.

Moore, M. S. and E. D. Schwoebel (2001). "Nuclear import in digitonin-permeabilized cells." Curr Protoc Cell Biol **Chapter 11**: Unit 11.17.

Morchoisne-Bolhy, S., M. C. Geoffroy, I. B. Bouhlel, A. Alves, N. Auduge, X. Baudin, K. Van Bortle, M. A. Powers and V. Doye (2015). "Intranuclear dynamics of the Nup107-160 complex." Mol Biol Cell **26**(12): 2343-2356.

Moscoso, L. M., G. C. Chu, M. Gautam, P. G. Noakes, J. P. Merlie and J. R. Sanes (1995). "Synapse-associated expression of an acetylcholine receptor-inducing protein, ARIA/heregulin, and its putative receptors, ErbB2 and ErbB3, in developing mammalian muscle." Dev Biol **172**(1): 158-169.

Nadal, C. and F. Zajdela (1967). "[Hepatic polyploidy in the rat. IV. Experimental changes in the nucleolar volume of liver cells and their mechanisms of regulation]." Exp Cell Res **48**(3): 518-528.

Nakamura, K. and S. F. Morrison (2011). "Central efferent pathways for cold-defensive and febrile shivering." J Physiol **589**(Pt 14): 3641-3658.

Nardozzi, J. D., K. Lott and G. Cingolani (2010). "Phosphorylation meets nuclear import: a review." Cell Communication and Signaling : CCS **8**: 32-32.

Nawar, N. A., J. Olsen, T. M. Jelic and C. He (2016). "Primary Urinary Bladder Angiosarcoma with Osteoclast-Like Multinucleated Giant Cells: A Case Report and Literature Review." Am J Case Rep **17**: 143-149.

Newlands, E. S., G. J. Rustin and M. H. Brampton (1996). "Phase I trial of elactocin." Br J Cancer **74**(4): 648-649.

Newlands, S., L. K. Levitt, C. S. Robinson, A. B. Karpf, V. R. Hodgson, R. P. Wade and E. C. Hardeman (1998). "Transcription occurs in pulses in muscle fibers." Genes Dev **12**(17): 2748-2758.

Newman, A. B., V. Kupelian, M. Visser, E. M. Simonsick, B. H. Goodpaster, S. B. Kritchevsky, F. A. Tylavsky, S. M. Rubin and T. B. Harris (2006). "Strength, but not muscle mass, is associated with mortality in the health, aging and body composition study cohort." J Gerontol A Biol Sci Med Sci **61**(1): 72-77.

Newmeyer, D. D., J. M. Lucocq, T. R. Burglin and E. M. De Robertis (1986). "Assembly in vitro of nuclei active in nuclear protein transport: ATP is required for nucleoplasmin accumulation." Embo j **5**(3): 501-510.

Niu, X., J. Hong, X. Zheng, D. B. Melville, E. W. Knapik, A. Meng and J. Peng (2014). "The nuclear pore complex function of Sec13 protein is required for cell survival during retinal development." J Biol Chem **289**(17): 11971-11985.

O'Connell, K., J. Gannon, P. Doran and K. Ohlendieck (2007). "Proteomic profiling reveals a severely perturbed protein expression pattern in aged skeletal muscle." Int J Mol Med **20**(2): 145-153.

O'Connor, R. S., S. T. Mills, K. A. Jones, S. N. Ho and G. K. Pavlath (2007). "A combinatorial role for NFAT5 in both myoblast migration and differentiation during skeletal muscle myogenesis." J Cell Sci **120**(Pt 1): 149-159.

Ogawa, M., H. Mizofuchi, Y. Kobayashi, G. Tsuzuki, M. Yamamoto, S. Wada and K. Kamemura (2012). "Terminal differentiation program of skeletal myogenesis is negatively regulated by O-GlcNAc glycosylation." Biochim Biophys Acta **1820**(1): 24-32.

Ohkawa, Y., C. Mallappa, C. S. Vallaster and A. N. Imbalzano (2012). "Isolation of nuclei from skeletal muscle satellite cells and myofibers for use in chromatin immunoprecipitation assays." Methods Mol Biol **798**: 517-530.

Orias, E., M. D. Cervantes and E. P. Hamilton (2011). "Tetrahymena thermophila, a unicellular eukaryote with separate germline and somatic genomes." Res Microbiol **162**(6): 578-586.

Pawlikowski, B., C. Pulliam, N. D. Betta, G. Kardon and B. B. Olwin (2015). "Pervasive satellite cell contribution to uninjured adult muscle fibers." Skeletal Muscle **5**: 42.

Pichavant, C. and G. K. Pavlath (2014). "Incidence and severity of myofiber branching with regeneration and aging." Skeletal Muscle **4**: 9-9.

Pichavant, C. and G. K. Pavlath (2014). "Incidence and severity of myofiber branching with regeneration and aging." Skelet Muscle **4**: 9.

Pollard, V. W., W. M. Michael, S. Nakielny, M. C. Siomi, F. Wang and G. Dreyfuss (1996). "A novel receptor-mediated nuclear protein import pathway." Cell **86**(6): 985-994.

Porpiglia, E., N. Samusik, A. T. Van Ho, B. D. Cosgrove, T. Mai, K. L. Davis, A. Jager, G. P. Nolan, S. C. Bendall, W. J. Fantl and H. M. Blau (2017). "High-resolution myogenic lineage mapping by single-cell mass cytometry." Nat Cell Biol **19**(5): 558-567.

Powers, M. A. and D. J. Forbes (2012). "Nuclear transport: beginning to gel?" Curr Biol **22**(23): R1006-1009.

Prigge, J. R., J. A. Wiley, E. A. Talago, E. M. Young, L. L. Johns, J. A. Kundert, K. M. Sonsteng, W. P. Halford, M. R. Capecchi and E. E. Schmidt (2013). "Nuclear double-fluorescent reporter for in vivo and ex vivo analyses of biological transitions in mouse nuclei." Mamm Genome.

Puck, T. T. and P. I. Marcus (1955). "A RAPID METHOD FOR VIABLE CELL TITRATION AND CLONE PRODUCTION WITH HELA CELLS IN TISSUE CULTURE: THE USE OF X-IRRADIATED CELLS TO SUPPLY CONDITIONING FACTORS." Proc Natl Acad Sci U S A **41**(7): 432-437.

Puck, T. T. and P. I. Marcus (1956). "Action of x-rays on mammalian cells." J Exp Med **103**(5): 653-666.

Puri, P. L., V. Sartorelli, X. J. Yang, Y. Hamamori, V. V. Ogryzko, B. H. Howard, L. Kedes, J. Y. Wang, A. Graessmann, Y. Nakatani and M. Levrero (1997). "Differential roles of p300 and PCAF acetyltransferases in muscle differentiation." Mol Cell **1**(1): 35-45.

Rabut, G., V. Doye and J. Ellenberg (2004). "Mapping the dynamic organization of the nuclear pore complex inside single living cells." Nat Cell Biol **6**(11): 1114-1121.

Rapp, F., S. Pauluzzi and J. S. Butel (1969). "Variation in properties of plaque progeny of PARA (defective simian papovavirus 40)-adenovirus 7." J Virol **4**(5): 626-631.

Ratnayake, D. and P. D. Currie (2017). "Stem cell dynamics in muscle regeneration: Insights from live imaging in different animal models." BioEssays **39**(6): n/a-n/a.

Ravid, K., J. Lu, J. M. Zimmet and M. R. Jones (2002). "Roads to polyploidy: the megakaryocyte example." J Cell Physiol **190**(1): 7-20.

Regot, S., E. de Nadal, S. Rodriguez-Navarro, A. Gonzalez-Novo, J. Perez-Fernandez, O. Gadal, G. Seisenbacher, G. Ammerer and F. Posas (2013). "The Hog1 stress-activated protein kinase targets nucleoporins to control mRNA export upon stress." J Biol Chem **288**(24): 17384-17398.

Ribbeck, K. and D. Gorlich (2001). "Kinetic analysis of translocation through nuclear pore complexes." Embo j **20**(6): 1320-1330.

Richey, J., S. Rogers, D. H. Van Thiel and R. Lester (1977). "Giant multinucleated hepatocytes in an adult with chronic active hepatitis." Gastroenterology **73**(3): 570-574.

Rigbolt, K. T., T. A. Prokhorova, V. Akimov, J. Henningsen, P. T. Johansen, I. Kratchmarova, M. Kassem, M. Mann, J. V. Olsen and B. Blagoev (2011). "System-wide temporal characterization of the proteome and phosphoproteome of human embryonic stem cell differentiation." Sci Signal **4**(164): rs3.

Robbins, J., S. M. Dilworth, R. A. Laskey and C. Dingwall (1991). "Two interdependent basic domains in nucleoplasmin nuclear targeting sequence: identification of a class of bipartite nuclear targeting sequence." Cell **64**(3): 615-623.

Ross, J. J., M. J. Duxson and A. J. Harris (1987). "Formation of primary and secondary myotubes in rat lumbrical muscles." Development **100**(3): 383-394.

Rosser, B. and E. Bandman (2003). "Heterogeneity of protein expression within muscle fibers." Journal of Animal Science **81**(14_suppl_2): E94-E101.

Sabri, N., P. Roth, N. Xylourgidis, F. Sadeghifar, J. Adler and C. Samakovlis (2007). "Distinct functions of the Drosophila Nup153 and Nup214 FG domains in nuclear protein transport." J Cell Biol **178**(4): 557-565.

Saeter, G., P. E. Schwarze, J. M. Nesland, N. Juul, E. O. Pettersen and P. O. Seglen (1988). "The polyploidizing growth pattern of normal rat liver is replaced by divisional, diploid growth in hepatocellular nodules and carcinomas." Carcinogenesis **9**(6): 939-945.

Sakai, H., I. Okafuji, R. Nishikomori, J. Abe, K. Izawa, N. Kambe, T. Yasumi, T. Nakahata and T. Heike (2012). "The CD40-CD40L axis and IFN-gamma play critical roles in Langhans giant cell formation." Int Immunol **24**(1): 5-15.

Salamon, M., C. Millino, A. Raffaello, M. Mongillo, C. Sandri, C. Bean, E. Negrisolo, A. Pallavicini, G. Valle, M. Zaccolo, S. Schiaffino and G. Lanfranchi (2003). "Human MYO18B, a novel unconventional myosin heavy chain expressed in striated muscles moves into the myonuclei upon differentiation." J Mol Biol **326**(1): 137-149.

Saroufim, M.-A., P. Bensidoun, P. Raymond, S. Rahman, M. R. Krause, M. Oeffinger and D. Zenklusen (2015). "The nuclear basket mediates perinuclear mRNA scanning in budding yeast." The Journal of Cell Biology **211**(6): 1131-1140.

Savas, J. N., B. H. Toyama, T. Xu, J. R. Yates and M. W. Hetzer (2012). "Extremely Long-Lived Nuclear Pore Proteins in the Rat Brain." Science **335**(6071): 942-942.

Scampini, G., A. Nava, A. J. Newman, P. Della Torre and G. Mazue (1993). "Multinucleated hepatocytes induced by rifabutin in rats." Toxicol Pathol **21**(4): 369-376.

Schiaffino, S. and C. Reggiani (1994). "Myosin isoforms in mammalian skeletal muscle." J Appl Physiol (1985) **77**(2): 493-501.

Schindelin, J., I. Arganda-Carreras, E. Frise, V. Kaynig, M. Longair, T. Pietzsch, S. Preibisch, C. Rueden, S. Saalfeld, B. Schmid, J. Y. Tinevez, D. J. White, V. Hartenstein, K. Eliceiri, P. Tomancak and A. Cardona (2012). "Fiji: an open-source platform for biological-image analysis." Nat Methods **9**(7): 676-682.

Schindelin, J., C. T. Rueden, M. C. Hiner and K. W. Eliceiri (2015). "The ImageJ ecosystem: An open platform for biomedical image analysis." Mol Reprod Dev **82**(7-8): 518-529.

Schipke, J., E. Banmann, S. Nikam, R. Voswinckel, K. Kohlstedt, A. E. Loot, I. Fleming and C. Mühlfeld (2014). "The number of cardiac myocytes in the hypertrophic and hypotrophic left ventricle of the obese and calorie-restricted mouse heart." Journal of Anatomy **225**(5): 539-547.

Schmid, M., G. Arib, C. Laemmli, J. Nishikawa, T. Durussel and U. K. Laemmli "Nup-PI: The Nucleopore-Promoter Interaction of Genes in Yeast." Molecular Cell **21**(3): 379-391.

Schmidt, H. B. and D. Görlich (2016). "Transport Selectivity of Nuclear Pores, Phase Separation, and Membraneless Organelles." Trends in Biochemical Sciences **41**(1): 46-61.

Schupbach, T. and E. Wieschaus (1986). "Germline autonomy of maternal-effect mutations altering the embryonic body pattern of Drosophila." Dev Biol **113**(2): 443-448.

Seglen, P. O. (1997). "DNA ploidy and autophagic protein degradation as determinants of hepatocellular growth and survival." Cell Biol Toxicol **13**(4-5): 301-315.

Sekimoto, T. and Y. Yoneda (2012). "Intrinsic and extrinsic negative regulators of nuclear protein transport processes." Genes Cells **17**(7): 525-535.

Serra, C., D. Palacios, C. Mozzetta, S. V. Forcales, I. Morantte, M. Ripani, D. R. Jones, K. Du, U. S. Jhala, C. Simone and P. L. Puri (2007). "Functional interdependence at the chromatin level between the MKK6/p38 and IGF1/PI3K/AKT pathways during muscle differentiation." Mol Cell **28**(2): 200-213.

Shalakhmetova, T. M., B. A. Umbayev, S. Z. Kolumbayeva and B. N. Kudryavtsev (2009). "About mechanisms of formation of multinuclear hepatocytes during toxic action of N-nitrosodimethylamine on rats." Cell and Tissue Biology **3**(1): 61.

Sharples, A. P., C. E. Stewart and R. A. Seaborne (2016). "Does skeletal muscle have an 'epi'-memory? The role of epigenetics in nutritional programming, metabolic disease, aging and exercise." Aging Cell **15**(4): 603-616.

Shi, X. and D. J. Garry (2006). "Muscle stem cells in development, regeneration, and disease." Genes Dev **20**(13): 1692-1708.

Shinin, V., B. Gayraud-Morel, D. Gomes and S. Tajbakhsh (2006). "Asymmetric division and cosegregation of template DNA strands in adult muscle satellite cells." Nat Cell Biol **8**(7): 677-682.

Shumaker, D. K., R. I. Lopez-Soler, S. A. Adam, H. Herrmann, R. D. Moir, T. P. Spann and R. D. Goldman (2005). "Functions and dysfunctions of the nuclear lamin Ig-fold domain in nuclear assembly, growth, and Emery-Dreifuss muscular dystrophy." Proc Natl Acad Sci U S A **102**(43): 15494-15499.

Smith, E. R., X. Y. Zhang, C. D. Capo-Chichi, X. Chen and X. X. Xu (2011). "Increased expression of Syne1/nesprin-1 facilitates nuclear envelope structure changes in embryonic stem cell differentiation." Dev Dyn **240**(10): 2245-2255.

Snow, C. J., A. Dar, A. Dutta, R. H. Kehlenbach and B. M. Paschal (2013). "Defective nuclear import of Tpr in Progeria reflects the Ran sensitivity of large cargo transport." The Journal of Cell Biology **201**(4): 541-557.

Soniat, M., T. Cagatay and Y. M. Chook (2016). "Recognition Elements in the Histone H3 and H4 Tails for Seven Different Importins." J Biol Chem **291**(40): 21171-21183.

Soonpaa, M. H. and L. J. Field (1998). "Survey of Studies Examining Mammalian Cardiomyocyte DNA Synthesis." Circulation Research **83**(1): 15-26.

Spalding, K. L., R. D. Bhardwaj, B. A. Buchholz, H. Druid and J. Frisén (2005). "Retrospective Birth Dating of Cells in Humans." Cell **122**(1): 133-143.

Strambio-De-Castillia, C., M. Niepel and M. P. Rout (2010). "The nuclear pore complex: bridging nuclear transport and gene regulation." Nat Rev Mol Cell Biol **11**(7): 490-501.

Su, J., C. Ekman, N. Oskolkov, L. Lahti, K. Strom, A. Brazma, L. Groop, J. Rung and O. Hansson (2015). "A novel atlas of gene expression in human skeletal muscle reveals molecular changes associated with aging." Skelet Muscle **5**: 35.

Su, J., C. Ekman, N. Oskolkov, L. Lahti, K. Ström, A. Brazma, L. Groop, J. Rung and O. Hansson (2015). "A novel atlas of gene expression in human skeletal muscle reveals molecular changes associated with aging." Skeletal Muscle **5**: 35.

Swindell, W. R. (2009). "Genes and gene expression modules associated with caloric restriction and aging in the laboratory mouse." BMC Genomics **10**(1): 1-28.

Tajbakhsh, S. (2005). "Skeletal muscle stem and progenitor cells: Reconciling genetics and lineage." Experimental Cell Research **306**(2): 364-372.

Tapley, E. C. and D. A. Starr (2013). "Connecting the nucleus to the cytoskeleton by SUN-KASH bridges across the nuclear envelope." Curr Opin Cell Biol **25**(1): 57-62.

Ten Broek, R. W., S. Grefte and J. W. Von den Hoff (2010). "Regulatory factors and cell populations involved in skeletal muscle regeneration." Journal of Cellular Physiology **224**(1): 7-16.

Terry, L. J., E. B. Shows and S. R. Wente (2007). "Crossing the nuclear envelope: hierarchical regulation of nucleocytoplasmic transport." Science **318**(5855): 1412-1416.

Terry, L. J. and S. R. Wente (2007). "Nuclear mRNA export requires specific FG nucleoporins for translocation through the nuclear pore complex." J Cell Biol **178**(7): 1121-1132.

Tidball, J. G. and S. A. Villalta (2010). "Regulatory interactions between muscle and the immune system during muscle regeneration." American Journal of Physiology - Regulatory, Integrative and Comparative Physiology **298**(5): R1173-R1187.

Timney, B. L., J. Tetenbaum-Novatt, D. S. Agate, R. Williams, W. Zhang, B. T. Chait and M. P. Rout (2006). "Simple kinetic relationships and nonspecific competition govern nuclear import rates in vivo." J Cell Biol **175**(4): 579-593.

Toyama, Brandon H., Jeffrey N. Savas, Sung K. Park, Michael S. Harris, Nicholas T. Ingolia, John R. Yates Iii and Martin W. Hetzer (2013). "Identification of Long-Lived Proteins Reveals Exceptional Stability of Essential Cellular Structures." Cell **154**(5): 971-982.

Tran, E. J., M. C. King and A. H. Corbett (2014). "Macromolecular transport between the nucleus and the cytoplasm: Advances in mechanism and emerging links to disease." Biochim Biophys Acta **1843**(11): 2784-2795.

Tran, E. J. and S. R. Wente (2006). "Dynamic nuclear pore complexes: life on the edge." Cell **125**(6): 1041-1053.

Trichia, H., O. Ignatova, J. Lekka, M. Papazian and P. Manikis (2016). "Malignant Myoepithelioma of the Breast Clinically and Histologically Masquerading as Angiosarcoma: Cytological Findings and Review of the Literature." Acta Cytol **60**(3): 260-266.

Tu, L. C. and S. M. Musser (2011). "Single molecule studies of nucleocytoplasmic transport." Biochim Biophys Acta **1813**(9): 1607-1618.

Turner, J. G. and D. M. Sullivan (2008). "CRM1-mediated nuclear export of proteins and drug resistance in cancer." Curr Med Chem **15**(26): 2648-2655.

Tyanova, S., T. Temu, P. Sinitcyn, A. Carlson, M. Y. Hein, T. Geiger, M. Mann and J. Cox (2016). "The Perseus computational platform for comprehensive analysis of (prote)omics data." Nat Methods **13**(9): 731-740.

Uv, A. E., P. Roth, N. Xylourgidis, A. Wickberg, R. Cantera and C. Samakovlis (2000). "members only encodes a Drosophila nucleoporin required for Rel protein import and immune response activation." Genes & Development **14**(15): 1945-1957.

Uzer, G., W. R. Thompson, B. Sen, Z. Xie, S. S. Yen, S. Miller, G. Bas, M. Styner, C. T. Rubin, S. Judex, K. Burridge and J. Rubin (2015). "Cell Mechanosensitivity to Extremely Low-Magnitude Signals Is Enabled by a LINCed Nucleus." Stem Cells **33**(6): 2063-2076.

Vitale, I., L. Senovilla, M. Jemaa, M. Michaud, L. Galluzzi, O. Kepp, L. Nanty, A. Criollo, S. Rello-Varona, G. Manic, D. Metivier, S. Vivet, N. Tajeddine, N. Joza, A. Valent, M. Castedo and G. Kroemer (2010). "Multipolar mitosis of tetraploid cells: inhibition by p53 and dependency on Mos." Embo j **29**(7): 1272-1284.

Voeltz, G. K. and W. A. Prinz (2007). "Sheets, ribbons and tubules [mdash] how organelles get their shape." Nat Rev Mol Cell Biol **8**(3): 258-264.

Walsh, S., A. Ponten, B. K. Fleischmann and S. Jovinge (2010). "Cardiomyocyte cell cycle control and growth estimation in vivo--an analysis based on cardiomyocyte nuclei." Cardiovasc Res **86**(3): 365-373.

Walther, T. C., A. Alves, H. Pickersgill, I. Loiodice, M. Hetzer, V. Galy, B. B. Hulsmann, T. Kocher, M. Wilm, T. Allen, I. W. Mattaj and V. Doye (2003). "The conserved Nup107-160 complex is critical for nuclear pore complex assembly." Cell **113**(2): 195-206.

Weihua, Z., Q. Lin, A. J. Ramoth, D. Fan and I. J. Fidler (2011). "Formation of solid tumors by a single multinucleated cancer cell." Cancer **117**(17): 4092-4099.

Weindruch, R., T. Kayo, C. K. Lee and T. A. Prolla (2001). "Microarray profiling of gene expression in aging and its alteration by caloric restriction in mice." J Nutr **131**(3): 918s-923s.

Welle, S., A. I. Brooks, J. M. Delehanty, N. Needler and C. A. Thornton (2003). "Gene expression profile of aging in human muscle." Physiological Genomics **14**(2): 149-159.

Wilkie, G. S. and E. C. Schirmer (2008). "Purification of nuclei and preparation of nuclear envelopes from skeletal muscle." Methods Mol Biol **463**: 23-41.

Williams, G. T. and W. J. Williams (1983). "Granulomatous inflammation--a review." J Clin Pathol **36**(7): 723-733.

Wohlschlaeger, J., B. Levkau, G. Brockhoff, K. J. Schmitz, M. von Winterfeld, A. Takeda, N. Takeda, J. Stypmann, C. Vahlhaus, C. Schmid, N. Pomjanski, A. Bocking and H. A. Baba (2010).

"Hemodynamic support by left ventricular assist devices reduces cardiomyocyte DNA content in the failing human heart." Circulation **121**(8): 989-996.

Worman, H. J., C. Östlund and Y. Wang (2010). "Diseases of the Nuclear Envelope." Cold Spring Harbor Perspectives in Biology **2**(2): a000760.

Wu, J., X. Ji, L. Zhu, Q. Jiang, Z. Wen, S. Xu, W. Shao, J. Cai, Q. Du, Y. Zhu and J. Mao (2013). "Up-regulation of microRNA-1290 impairs cytokinesis and affects the reprogramming of colon cancer cells." Cancer Lett **329**(2): 155-163.

Xu, L., X. Yao, X. Chen, P. Lu, B. Zhang and Y. T. Ip (2007). "Msk is required for nuclear import of TGF-{beta}/BMP-activated Smads." J Cell Biol **178**(6): 981-994.

Xue, Q. L., J. D. Walston, L. P. Fried and B. A. Beamer (2011). "Prediction of risk of falling, physical disability, and frailty by rate of decline in grip strength: the women's health and aging study." Arch Intern Med **171**(12): 1119-1121.

Yamamoto, D. L., R. I. Csikasz, Y. Li, G. Sharma, K. Hjort, R. Karlsson and T. Bengtsson (2008). "Myotube formation on micro-patterned glass: intracellular organization and protein distribution in C2C12 skeletal muscle cells." J Histochem Cytochem **56**(10): 881-892.

Yasuda, K., K. Sugiura, T. Takeichi, Y. Ogawa, Y. Muro and M. Akiyama (2014). "Nuclear envelope localization of Ran-binding protein 2 and Ran-GTPase-activating protein 1 in psoriatic epidermal keratinocytes." Exp Dermatol **23**(2): 119-124.

Yasuda, Y., Y. Miyamoto, T. Saiwaki and Y. Yoneda (2006). "Mechanism of the stress-induced collapse of the Ran distribution." Exp Cell Res **312**(4): 512-520.

Youn, M. Y., I. Takada, Y. Imai, H. Yasuda and S. Kato (2010). "Transcriptionally active nuclei are selective in mature multinucleated osteoclasts." Genes Cells **15**(10): 1025-1035.

Zahn, J. M., R. Sonu, H. Vogel, E. Crane, K. Mazan-Mamczarz, R. Rabkin, R. W. Davis, K. G. Becker, A. B. Owen and S. K. Kim (2006). "Transcriptional Profiling of Aging in Human Muscle Reveals a Common Aging Signature." PLoS Genetics **2**(7): e115.

Zambon, A. C., S. Gaj, I. Ho, K. Hanspers, K. Vranizan, C. T. Evelo, B. R. Conklin, A. R. Pico and N. Salomonis (2012). "GO-Elite: a flexible solution for pathway and ontology over-representation." Bioinformatics **28**(16): 2209-2210.

Zhang, M. and I. S. McLennan (1995). "During secondary myotube formation, primary myotubes preferentially absorb new nuclei at their ends." Dev Dyn **204**(2): 168-177.

Zykovich, A., A. Hubbard, J. M. Flynn, M. Tarnopolsky, M. F. Fraga, C. Kerksick, D. Ogborn, L. MacNeil, S. D. Mooney and S. Melov (2014). "Genome-wide DNA methylation changes with age in disease-free human skeletal muscle." Aging Cell **13**(2): 360-366.

Zykovich, A., A. Hubbard, J. M. Flynn, M. Tarnopolsky, M. F. Fraga, C. Kerksick, D. Ogborn, L. MacNeil, S. D. Mooney and S. Melov (2014). "Genome-wide DNA methylation changes with age in disease-free human skeletal muscle." Aging Cell **13**(2): 360-366.